

Novel Carbon-Based Microelectrodes for Neurotransmitter Detection

Alexander G. Zestos  
Williamsburg, VA

B.S., The College of William and Mary, 2007  
M.S., The College of William and Mary, 2008

A Dissertation presented to the Graduate Faculty of the University of Virginia in  
Candidacy for the Degree of Doctor of Philosophy

Department of Chemistry

University of Virginia  
May, 2014

---

---

---

---

© Copyright by  
Alexander G. Zestos  
All rights reserved  
May 2014

**Abstract**

Carbon-fiber microelectrodes (CFMEs) are used with fast scan cyclic voltammetry (FSCV) to detect neurotransmitters *in vivo*. CFMEs are typically constructed from glass capillaries pulled to a fine taper or from a polyimide-coated capillary that is 90  $\mu\text{m}$  in outer diameter. Though glass has been used for over twenty years, alternative insulations are sought that can be used to insulate alternative nanomaterials that cannot withstand a vertical capillary puller.

Polyimide coated capillaries can be used to insulate nanomaterials, though the manufacturing process is tedious and not amenable to mass production.

Here, a new fabrication method is developed to insulate carbon-fiber and other microelectrodes with a thin epoxy coating. A  $\text{CO}_2$  laser was used to etch channels in a Teflon mold where carbon fibers were epoxy insulated in the oven. They were then silver epoxied to gold pin that connected to the head stage of the potentiostat to form an electrode. Epoxy insulated CFMEs perform comparably to glass insulated CFMEs and have been successfully used as *in vivo* sensors.

This thesis will examine electrodes made from alternative nanomaterials with epoxy insulation. The thoroughly examined poly(vinyl alcohol) (PVA) carbon nanotube (CNT) fiber was epoxy insulated to form an electrode material and used to detect dopamine with fast scan cyclic voltammetry. Wet spun polyethyleneimine (PEI) CNT fiber microelectrodes were also constructed using epoxy insulation. PEI-CNT fiber microelectrodes displayed increased sensitivity and faster electron transfer kinetics with respect to PVA-CNT fiber microelectrodes. PEI-CNT fiber microelectrodes also exhibited a resistance to surface fouling from serotonin and 5-hydroxyindoleacetic acid (5-HIAA), a

metabolite interferant of serotonin that is present in concentrations ten-times higher than serotonin.

Recently, chlorosulfonic-acid was found to be the first true solvent for carbon nanotubes. Chlorosulfonic acid wet-spun CNT fibers were also used to make electrodes using epoxy insulation. These electrodes were found to be more sensitive than other carbon nanotube fiber microelectrodes due to their larger surface areas, lack of polymer/surfactant impurities, and the lack of the use of sonication which reduces CNT length and lowers conductivity. The sensitivity towards dopamine found to be independent of the wave application frequency, similar to PEI-CNT and CNT-Yarn fiber electrodes. This could allow us to measure neurotransmission closer to the rate at which actually occurs. Lastly, plasma enhanced chemical vapor deposition (PECVD) was used to grow carbon nanopetals (edge-plane graphene) onto metal wires. The high conductivity of the metal substrate is appealing because it would not hinder electron transfer. PECVD is used because it covers the entire wire in carbon for a complete surface coverage without the use of metal catalysts that can be difficult to deposit onto metal surfaces.

Dedicated to my parents, Dr. George K. Zestos and Eva Zestos, for their continual encouragement and support.

## Acknowledgments

The author is grateful to Christopher Jacobs, Michael Nguyen, Elefterios Trikantopoulos, and Brian Poe for their contributions to this dissertation. Christopher Jacobs has made and tested CNT fiber and yarn microelectrodes and has provided insight into the discussion section. Michael Nguyen has carried out the *in vivo* testing of epoxy insulated carbon-fiber and carbon nanotube fiber microelectrodes. Elefterios Trikantopoulos has assisted in making and testing PEI and acid spun CNT fiber microelectrodes. Brian L. Poe has laser etched channels into Teflon molds to form epoxy insulated CFMEs. A special thanks goes to my advisor, Dr. B. Jill Venton, for her mentorship and vision.

## Table of Contents

Chapter 1: Introduction.....	1
1.1.Fast-scan cyclic voltammetry for neurotransmitter detection in vivo....	2
1.2 Electrochemistry/Electrode Fabrication.....	4
1.2.1 Fast-scan cyclic voltammetry for neurotransmitter detection in vivo.....	4
1.2.2. Glass insulated carbon-fiber microelectrodes.....	6
1.3 Alternative Insulations for Electrode Materials.....	7
1.4 Insulations for Metal Electrodes.....	8
1.5 Carbon Nanotubes.....	9
1.5.1 Carbon Nanotubes Introduction.....	9
1.5.2. Carbon Nanotube Based Electrochemical Sensors.....	10
1.5.3. Carbon Nanotube Based Detection of Dopamine.....	11
1.5.4. Dip Coating CNTs onto Carbon Fibers for Neurotransmitter Detection.....	12
1.5.5. Effect of Functional Groups on the Sensitivity of CNT modified CFMEs.....	14
1.5.6. Nafion-CNT Coatings on Carbon Fibers.....	15
1.5.7: Vertically Aligned CNT Forests grown on CFMEs.....	17
1.5.8: Wet Spinning Carbon Nanotube Fibers.....	18
1.5.9.: Electrospinning of CNT Fibers.....	20
1.5.10: Carbon Nanotube-Polymer Composite Fiber Sensors.....	21
1.5.11: Carbon Nanotube Fiber Microelectrodes.....	22
1.5.12: Wet spinning of Poly(ethyleneimine) (PEI)-CNT Fibers.....	23

1.5.13: Carbon Nanotube Fibers for Neurotransmitter Detection.....	25
1.5.14: Carbon Nanotube Yarn Electrodes.....	28
1.5.15: Acid Wet-Spun Carbon Nanotube Fibers.....	30
1.5.16: Growth of Vertically Aligned CNTs using Chemical Vapor Deposition.....	34
1.6: Carbon Nanofiber Electrode Array Development .....	35
1.7: Overview.....	37
Chapter 2: Epoxy insulated carbon fiber and carbon nanotube fiber Microelectrodes.....	47
2.1: Abstract.....	48
2.2: Introduction.....	49
2.3: Methods and Materials.....	51
2.3.1 Chemicals and Materials.....	51
2.3.2 Instrumentation.....	52
2.3.3. Electrode Construction.....	53
2.3.4. Animals.....	54
2.4 Results.....	54
2.4.1. Electrode Construction.....	55
2.4.2.: Comparison of epoxy, glass, and polyimide capillary insulation....	56
2.4.3.: Epoxy-insulated electrode characterization.....	58
2.4.4: Optimization: Armstrong Epoxy vs. SU-8.....	60
2.4.5: Stability Experiment .....	62
2.4.6.: Stimulated Dopamine Release In vivo.....	63
2.4.7.: Carbon Nanotube (CNT)-Fiber Microelectrodes.....	65

2.5: <i>Conclusions</i> .....	67
Chapter 3: Polyethyleneimine Carbon Nanotube Fiber Electrodes For Enhanced Detection of Neurotransmitters.....	72
3.1: Abstract.....	73
3.2: Introduction.....	74
3.3: Methods and Materials.....	76
3.3.1 Chemicals and Materials.....	76
3.3.2 Instrumentation.....	77
3.3.3 Scanning electron microscopy.....	77
3.3.4 <i>Electrode Construction</i> .....	77
3.4 Results.....	79
3.4.1: Synthesis and Characterization of PEI-CNT Fibers.....	79
3.4.2.: Comparison of PVA-CNT and PEI-CNT Fiber Electrodes.....	81
3.4.3: Characterization of dopamine detection at PEI-CNT fiber microelectrodes.....	84
3.4.4.: Characterization of serotonin and 5-HIAA detection at PEI-CNT fiber microelectrodes .....	88
3.5: Conclusion.....	94
Chapter 4: High Temporal Resolution Measurements by Carbon Nanotube Fiber and Yarn Microelectrodes.....	98
4.1: Abstract.....	99
4.2: Introduction.....	100
4.3: Methods and Materials.....	102
4.3.1.: Chemicals and Materials.....	102
4.3.2.: Instrumentation.....	103

4.3.3.: Scanning Electron Microscopy.....	103
4.3.4: Carbon Nanotube Fiber and Yarn Microelectrode Preparation.....	104
4.4: Results.....	106
4.4.1: Synthesis of Carbon Nanotube Fibers and Yarns.....	106
4.4.2.: Surface Characterization.....	108
4.4.3.: Electrochemical Characterization.....	110
4.4.4.: Frequency Independent Response.....	115
4.5: Conclusion and Discussion.....	118
Chapter 5: Carbon Nanopetals Grown on Metal Wires for Dopamine Detection.....	124
5.1: Abstract.....	125
5.2: Introduction.....	126
5.3: Methods and Materials.....	128
5.3.1.: Chemicals and Materials.....	128
5.3.2.: Instrumentation.....	129
5.3.3: Plasma Enhanced Chemical Vapor Deposition.....	129
5.3.4.: Scanning Electron Microscopy.....	130
5.3.5.: Electrode Construction.....	130
5.4: Results.....	131
5.4.1.: Surface Characterization.....	131
5.4.2.: Background Charging Currents.....	133
5.4.3: Detection of Dopamine.....	135
5.4.4 Adsorption Studies.....	141
5.4.5 Stability Study.....	142

5.4.6. Effect of Growth Time.....	143
5.5: Discussion.....	145
5.6: Conclusion.....	149
Chapter 6: Conclusions and Future Directions.....	156
6.1.: Overview.....	157
6.2.: Comparison of Alternative Electrode Materials.....	158
6.2.1.: Synthesis and Characterization.....	158
6.2.2.: Sensitivity.....	159
6.2.3.: Electron Transfer.....	160
6.2.4.: Reversibility.....	161
6.2.5. Temporal Resolution.....	162
6.2.6.: Anti-fouling Properties.....	163
6.2.7.: Acid Spun CNT Fibers.....	164
6.3.: Future Directions.....	164
6.3.1.: <i>In vivo</i> Testing.....	164
6.3.2 Growth of Carbon Using Chemical Vapor Deposition.....	166
6.3.3.: Conclusions and Future of the Field.....	168

## Table of Figures

### Chapter 1

<b>Figure 1.1:</b> Waveform applied for fast scan cyclic voltammetry.....	5
<b>Figure 1.2:</b> Scanning electron micrograph (SEM) image of a glass capillary insulated CFME.....	6
<b>Figure 1.3:</b> Structure of single wall carbon nanotube (SWCNT).....	10
<b>Figure 1.4 :</b> Comparison between bare and CNT coated disk electrodes.....	13
<b>Figure 1.5 :</b> Current vs. time trace depicting 40 fold increase in sensitivity after dipping in CNT suspension to form CNT forest electrode.....	18
<b>Figure 1.6:</b> Schematic of wet spinning apparatus setup.....	20
<b>Figure 1.7:</b> SEM Of PANi-CNT fiber.....	22
<b>Figure 1.8 :</b> CNT fiber completely sealed by epoxy resin to form CNT-microelectrode.....	27
<b>Figure 1.9:</b> Mechanism of CNT fiber formation.....	32
<b>Figure 1.10:</b> SEM of aligned CNT-fiber spun with chlorosulfonic acid.....	34

### Chapter 2

<b>Figure 2.1:</b> Pictures of epoxy coated electrodes.....	56
<b>Figure 2.2:</b> Example FSCV data for different electrode insulations.....	58
<b>Figure 2.3:</b> Characterization of epoxy-insulated electrodes.....	59
<b>Figure 2.4:</b> Comparison of SU-8 vs. Armstrong C7 epoxy insulation.....	61
<b>Figure 2.5:</b> Stability Experiment.....	63
<b>Figure 2.6:</b> Dopamine detection <i>in vivo</i> at an epoxy-insulated microelectrode...	64
<b>Figure 2.7:</b> Epoxy-insulated CNT fiber microelectrode.....	67

### Chapter 3

<b>Figure 3.1:</b> SEM Image of PEI-CNT Fiber.....	81
--	----

<b>Figure 3.2:</b> Comparison of PEI-CNT and PVA-CNT fiber microelectrodes.....	83
<b>Figure 3.3:</b> Adsorption Studies.....	86
<b>Figure 3.4:</b> Stability and Switching Potential Studies.....	88
<b>Figure 3.5:</b> Serotonin Fouling.....	90
<b>Figure 3.6:</b> 5-HIAA Fouling.....	92
<b>Chapter 4</b>	
<b>Figure 4.1:</b> SEM Images of Carbon Nanotube Fibers and Yarn.....	110
<b>Figure 4.2:</b> Acid Spun-CNT Fiber Microelectrode Data.....	112
<b>Table 4.1:</b> Table of Electrochemical Data.....	114
<b>Figure 4.3:</b> Frequency Independent Response.....	116
<b>Figure 4.4:</b> High Temporal Resolution Measurements.....	118
<b>Chapter 5</b>	
<b>Figure 5.1:</b> Carbon nanopetal surfaces.....	132
<b>Figure 5.2:</b> Background Charging Currents.....	134
<b>Figure 5.3:</b> Detection of Dopamine.....	138
<b>Table 5.1:</b> Electrochemical Data.....	141
<b>Figure 5.4.:</b> Adsorption Studies.....	142
<b>Figure 5.5:</b> Stability Study.....	143
<b>Figure 5.6:</b> Effect of Growth Time.....	145
<b>Chapter 6</b>	
<b>Table 6.1:</b> Electrochemical Properties of alternative nanomaterial based electrodes.....	159

# Chapter 1: Introduction

---

## 1.1 Introduction

Dopamine is an important neurotransmitter which functions in reward, cognition, voluntary movement, addiction, and learning.<sup>1-5</sup> The detection of dopamine is important for studying diseases such as Parkinson's disease and depression.<sup>6</sup> Traditionally, glass insulated carbon-fiber microelectrodes (CFMEs) have been used to detect neurotransmitter concentrations such as dopamine in biological samples.<sup>7-11</sup> *In vivo* voltammetry has been instrumental for the detection of neurotransmitters and monitoring of neurotransmission in the brain especially in response to certain receptor agonist or antagonist drugs, which could allow us to understand more about human disease states such as Parkinson's disease.<sup>12-14</sup> This thesis seeks to explore novel methods of electrode fabrication for neurotransmitter detection. Novel microelectrodes are being explored due to their usage possible usage as chronic sensors<sup>15</sup>, increased sensitivity<sup>16</sup>, resistance to surface fouling<sup>17</sup>, and faster electron transfer kinetics with respect to carbon-fiber microelectrodes<sup>16</sup>. This thesis will examine novel methods of developing electrode materials. Both alternative insulations and alternative electrode materials will be examined (carbon nanotube fibers and metal wires). I will attempt to optimize superior electrode technology through novel methods of construction.

First and foremost, an epoxy insulation will be chosen to replace the glass capillary insulation. Glass has been used for over twenty years, however, it has certain drawbacks such as it breaking *in vivo*, which is why it cannot be used for

testing in higher order primates or for long-term chronic measurements. Carbon nanotube fibers have been epoxy insulated to create carbon nanotube fiber microelectrodes through this novel electrode development procedure.

Polyethyleneimine (PEI) carbon nanotube fiber microelectrodes have been created using the epoxy insulation. They have displayed superior characteristics to PVA carbon nanotube fiber microelectrodes such as higher sensitivities, faster electron transfer kinetics, and a resistance to surface fouling by serotonin and 5-HIAA. The same epoxy insulation was used to form acid-spun carbon carbon nanotube fiber microelectrodes. CNTs were dissolved in chlorosulfonic acid without the use of sonication, surfactants, or polymer coatings that would serve as impurities. They are then syringed into water or acetone, which displaced the acid to form vertically aligned CNT fibers. Along with PEI CNT fibers and CNT-yarns, they have displayed a sensitivity towards dopamine that is independent of the wave application frequency. This could be useful in detecting dopamine at frequencies at which neurotransmission actually occurs. Lastly, I will also study carbon nanopetals grown onto metal wire electrodes for the detection of neurotransmitters. The idea of this study is to coat a substrate with carbon nanotubes that is more conductive than the carbon fiber to not slow down electron transfer. This method has been used to form a wide variety of metal electrodes. The carbon coating method creates novel electrode materials out of metals that were previously unable to detect dopamine before carbon coating.

## 1.2 Electrochemistry/Electrode Fabrication

### 1.2.1 Fast-scan cyclic voltammetry for neurotransmitter detection *in vivo*.

Fast scan cyclic voltammetry (FSCV) is an electroanalytical technique that can be used to measure neurotransmitter concentrations *in vivo*.<sup>18</sup> A carbon fiber (typically 7  $\mu\text{m}$  in diameter) is used as the working electrode, while the reference electrode is often an Ag/AgCl wire (.197 V). A commonly used waveform for dopamine detection ramps the voltage linearly from the holding potential (-0.4 V) to the switching potential (1.3 V) and back at a scan rate of 400 V/sec to oxidize and, subsequently, reduce the analyte (Figure 1.1a). The background charging current (Figure 1.1b) is a function of the scan rate and electroactive surface area of the electrode. Background subtraction reveals the cyclic voltammogram (CV) of the analyte being detected. In Fig. 1.1b, the black line is subtracted from the red line to give the background subtracted CV (Figure 1.1c) for dopamine. Dopamine is oxidized to dopamine-o-quinone (DOQ) and DOQ is reduced back to dopamine<sup>19</sup>. The shape and position of the cyclic voltammogram is a molecular fingerprint for the specific molecule being detected. FSCV has been used for the detection of neurotransmitters in *Drosophila melanogaster*<sup>20</sup>, rats<sup>21</sup>, brain slices<sup>22</sup>, and primates such as monkeys<sup>23</sup> and humans<sup>24</sup>. The interaction of dopamine with the surface of the carbon fiber is adsorption controlled partly because its amine group is positively charged (protonated) at physiological pH<sup>19</sup>. It undergoes an electrostatic interaction with the negatively charged oxides at the surface of the carbon fiber in addition to

hydrogen bonding and dipole-dipole interactions<sup>25</sup>. Current is directly proportional to both concentration and scan rate for adsorption controlled processes.

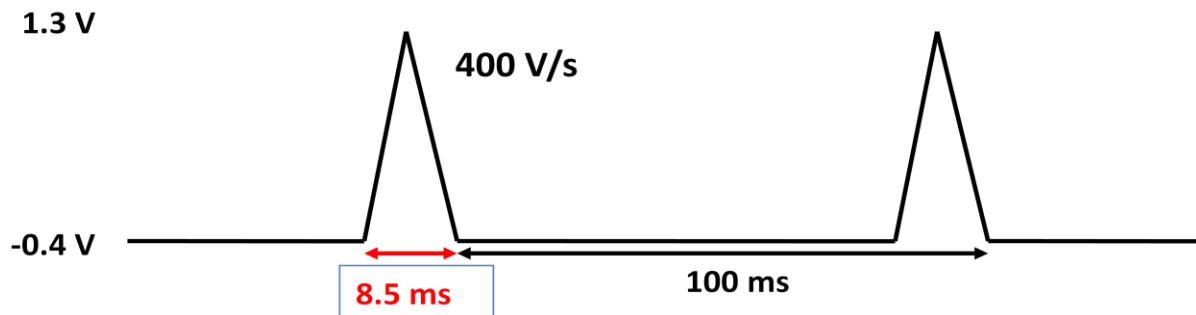
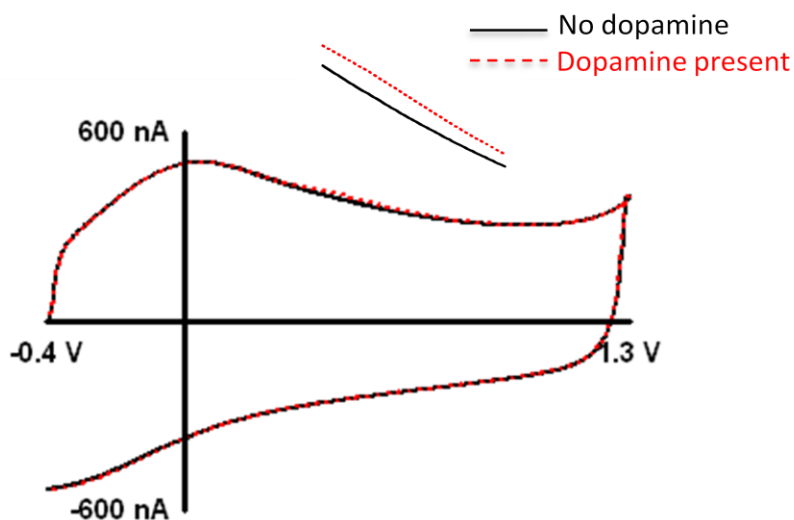
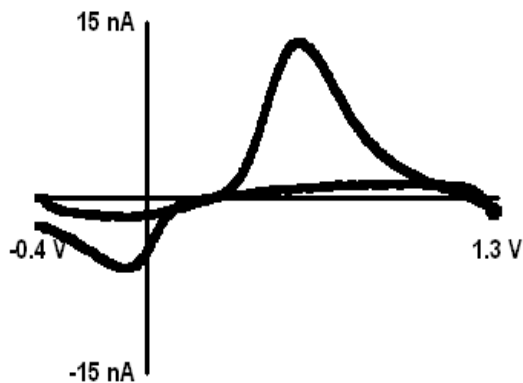


**Figure 1.1 A:** Waveform applied for fast scan cyclic voltammetry



**B:** Background capacitive charging current of a CFME using FSCV. The background is subtracted from the signal (the red from the black lines) to form the cyclic voltammogram.



**C:** Cyclic Voltammogram for Dopamine

### 1.2.2 Glass insulated carbon-fiber microelectrodes

Carbon-fiber microelectrodes have been utilized for the detection of neurotransmitters *in vivo*.<sup>8</sup> The electrodes are traditionally insulated in glass capillary tubes pulled to a fine taper using a vertical capillary puller.<sup>12,26-29</sup> The carbon fiber protrudes through the tapered end of the glass capillary and is usually cut to 50-100 microns as shown in Figure 1.2. The electrode is then backfilled with potassium chloride to create an electrical connection. Although glass insulations have been used for over twenty years and are the standard for neurochemical detection, they have certain drawbacks. First, alternative nanomaterials such as carbon nanotube fibers cannot be insulated with glass capillary insulation.<sup>30</sup> Vertical capillary pullers cannot be used with carbon nanotube fibers/yarns because of the altered tensile strengths and thicknesses. Second, glass insulations are currently not allowed for *in vivo* testing of non-human primates such as monkeys because of possible shattering or breakage in tissue.<sup>23</sup> The epoxy insulation described in Chapter 2 provides alternative insulation to glass that does not require the use of a vertical capillary puller.<sup>31</sup>

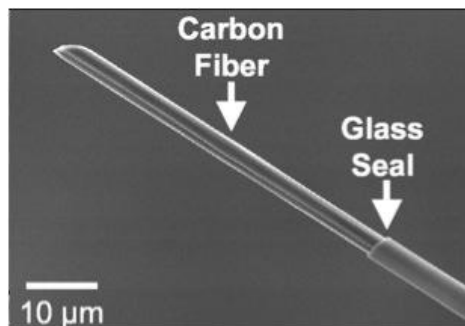


**Figure 1.2:** Scanning electron micrograph (SEM) image of a glass capillary insulated CFME.

### ***1.3 Alternative Insulations for Electrode Materials***

Novel electrode construction techniques have been examined for many years. The Baker group has studied the pyrolysis of parylene C to coat conical quartz electrodes to create electrodes with high thermal stabilities.<sup>32</sup> The chemical vapor deposition and subsequent pyrolysis of parylene C created a very conductive substrate that can be used for electrochemical detection. The subsequent vapor deposition of parylene provides the insulation, while masking in polydimethylsiloxane (PDMS) during vapor deposition preserves the electroactive region. Another quartz electrode involves the pyrolysis of methane inside of pulled quartz capillaries.<sup>33</sup> The resulting pyrolytic carbon forms a film on the inside of the capillary resulting in microring geometry. These electrodes can detect 1  $\mu$ M dopamine.

In the past, many alternative insulations have been examined in addition to glass insulations for carbon-fiber microelectrodes<sup>34</sup>. Poly(oxyphenylene) and a copolymer of 2-allylphenol and phenol were electropolymerized onto the surface of the carbon fiber upon applying a positive potential.<sup>34,35</sup> The polymers provided a thin insulation on the carbon fiber; however, the fibers must be masked using a compound such as paraffin wax in order to preserve the electroactive area of the electrode (the non-insulated region). The removal of the masking agent in addition to the lack of robustness of the thin and flimsy (nm thick) insulation provides many experimental challenges. Varying polymer concentrations, times of electrodeposition, and pH provide insulations of variable thicknesses that are not easily reproducible.

Another insulation for carbon-fiber microelectrodes involve the anodic electrophoretic deposition of paint onto the surface of carbon fiber to serve as the insulator.<sup>36,37</sup> The anodic paint consists of an aqueous dispersion of poly(acrylic carboxylic acid), Glassphor ZQ 84-3211, and resins of micellar structure. The negatively charged water soluble portion of the polymer has carboxylate end groups that are neutralized by acidification that leads to the precipitation of micelles. These negatively charged micelles are electrophoretically attracted to the anode. Water hydrolysis produces protons that precipitate the micelles as a thin, uniform, and tightly adhered polymer film on the electrode surface. Compared to the electrodeposition of polymers containing phenolic compounds, the insulation of carbon fibers by anodic electrophoretic deposition is much simpler, has a shorter processing time, and is less toxic.

#### ***1.4 Insulations for Metal Electrodes***

The use of epoxy insulations for electrodes has been examined by the Wightman group where conical epoxyite insulated Tungsten wire tips were used as substrates for the preparation of platinum and gold ultramicroelectrodes (UMEs).<sup>38</sup> Gold and platinum were electroplated onto the surface of the tungsten, then coated with a photoresist followed by pyrolysis. Epoxyite epoxy was used to coat the entire electrode except for the tip, which provided an exposed carbon surface able to perform voltammetric measurements. These novel UMEs had similar electrochemical behavior to electrodes made from wires or carbon fibers insulated with glass capillaries<sup>38</sup>. Selimovic et al created a new method to form epoxy embedded macro-electrodes to integrate electrochemical detection with

microchip-based analysis systems.<sup>39</sup> The use of a teflon mold was ideal because of its non-stick properties, which allows for the curing of epoxy onto the surface of electrodes, and their subsequent removal from the mold.

Chapter 2 will discuss the development of a novel epoxy insulation for carbon fiber and carbon nanotube fiber microelectrodes. The use of a non-stick teflon mold will be used as a substrate to coat the electrode materials. Silver epoxy will be used to connect one protruding end to a gold pin that fits into the head stage of the potentiostat to form an electrode. This novel electrode development facilitated rapid testing of novel electrode materials including carbon nanotube fiber electrodes and metal electrodes coated in carbonaceous materials.

## ***1.5 Carbon Nanotubes***

### ***1.5.1 Carbon Nanotubes Introduction***

Iijima discovered carbon nanotubes in 1991.<sup>40</sup> The novel carbon nanotubes were produced in a similar fashion to C<sub>60</sub> and other fullerenes. Iijima utilized arc discharge synthesis where needles grew at the negative end of the electrode used for discharge. The carbon-atom hexagons were arranged in a helical fashion about the needle axis in diameters ranging from 4-30 nm and up to 1 mm in length. The nanotubes resembled layers of graphite sheets rolled up with respect to the needle axis. Iijima and co-workers analyzed electron diffraction patterns of the newly created carbon nanotubes to verify their hexagonal orientation and highly sp<sup>2</sup> hybridized chemical structure. This highly sp<sup>2</sup> hybridized structure gives the nanotubes superior mechanical properties and

very high conductivity with respect to other carbon-based materials. Iijima and co-workers further characterized carbon nanotubes by discovering single wall carbon nanotubes (SWCNTs) (see Figure 1.3) that form in the gas phase as opposed to the MWCNTs that grow on the carbon cathode during carbon arc synthesis.<sup>41</sup> The authors used iron as a homogeneous catalyst in the vapor phase that assisted in the formation of single shelled tubules. The mirror symmetry in diffraction patterns confirmed the presence of single shelled tubules. CNTs have thermal stability up to 1400°C in a vacuum oven and gas adsorption properties such as to hydrogen, and electrical superconductivity<sup>42</sup>.

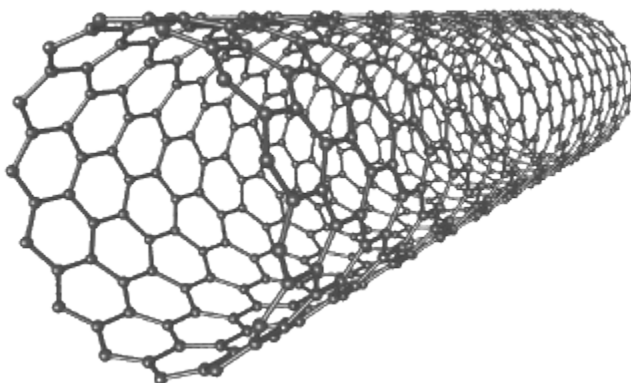


**Figure 1.3:** Structure of single wall carbon nanotube (SWCNT).

### ***1.5.2 Carbon Nanotube Based Electrochemical Sensors***

Carbon nanotube based electrodes have been used for the detection of neurotransmitters.<sup>16</sup> The high conductivity of CNTs makes them attractive as electrode sensing materials.<sup>43</sup> CNT electrodes have been utilized as detectors for neurotransmitters/ neurochemicals<sup>44</sup>, proteins<sup>45</sup>, DNA<sup>46</sup>, and as enzyme sensors<sup>47</sup>. CNT electrodes can detect proteins through direct and indirect

electrochemistry, chemical reactions, and through the gating of FET (Field emission transistors)<sup>45</sup>. Wang's group designed a novel CNT-based electrode for direct amperometric and voltammetric determination of insulin.<sup>48</sup> Other proteins detected were streptavidin and albumin<sup>49</sup>. CNT based electrodes have also been used as enzyme sensors to detect sugars such as glucose and galactose<sup>50-53</sup> in addition to other biological compounds such as cholesterol<sup>54</sup> and DNA.<sup>55,56</sup> The addition of CNTs to enzyme sensors further facilitates the tunneling of electrons through the delocalization of electrons due to  $sp^2$  hybridization. They also have electrocatalytic effects for hydrogen peroxide or glucose detection on their edge plane sites<sup>57</sup>.

### ***1.5.3 Carbon-Nanotube Based Detection of Dopamine***

Britto et al developed the first carbon nanotube paste electrode for the detection of dopamine using voltammetry.<sup>58</sup> MWCNTs were blended with a binder such as bromoform to create a CNT paste. The paste was packed into a glass capillary to form a carbon nanotube paste electrode. Cyclic voltammetry (CV) and differential pulse voltammetry (DPV) were both used to study the oxidation of dopamine. As opposed to other carbon based electrodes, a perfect/ideal Nernstian reversibility ( $\sim 30$  mV) peak separation was seen for CNT paste electrodes, which was not expected from carbon based electrodes most likely due to the higher conductivity of the carbon nanotubes. Furthermore, no decrease in sensitivity was seen when the electrode was implanted into goat brain tissue. Further work from the same group saw improved charged transfer at

carbon nanotube electrodes for the electrocatalytic reduction of dissolved oxygen, which is important for fuel cells.<sup>59</sup>

#### ***1.5.4 Dip Coating CNTs onto Carbon Fibers for Neurotransmitter Detection***

The Venton group has developed several strategies for making carbon nanotube modified electrodes for neurotransmitter detection<sup>16,30</sup>. Carbon nanotubes increase sensitivity and have faster electron transfer kinetics. Dip-coating a carbon fiber microelectrode in a suspension of carbon nanotubes in an organic solvent such as dimethylformamide (DMF) results in a more sensitive electrode.<sup>60</sup> However, this dip-coating procedure is not reproducible and decreases signal to noise ratios (S/N).<sup>60</sup> Venton and Swamy saw 2-6 fold increases in sensitivity in dopamine and serotonin detection using fast scan cyclic voltammetry with respect to disk electrodes without sacrificing temporal resolution as other pre-treatments have been known to do (Figure 1.4)<sup>60</sup>. The increase in sensitivity was likely a result of the increase in the number of adsorption sites because of the increase in the surface area by carbon nanotube modifications. The carbon nanotubes also increased electron transfer kinetics at relatively lower switching potentials and slower scan rates, which did not result in the over-oxidation of the surface of the carbon fiber.

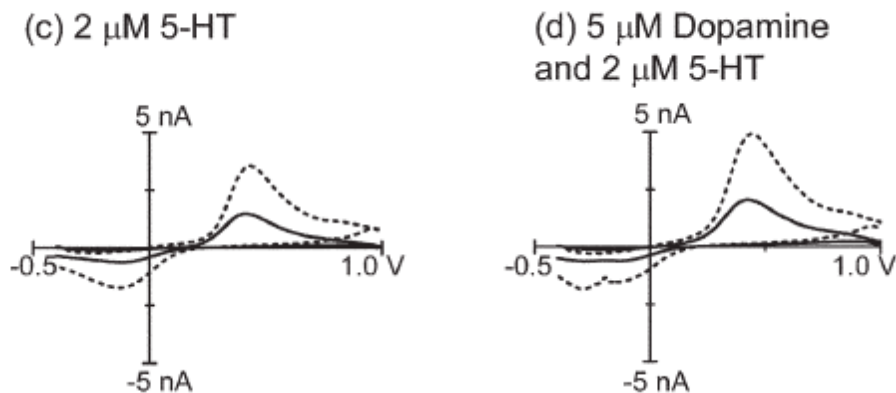


**Figure 1.4** : Comparison between bare (solid line) and CNT coated (dashed line) disk electrodes. C) Background subtracted CVs for 2  $\mu\text{M}$  serotonin. D) Background subtracted CVs for 2  $\mu\text{M}$  serotonin and 5  $\mu\text{M}$  dopamine.<sup>60</sup> Reprinted from Reference 60.

The carbon nanotube coatings also aided in co-detecting serotonin and dopamine<sup>60</sup>. These two neurotransmitters both oxidize at 600 mV, and their reduction potentials differ by approximately only 200 mV with FSCV<sup>60</sup>. A special waveform applied for serotonin detection that reduces fouling does not present the reduction peak of dopamine, which makes it difficult to co-detect both molecules. Serotonin produces hydroxylated dimers and oxidation products that irreversibly adsorb to the surface of the carbon fiber, which block sites for further adsorption<sup>60</sup>. Disk carbon fiber electrodes lost approximately 40% of their sensitivity over time, while carbon nanotube modified carbon fiber microelectrodes (CFMEs) lost less than 10% of their signal. Oxidative by-products of serotonin do adsorb to the CNT surface, but do not inhibit electron transfer. This means that the surface is not as easily passivated after CNT dip coating<sup>60</sup>.

The mechanism of the resistance to fouling to CNT materials is not completely understood. It has been shown that the extent of fouling is dependent on applied waveform; however, not all CNT materials are anti-fouling, as shown by the Macpherson group<sup>61</sup>. Studies of thin carbon films have found that adding oxide groups while maintaining a high  $sp^2$  conjugation also helps with resistance to serotonin fouling<sup>62</sup>. PVA-CNT fiber microelectrodes were also resistant to fouling by large concentrations of dopamine and CNTs were found to resist the first phase of fouling, the growth of the insulating layer from the polymerization products<sup>63</sup>. Resistance to fouling at CNT ends is often attributed to the higher density of edge plane sites that are more prevalent in CNT materials. Indeed, some studies of edge-plane pyrolytic graphite electrodes have found that they have similar anti-fouling properties to CNT based electrodes<sup>64</sup>. In chapter 3, the anti-fouling properties of PEI-CNT fiber microelectrodes will also be discussed. PEI-CNT fiber microelectrodes were found to be anti-fouling with respect to physiological concentrations of both serotonin and 5-hydroxyindoleacetic acid (5-HIAA).

#### ***1.5.5 Effect of Functional Groups on the Sensitivity of CNT modified CFMEs***

Jacobs et. al continued this work by dip coating carbon fiber microelectrodes with CNTs functionalized with carboxylic acid, amides, and octadecylamine.<sup>16</sup> Dip-coating CFMEs with carboxylic acid and amide functionalized CNTs increased sensitivity 2-6 fold, however, dip coating with octadecyl amine displayed no increase in sensitivity because of increased

electrostatic interactions between the positively charged (cationic) species such as dopamine and the negatively charged carboxylic groups. On the other hand, the positively charged octadecylamine repelled the positively charged dopamine. Similarly, the electron transfer kinetics were much faster for the amide and carboxylic CNT coatings rather the octadecyl amine CNT coatings. The long and bulky alkyl chain (18 Cs) was thought to sterically hinder electron transfer, therefore, significantly decreasing conductivity.

#### **1.5.6 Nafion-CNT Coatings on Carbon Fibers**

Nafion was also used to coat carbon-fiber microelectrodes along with CNTs<sup>65</sup>. Nafion is a cation exchange polymer with a negative charge that is used to attract cationic species and repel anionic species (ATP or ascorbic acid). Dip coating in CNT-Nafion suspensions increased sensitivity (peak oxidative current) 4-fold compared to bare electrodes and 2-fold compared to Nafion coated electrodes, and the electrodes were six times as sensitive to adenosine over ATP. This can be explained by the fact that ATP is a negatively charged molecule (from the triphosphate groups), which undergoes an electrostatic repulsion with respect to the negatively charged Nafion. On the other hand, the neutrally charged adenosine is not repulsed by the Nafion.

The aforementioned Nafion-CNT coatings have been thoroughly compared to overoxidized polypyrrole (oPPY)-CNT coatings.<sup>66</sup> Both types of electrodes were 3-4 fold more sensitive to dopamine than bare CFMEs without sacrificing temporal resolution or time response. Polypyrrole was electropolymerized and overoxidized onto the surface of the carbon fiber to form

oPPY-CNT coatings. OPPY-coatings had faster electron transfer kinetics, more sensitivity *in vivo* and maintained selectivity over anions. The reason for this is that Nafion is known to wrap nanotubes, which makes it electrostatically repel anions from the CNTs in the Nafion-CNT coating.

However, the deposition of Nafion onto the surface of CFMEs is not only achieved by dip-coating. Hashemi et. al electrodeposited Nafion onto the surface of CFMEs<sup>67</sup>. Nafion was electrodeposited onto the surface of CFMEs at a potential of 4.0 V. The author electrodeposited Nafion onto the surface of CFMEs, so that they would deposit a thin and uniform layer of Nafion. They did this primarily to electrostatically repel the metabolite interferant 5-hydroxyindole acetic acid (5-HIAA) from the surface of CFMEs during the *in vivo* detection of serotonin. 5-HIAA is a breakdown product of serotonin that has physiological concentrations ten-times greater than that of serotonin. 5-HIAA is repelled by the Nafion because it is negatively charged, while serotonin is not. However, the electrodeposition of Nafion on the surface makes electrodes highly absorptive, which can delay time responses *in vivo*.

The Andrews group also compared the anti-fouling properties of Nafion in comparison to base-hydrolyzed cellulose acetate (BCA) and fibronectin<sup>68</sup>. CFMEs immersed in brain tissue were tested with the three coatings. BCA was found to be relatively fouling resistant. Fibronectin coatings were fouled significantly exhibiting moderate losses in sensitivity. On the other hand, Nafion coatings (without CNTs) increased sensitivity for both dopamine and norepinephrine, but not for serotonin. Substantial fouling occurred in CFMEs that

were both electrodeposited and dip-coated with Nafion, comparable to bare CFMEs. Thus, this supports the hypothesis that CNTs could play a role in the anti-fouling process.

### ***1.5.7 Vertically Aligned CNT Forests grown on CFMEs***

Methods have been developed to grow vertically aligned CNT forests on the surface of a carbon fiber using a chemical self-assembly method<sup>69</sup>. Evenly dip coating CNTs onto a carbon fiber is difficult because a dense and uniform layer of CNTs is hard to deposit on the electrode surface. Usually, large CNT aggregates are formed, which creates low reproducibility and much noise. In this study, carbon fibers were coated first in an iron-hydroxide decorated Nafion film and then in a suspension of short carboxylic acid functionalized CNTs suspended in dimethylformamide (DMF). A polished disk carbon-fiber microelectrode was used to have an even and uniform surface for CNT forest self-assembly. The self-assembly method caused the CNTs to stand on the ends, which is efficacious because the ends of CNTs are likely to be the best sites for electron transfer.<sup>69</sup>

The authors saw a remarkable 30 – 40 fold increase sensitivity upon applying the self-assembled coating without such a marked increase in the background current. The CNT forest coated electrodes had the same sensitivity as disk uncoated carbon fibers at 10 Hz upon increasing the wave application frequency to 90 Hz which allowed the authors to scan at much higher frequencies without compromising sensitivity (see Figure 1.5). Six other analytes

increased in sensitivity at vertically aligned carbon nanotube electrodes. The electrode was also used to measure endogenous dopamine changes in the ventral nerve cord (VNC) of *Drosophila*. The SWCNT forest electrodes actually detected higher current for dopamine at 90 Hz than the bare electrodes could detect at 10 Hz.

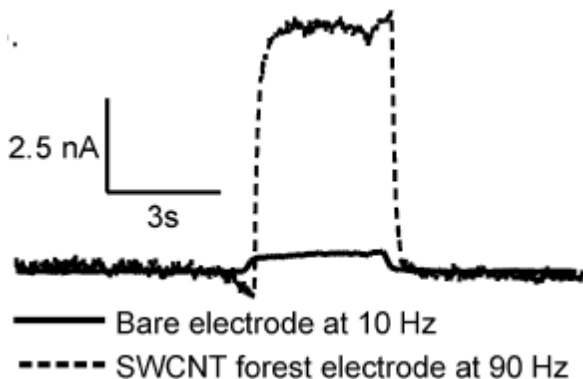


**Figure 1.5 :** Current vs. time trace depicting 40 fold increase in sensitivity after dipping in CNT suspension to form CNT forest electrode<sup>69</sup>. Reprinted from reference 69.

### 1.5.8 Wet Spinning Carbon Nanotube Fibers

In 2000, a group of French scientists made a breakthrough discovery with the development of carbon nanotube fibers.<sup>70</sup> Carbon nanotube fibers were thin (10 – 100 microns in diameter) and made of only carbon nanotubes. Carbon nanotubes were sonicated and separated in water using a tissue sonicator with the presence of the surfactant, sodiumdodecyl sulfate (SDS). SDS is negatively charged with a long hydrophobic carbon chain. Surfactant separated carbon nanotubes from bundling and aggregating. It adsorbed to the surface of the nanotubes, and the negative charge from the sulfate group produced an electrostatic repulsion of like charges that separated the nanotubes. SWCNT suspensions were then syringed into a 5% aqueous solution of poly(vinyl alcohol)

(PVA) that was rotated using a moving stage as shown in Figure 1.6. Diameters of the fibers could be altered with the use of different flow rates through the syringe and speed (revolutions per minute, rpms) of the rotating stage.

Amphiphilic properties of PVA allowed adsorption to the surface of the CNTs and, therefore, displaced the charged SDS surfactant. However, unlike SDS, the neutral PVA cannot provide efficient stabilization against the van der Waals attractive forces of the nanotubes, which causes them to attract and aggregate into ribbons in the aqueous solution. Repeatedly washing the ribbons in water, pulling them out of aqueous solution, and allowing them to dry washes away the excess polymer and surfactant, thus purifying the ribbons into carbon nanotube fibers.

The carbon nanotube fibers displayed outstanding physical and mechanical properties in comparison to traditional carbon fibers. The authors saw a Young's Modulus that was an order of magnitude greater than the modulus of high-quality bucky paper. The fibers also displayed conductivity with a resistivity of 0.1 ohm-cm. Interestingly, when the fibers were analyzed with scanning electron microscopy, the inner shell of the CNT-fiber cylinder was found to contain mainly SWCNTs, while the outer layer contained mostly non-conductive  $sp^3$  hybridized carbonaceous impurities. These carbon impurities were randomly dispersed in the initial ribbons, but moved to the outer edges of the carbon fiber due to capillary action and water evaporation from the original ribbons as they formed fibers. These impurities sparked the interest in further

purifying these fibers as will be discussed later on in the introduction of this thesis.

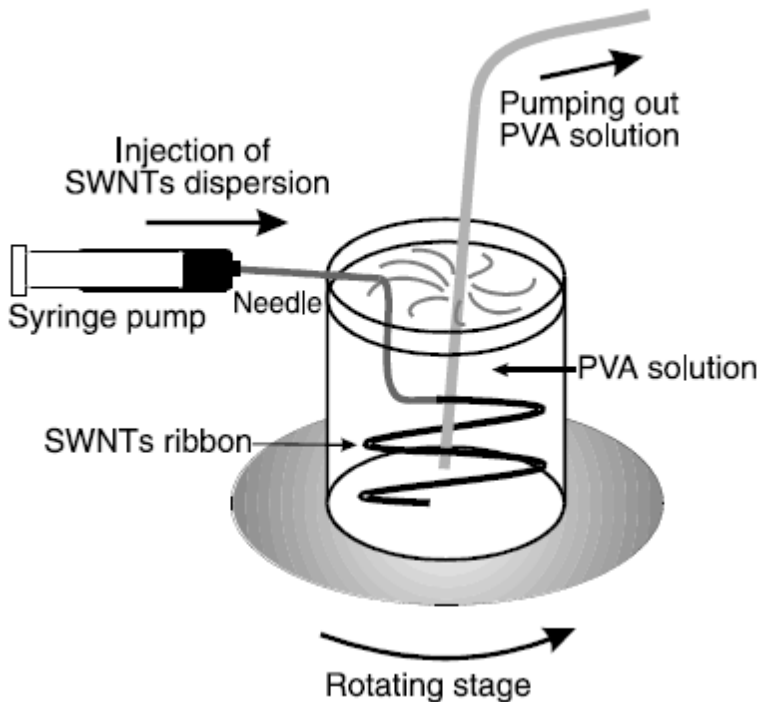


**Figure 1.6:** Schematic of wet spinning apparatus setup.<sup>70</sup> Reprinted from Reference 70.

### 1.5.9 Electrospinning of CNT Fibers

The process of electrospinning has also been used to develop carbon nanotube fibers and yarns.<sup>71,72</sup> Electrospinning involves the applying a high voltage to a liquid droplet that supercharges the liquid droplet. Electrostatic repulsion counteracts the surface tension, which subsequently stretches the droplet. Once the droplet is stretched passed a certain critical point, a stream of liquid is known to erupt from the surface, called a Taylor cone. Specific variables that can be varied in electrospinning are molecular weight of the polymer, viscosity of the solution, potential, distance between the capillary and the

collection screen, temperature, size of the target, and needle gauge. CNT fibers have been produced by co-electrospinning with polylactic acid (PLA) and polyacrylonitrile (PAN) with HiPCO (high pressure CO) CNTs. The spinning distance was 15 cm and the voltage 25 kV. The fibers were graphitized at 1100°C and then spun into yarns. Raman spectroscopy confirmed the presence of SWNTs in the PLA and PAN matrix. Unfortunately, AFM and TEM images of PAN and PLA nanofibrils display an agglomerated microstructure that accounts for a heterogeneous distribution of SWNTs. This is thought to be detrimental to the mechanical properties and conductivity of the polymer fibers. If clumps of SWNTs are spread randomly throughout the polymer fiber, then this casts doubt on the use of PAN/PLA-CNT fibers as possible electrode materials.

#### ***1.5.10 Carbon Nanotube-Polymer Composite Fiber Sensors***

CNTs have also been used for a wide variety of alternative chemical sensors. Recently, carbon nanotube/polyaniline (PANi) composite nanofibers have been synthesized via a simple polymerization mechanism to produce high-performance chemosensors as displayed in Figure 1.7.<sup>73</sup> SWCNTs were dispersed in 1.0 M HCl and then aniline plus an aniline dimer initiator were added to form the composite CNT/PANi nanofiber (~20 nm diameter). The conductivity of the nanofibers could be widely tuned based ( $10^{-4}$  to  $10^2$  S/cm) based on varying pH and SWCNT loadings. The great increase in conductivity of the composite fibers can be explained by CNTs interacting with polymer chains that lower the hopping length that exists in pure PANi nanofibers. Electron transfer occurs from the nanotubes to the LUMO of the conjugated polymer, which

increases charge carrier mobility. The highly conductive composite nanofibers detected  $\text{NH}_3$  vapor (100 ppb) much quicker than pristine PANi fibers by responding to a 20-fold increase in resistance (120 s vs. 1000 s) as shown by the I-V relationships from the four-probe measurement.

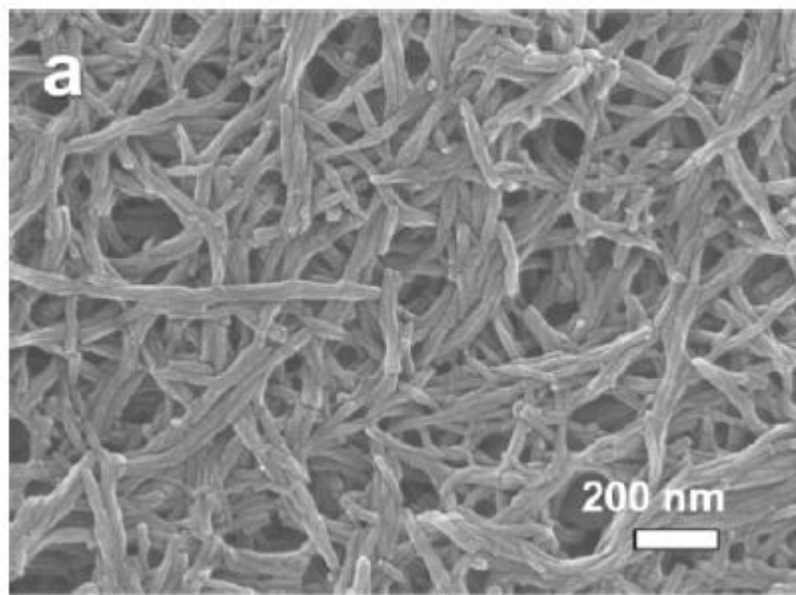


**Figure 1.7:** SEM Of PANi-CNT fiber.<sup>73</sup> Reprinted from Reference 73.

#### **1.5.11 Carbon Nanotube Fiber Microelectrodes**

Joseph Wang's research group was the first to use poly(vinyl alcohol) (PVA) wet-spun carbon nanotube fibers as microelectrodes.<sup>74</sup> The CNT fibers were heat treated at 300°C for sixty minutes and pushed into glass capillaries to form microelectrodes. Scanning electron microscopy (SEM) revealed that heat treated fibers fractured the skin of the fiber, which removed much of the non-conductive poly(vinyl alcohol) polymer and  $\text{sp}^3$  hybridized carbonaceous impurities, while also exposing internal nanofelt porous conducting bundles of nanotubes. Untreated fibers revealed a uniform porous structure, which mirrored the aligned surface of the CNT. Treated fibers were also found to be

more conductive because of their much larger background charging currents in cyclic voltammetry, which is a function of the much larger double layer capacitance. This conductivity is a result of the fact that thermally activated fibers have had their non-conductive carbonaceous and polymer purities removed and because of the highly catalytic ends of the nanotubes (as opposed to the sidewalls) are being exposed at the tips of the fibers. Heat treated carbon nanotube fibers yielded significantly higher current densities for 100  $\mu\text{M}$  dopamine and hydrogen peroxide than carbon fibers and untreated carbon nanotube fibers using hydrodynamic voltammetry. Likewise, chronoamperometric signals were much higher for dopamine and hydrogen peroxide for CNT fibers as opposed to carbon fibers. Hydrodynamic voltammetry measurements for NADH showed that treated CNT fiber electrodes yielded redox activity at potentials above 0.1 V, while redox activity is only observed above 0.6 V for both untreated CNT fibers and for carbon fiber microelectrodes. The electrocatalytic activity of CNT fibers facilitates the minimizing of NADH passivation and hence, surface fouling at these lower voltages.

#### ***1.5.12 Wet spinning of Poly(ethyleneimine) (PEI)-CNT Fibers***

An alternative method was used to wetspin carbon nanotube fibers in a very similar manner by substituting poly(vinyl alcohol) (PVA) with poly(ethyleneimine) (PEI)<sup>75</sup>. CNT fibers were spun into PEI (40% in MeOH, MW = 40,000) which was used as the coagulant. Three surfactants, cetyltrimethylammonium bromide (CTAB), lithium dodecyl sulfate (LDS), and sodium dodecylbenzenesulfonate (SDBS) were used to separate nanotubes. PEI

was found to intercalate into SWCNT bundles that increased conductivity, rigidity, and Young's Modulus. SEM images showed regions of polymer incorporation that were much less extensive than for PVA-formed CNT fibers. The conductivity of these fibers ( $100 - 200 \text{ S cm}^{-1}$ ) are 10 fold greater than SWCNTs made from the pulse laser vaporization (PLV) method, and 100 fold greater than the PVA wet spun CNT fibers. The reactive amine group on the PEI polymer interacted with the carbon nanotubes by physisorption to the walls of the nanotubes. The amine group donates a pair of electrons to the SWCNT sidewalls initiating an intermolecular charge transfer, which significantly increases the conductivity of the fiber. Electron dispersive spectroscopy (EDS) showed no presence of sulfur on the surface of the nanotube fibers, which may show that the surfactants (SDBS, LDS, etc.) could have been removed during the coagulation process. A new conductive fiber may prove to be very beneficial for the purpose of using these fibers for electrochemistry.

Our lab has developed a new method of constructing carbon nanotube fiber microelectrodes by epoxy insulating a CNT fiber and then silver epoxying it to a gold pin that fits into the headstage of the potentiostat.<sup>31</sup> Chapter 3 delves deeper into the use of polyethyleneimine carbon nanotube fiber microelectrodes for neurotransmitter detection. Previously, PEI-CNT fibers have not been used as electrode materials. The higher conductivity of the PEI-CNT fiber with respect to the PVA-CNT fiber makes these fibers suitable as electrodes for the detection of neurotransmitters using fast scan cyclic voltammetry. A comparison to PVA-CNT fiber microelectrodes, adsorption properties, stabilities *in vitro*, and a resistance

to serotonin and 5-hydroxyindole acetic acid (5-HIAA) fouling will be thoroughly examined with these novel PEI-CNT fiber microelectrodes.

### **1.5.13 Carbon Nanotube Fibers for Neurotransmitter Detection**

Carbon nanotube fibers have further been used to form microelectrodes for small molecule detection using electrochemistry.<sup>74</sup> It has been widely expected that carbon nanotube fibers could be used as neurotransmitter detectors *in vivo*. One of the problems of dopamine detection *in vivo* is that there is often the presence of anionic interferants such as ascorbic acid that are present in concentrations sometimes 100-1000 times higher than dopamine. Furthermore, ascorbic acid is oxidized at similar potentials as dopamine which causes overlapping signals to occur that can prevent the correct concentration estimate of dopamine.

Using differential pulse voltammetry (DPV), carbon nanotube fibers were compared to glassy carbon electrodes (GCEs) in the detection of both dopamine (DA) and ascorbic acid (AA).<sup>76</sup> At GCEs, dopamine oxidation shifted 80 mV with respect to carbon nanotube fibers but still could not distinguish between dopamine and ascorbic acid. However, current density increased by more than one magnitude at carbon nanotube fiber electrodes compared to GCEs. The amplitude of AA peaks was much lower than that of dopamine, even though it was present at a concentration 10-fold greater than that of dopamine. An electrostatic barrier at the surface of the carbon nanotube fiber could explain this phenomenon. Carbon nanotube fibers contain negatively charged oxide and carboxyl group that electrostatically interact with the positively charged

dopamine. However, the anionic AA is negatively charged and is electrostatically repelled by this negative charge, which inhibits adsorption and charge transfer to the negatively charged surface of the CNT fiber. Also, the aromatic group of dopamine undergoes favorable  $\pi$ - $\pi$  interactions with the  $sp^2$  hybridized CNTs, which further facilitates adsorption to the surface of the carbon nanotube fiber microelectrode. The higher porosity of the CNT fibers also provided further sites for analyte adsorption. When dopamine and ascorbic acid were present in equal amounts, the ascorbic acid signal was similar to that of the noise. When ascorbic acid was present at an order of magnitude greater than that of dopamine, the signal for dopamine is still significantly higher than that of ascorbic acid.

Viry et al further developed carbon nanotube fiber microelectrodes for the detection of NADH using cyclic voltammetry and to manufacture glucose biosensors.<sup>77,78</sup> The glucose sensor was formed by adsorbing a mediator onto the surface of the carbon nanotube fiber. Figure 1.8 shows the CNT fiber enclosed by epoxy resin to form a CNT-fiber microelectrode. At a potential of 0 volts, analytes were oxidized by applying a potential and via the dehydrogenase enzyme. The authors concentrated on several surface modifications for the CNT fibers to make them more sensitive, selective, and responsive to the analytes. They began this procedure by dipping CNT fibers in tetrahydrofuran (THF) and, subsequently, drying to deposit a layer of the insoluble organic molecule on the surface of the CNT fiber. The CNT fibers were hot stretched and pulled to 500% length in a hot flow of air, which produced a substantial increase of CNT alignment along the axis of the fiber. The authors hypothesize that analytes are

more likely to adsorb to a well-organized and aligned interface as produced by CNT fiber stretching, which aligns CNTs. The CNT fibers were then dipped into a solution of polyoxometalate ( $\text{H}_3\text{PMo}_{12}\text{O}_{40}$ ) (POM) in 0.5 M sulfuric acid to exfoliate graphite and carbon particles followed by dipping in a buffered solution of pH 8 to desorb the POMs from the surface. The background capacitive charging current increased three-fold, which indicates that the electroactive surface area increased substantially due to the increased porosity of the CNT fiber. The authors speculated that the POM layer created new holes in the CNT network via chemisorptions.

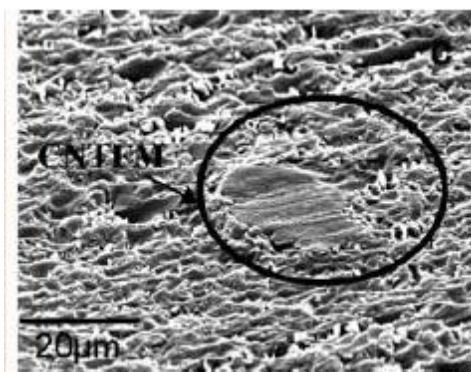


**Figure 1.8** : CNT fiber completely sealed by epoxy resin to form CNT-microelectrode.<sup>78</sup> Reprinted from Reference 78.

Ewing and Safina's research group utilized wet-spun PVA CNT fibers to prevent long-term dopamine fouling at the surface of an electrode<sup>63</sup>. Dopamine oxidation occurs by the way of a two electron transfer, which yields dopamine-ortho-quinone (DOQ). When the amine is protonated in the buffer, cyclization occurs forming leucodopaminechrome (LDC) that further forms dopaminechrome (DC) by undergoing another two-electron oxidation. A melanin polymer is formed from the free radical polymerization of dopaminechrome. Carbon nanotube fibers

resisted melanin polymer formation or surface fouling by way of their surface roughness, high electroactivity, fast response, and high chemical stability. The EDX spectra of CNT fibers show traces of nickel (catalyst remaining from CNT synthesis) and higher oxide concentrations with respect to carbon fibers, which explains their higher sensitivity towards dopamine as opposed to carbon fibers. For 100  $\mu\text{M}$  dopamine, the CNT fiber electrode displayed more stability against chemical fouling caused oxidation products of the analyte. After three hours of continuous oxidation, the current decreased by only 15% in CNT fibers, while it decreased by over 70% in carbon fibers.

#### ***1.5.14 Carbon Nanotube Yarn Electrodes***

The Sombers research group has recently developed carbon nanotube yarns as microelectrodes for neurotransmitter detection using FSCV. They grew MWCNT arrays on quartz substrates via the “chloride mediated chemical vapor deposition (CVD) method<sup>79</sup>.” They pulled out CNT ribbons from the array and then attached them to a spindle. The yarns were formed by drawing and then rotating the spindle (twist angle 20 degrees). The CNT yarns were then fabricated into disk microelectrodes using a polishing wheel. The yarn-electrodes displayed superior selectivity, sensitivity, and spatial resolution in comparison to traditional CFMEs<sup>80</sup>. CVs and background charging currents yielded faster electron transfer kinetics (reduced peak separation,  $\Delta E_p$ , for dopamine) and a greater mass transfer profile at the surface of the sensor, which increases sensitivity and substantially lowers the limit of detection in comparison to CFMEs. Signal enhancement (180%) is mainly due to the presence of oxygen

functionalized hydroxyl and carboxyl functionalities that electrostatically interact with the positively charged dopamine. A greater cathodic/anodic peak ratio of CNT yarns in comparison to CNTs was observed and could be a function of stronger reversibility of the oxidation to reduction reactions at the CNT surface. CNT yarns also could help resolve multiple analytes in complex mixtures. An extra peak was observed in the voltammogram of adenosine (~ 530 mV), which could help distinguish it from peroxide, histamine, and shifts in pH. The peak is most likely a result of adenosine polymerization onto the surface of the CNT yarn. The yarn electrode also better distinguished dopamine from ascorbic acid, serotonin, and DOPAC. CNT-yarn electrodes were further used to detect stimulated dopamine release in brain slices (striatum), which demonstrate their potential applicability as alternatives to traditional carbon fiber microelectrodes.

Carbon nanotube yarns can also be purchased from companies such as Nanocomp Technologies, Inc. and General Nano LLC. They use dry-spinning for the manufacturing of carbon nanotube yarns (CNTYs) as developed by the textile industry.<sup>30</sup> Aligned CNTs are synthesized in the furnace and then twisted to form a yarn. Our lab made carbon nanotube yarn electrodes (CNTYEs) by placing a CNTY in a polyimide coated fused silica capillary that was slipped into a pulled glass capillary that was back filled with 1 M potassium chloride and five minute epoxy was used to seal the polyimide-glass capillary interface. The electrodes were beveled at an angle perpendicular to the capillary. Background charging currents were found to be 4-fold larger for CNTYEs as opposed to disk CFMEs<sup>30</sup>. In addition to the increase in sensitivity of CNTYEs, dopamine was found to be

adsorption controlled to the surface of the CNT yarn as illustrated by concentration and scan rate experiments. As opposed to CFMEs, CNTYEs have an interesting property as their sensitivity for dopamine is independent of the wave application frequency. At lower frequencies, more time is spent at the negative holding potential, which electrostatically attracts the positively charged dopamine. This interesting property of CNTYEs was explained by the fact that rates of desorption of dopamine and dopamine-ortho-quinone (DOQ), the oxidation product, are equal to one another at CNTYEs. Higher desorption of DOQ would mean that surface coverage of DOQ decreases, which means that there is less dopamine adsorbed to the surface after reduction for CFMEs. Thus, CNTYEs could measure changes in neurotransmitters at a much faster timescale, closer to which neurotransmission actually occurs.

#### ***1.5.15 Acid Wet-Spun Carbon Nanotube Fibers***

Smalley et. al developed a novel method of creating carbon nanotube fibers without the use of polymers or surfactants.<sup>81</sup> They dispersed 8% of SWCNTs in 102 % sulfuric acid (including 2% excess sulfur trioxide). They produced the fibers in a custom-built apparatus used for mixing and extruded SWCNT fibers. The procedure was similar to wet-spinning though the coagulants that were used were diethyl ether, 5 wt% aqueous sulfuric acid, or water instead of the polymer coagulant. Furthermore, no surfactant or sonication was necessary to separate the carbon nanotubes from aggregating via van der Waals interactions. Fibers were dried in a vacuum followed by further annealing in a vacuum at 1100 °C. SEMs of the fibers displayed very high vertical alignment of

SWCNT ropes that are 20 to 30 nm. Raman ratio peaks of 20:1 (G:D peaks) also confirmed a highly ordered species. Mechanisms of vertical alignment lie in the swelling of the carbon nanotubes by sulfuric acid. Negatively charged anionic oxide groups from the sulfuric acid surround the individual nanotubes forming an energetically favorable charge transfer complex (see Figure 1.9).

Upon spinning into the coagulant, the anions are displaced by water, which collapses them into vertically aligned carbon nanotube fibers (~ 50 microns in diameter). This process is reversible because the nanotube fibers can be swollen again into CNT ropes upon subsequent suspension of the fibers into a solution of sulfuric acid. CNT fibers displayed mechanical strength and rigidity much superior to CNT fibers created from the traditional method of polymer wet spinning. The creation of a CNT fiber without the presence of sonication (that cuts nanotubes short and destroys conductivity), polymer, surfactant, and non-conductive carbonaceous impurities provides a potential method of developing highly conductive carbon nanotube fibers that could be used for the purpose of developing microelectrodes for the monitoring of neurotransmission.

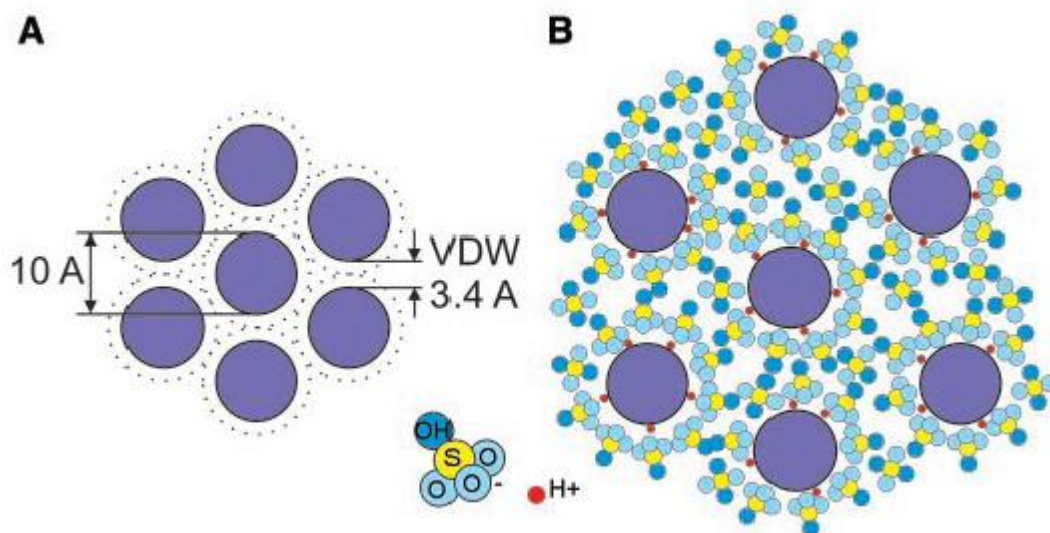


**Figure 1.9:** Mechanism of CNT fiber formation. A. SWNTs in van der waals contact. B. SWNT ropes after exposure to sulfuric acid. <sup>81</sup> Reprinted from Reference 81.

Pasquali et. al found that chlorosulfonic acid is the first “true solvent” for carbon nanotubes.<sup>82</sup> Therefore, carbon nanotubes could be dissolved in chlorosulfonic acid without having clumps of differently sized nanotubes suspended in solvents. Wet spinning was performed in the same manner as the before, with 2-6% of CNTs dissolved in chlorosulfonic acid spun into a coagulating bath of water or acetone to remove the acid using a spinning chamber in a custom built apparatus to collect fibers on a winding drum. The linear velocity of the drum was higher than the speed of the spinneret to produce high CNT alignment by constant stretching and tensioning of the filament. Four point probes were used to measure conductivity that greatly increased to 5 MS/m prior to iodine doping. Electrical conductivity was 10-fold greater than traditional undoped solid state fibers and 5-fold better than doped (with iodine) CNT fibers.

The fibers combined the great conductivity of metals with the specific strength of high performance carbon fibers.

The aim of this procedure was to fabricate CNTs that are longer and reduce the number of CNT ends in a fiber, producing greater strength and reducing CNT junctions, which, therefore, raise electrical (greater than steel, Ni, and Au) and thermal conductivity (30 fold higher than that of wet-spun fibers). They observed 5  $\mu\text{m}$  long CNT lengths as opposed to 0.5  $\mu\text{m}$ , which greatly enhanced conductivity. As before, the use of chlorosulfonic acid precludes the use of surfactants in the CNT dispersion and polymers to collapse the fibers into ribbons. SEM imaging displayed highly vertically aligned fibers composed of fibrils that were 10 to 100 nm in diameter (see Figure 1.10). Highly aligned fibril structures made the fibers ultraconductive due to increased CNT overlap. Decreased spacing between the highly aligned fibrils facilitated inter-CNT transport. Iodine doping of the fibers further increased conductivity (~5 to 10 fold) due to the increase in intra-CNT conductivity of the semiconducting CNTs and also increasing disorder, which helps relax the momentum conservation need for inter-CNT transport. The iodine fibers were so conductive and strong that they could support and conduct electricity to light a light-emitting diode lamp and also created a field-emitting device displaying metallic field emission<sup>82</sup>.

Chapter 4 will further examine chlorosulfonic acid spun CNT fibers as electrode materials for neurotransmitter detection using fast scan cyclic voltammetry. The use of acid spun CNT fibers is promising for a few reasons. First of all, the high conductivity of the CNT fibers makes it desirable as an

electrode material for voltammetry. Second, the CNT fiber formation precludes the use of polymers and surfactant that coat the CNT surface (such as poly(vinyl alcohol) and sodiumdodecyl sulfate) that coat the CNT surface, which decrease adsorption by blocking adsorption sites for biomolecules. Third, this method does not include the use of sonication to separate CNT bundles, which decreases CNT length and lowers conductivity. Finally, the use of the acid could oxidize the surface groups of the CNT fiber with negatively charged oxide groups that would make the electrode material electrostatically attract the cationic dopamine.

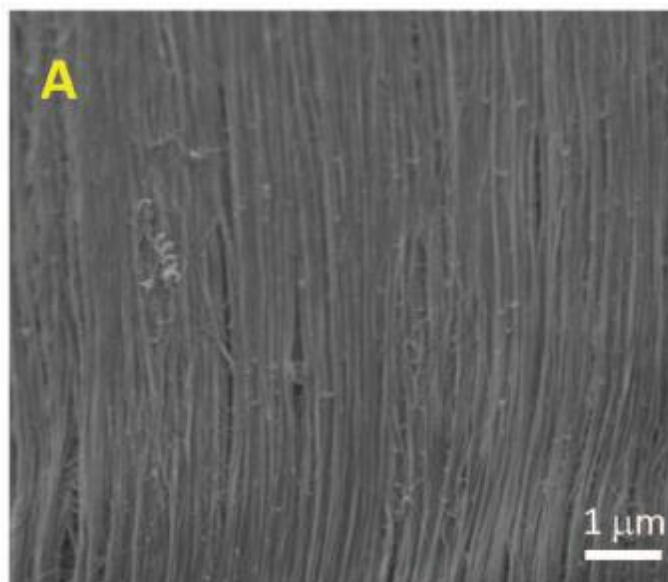


**Figure 1.10:** SEM of vertically aligned CNT fiber spun with chlorosulfonic acid.<sup>82</sup> Reprinted from Reference 82.

#### ***1.5.16 Growth of Vertically Aligned CNTs using Chemical Vapor Deposition***

The growth of carbon nanotube yarns using chemical vapor deposition could be potentially useful for neurotransmitter detection.<sup>79</sup> A novel method depicts a one step growth of aligned bulk carbon nanotubes by chloride mediated chemical vapor deposition. Using a quartz substrate, an iron chloride catalyst

was utilized along with acetylene to grow vertically aligned carbon nanotubes at 820°C at 10 Torr. Growth occurred over a time period of approximately 20 minutes to produce 2.1 mm length of vertically aligned CNTs. It was found that growth was highly dependent on both temperature and pressure. The vertically aligned CNTs were then spun into yarns. The mechanism of growth is that iron chloride reacts with acetylene to produce carbon-rich iron carbide ( $\text{FeC}_2$ ), and hydrogen chloride (HCl). Iron carbide then segregates into graphene layers, which initiates CNT growth in chloride mediated chemical vapor deposition (CM-CVD). Growth is triggered once bud-like CNT structures are formed. This one step CM-CVD growth of vertically aligned carbon nanotubes that can be spun into yarns is a promising method of producing CNT yarns that could be used as sensors.

The Meyyappan group has pioneered growing carbon nanotubes and nanofibers using plasma enhanced chemical vapor deposition (PECVD)<sup>83</sup>. PECVD differs from CVD in that includes a plasma source which arises from an alternating or direct current discharge between two electrodes. It is not currently known what the role of the plasma is in carbon growth or CNT growth is, but empirical evidence suggests that the electric field in the plasma enables vertically aligned CNTs or carbon than thermal CVD.<sup>84</sup>

### **1.6 Carbon Nanofiber Electrode Array Development using Plasma Enhanced Chemical Vapor Deposition**

Carbon nanofiber (CNF) arrays grown using plasma enhanced chemical vapor deposition have been developed by scientists at Oak Ridge National Laboratory for many electroanalytical measurements.<sup>85</sup> A thin layer of metal

catalyst was deposited onto a silicon wafer to begin the process. The fiber synthesis was performed using direct current-plasma enhanced chemical vapor deposition (PECVD) where the decomposition of acetylene on the nickel results in “tip-type” nanofibers. The CNF array was used as an electrode array where excitable cell matrices of both neuronal-like derived cell lines (PC-12) and primary cells (from the rat hippocampus) were cultured. The electrode arrays detected dopamine, norepinephrine, and 5-hydroxytyramide using linear sweep voltammetry, amperometry, and cyclic voltammetry over a 16-day period. The same group also used these vertically aligned carbon nanotube arrays for stimulation and extracellular recording of spontaneous and evoked neuroelectrical activity in organotypic hippocampal slice cultures<sup>86</sup> and as a neural chip that stimulated and monitored electrophysiological signals from brain tissue *in vivo*<sup>87</sup>.

Carbon nanofiber electrode arrays have also been used with fast scan cyclic voltammetry for neurotransmitter detection.<sup>88</sup> CNFs were prepared as arrays on silicon wafers as 3 x 3 electrode pads. Using plasma enhanced chemical vapor deposition (PECVD), vertically aligned CNFs were grown using ethylene feedstock and nickel catalysts at 700°C. Wireless Instantaneous Neurotransmitter Concentration Systems (WINCS) was used for the data analysis software to integrate FSCV and digital telemetry. Dopamine was detected in concentrations spanning from 500 nM to 2.5 μM. Dopamine detection was modeled and compared to CFME detection by taking into account measurements of the electroactive surface areas. CFMEs and CNTs were found

comparable in their response and sensitivity to dopamine detection, which illustrates the applicability of CNF arrays as electrodes to be used for neurochemical monitoring.

In chapter 5, the growth of edge plane graphene using plasma enhanced chemical vapor deposition onto metal wires will be discussed. This method of carbon growth is attractive for many reasons. First, it does not require the deposition of a metal catalyst onto the surface of the metal wire, which is tedious and often difficult to achieve. Second, it also has uniform surface coverage over the entire metal. This is important since we wish to create carbon coated metal electrodes that will be used for neurotransmitter detection using voltammetry. Metal is used as the substrate for its fast electron transfer kinetics, however, it must be coated with carbon since metal electrodes have a different overpotential for the oxidation of water that could interfere with the signal during voltammetry.

## **1.7 Overview**

This in depth literature review provided a broad overview of the alternative insulations and CNT-based microelectrodes that could be utilized for the monitoring of neurotransmitters. This thesis will examine several different methods of electrode development to produce alternative electrodes to the traditional glass capillary CFMEs including both alternative insulations and CNT fibers for electrode development.

Chapter 2 will examine alternative epoxy insulations that can be used to construct carbon fiber microelectrodes and carbon nanotube fiber electrodes without the use of glass or a vertical capillary puller. PEI (polyethyleneimine)-

CNT fiber microelectrodes are discussed in chapter 3 with special attention being paid to their sensitivity, electron transfer kinetics, and anti-fouling properties. Acid spun CNT-fiber microelectrodes will be examined in chapter 4 including their frequency independent properties in comparison CNT-yarn and PEI-CNT fiber electrodes. Chapter 5 will look at the growth of edge-plane graphene onto metal wires that can be used as electrodes for neurotransmitter detection. Finally, Chapter 6 will compare and contrast these different types of electrodes and look at future challenges in this field.

## Reference List

1. Vickrey, T. L.; Condrón, B.; Venton, B. J. Detection of Endogenous Dopamine Changes in *Drosophila melanogaster* Using Fast-Scan Cyclic Voltammetry. *Analytical Chemistry* **2009**, *81* (22), 9306-9313.
2. Watson, C. J.; Venton, B. J.; Kennedy, R. T. In vivo measurements of neurotransmitters by microdialysis sampling. *Anal. Chem.* **2006**, *78* (5), 1391-1399.
3. Wightman, R. M.; Amatore, C.; Engstrom, R. C.; Hale, P. D.; Kristensen, E. W.; Kuhr, W. G.; May, L. J. Real-time characterization of dopamine overflow and uptake in the rat striatum. *Neuroscience* **1988**, *25* (2), 513-523.
4. Wightman, R. M.; Zimmerman, J. B. Control of dopamine extracellular concentration in rat striatum by impulse flow and uptake. *Brain Res. Brain Res. Rev.* **1990**, *15* (2), 135-144.
5. Wightman, R. M.; Heien, M. L. A. V.; Wassum, K. M.; Sombers, L. A.; Aragona, B. J.; Khan, A. S.; Ariansen, J. L.; Cheer, J. F.; Phillips, P. E. M.; Carelli, R. M. Dopamine release is heterogeneous within microenvironments of the rat nucleus accumbens. *European Journal of Neuroscience* **2007**, *26* (7), 2046-2054.
6. Laurelle, M. Increased dopamine transmission in schizophrenia. *Nordic Journal of Psychiatry* **2001**, *55* (2), 82.
7. Cechova, S.; Venton, B. J. Transient adenosine efflux in the rat caudate-putamen. *J. Neurochem.* **2008**, *105* (4), 1253-1263.
8. Huffman, M. L.; Venton, B. J. Carbon-fiber microelectrodes for in vivo applications. *Analyst* **2009**, *134* (1), 18-24.
9. Huffman, M. L.; Venton, B. J. Electrochemical Properties of Different Carbon-Fiber Microelectrodes Using Fast-Scan Cyclic Voltammetry. *Electroanalysis* **2008**, *20* (22), 2422-2428.
10. Venton, B. J.; Wightman, R. M. Pharmacologically induced, subsecond dopamine transients in the caudate-putamen of the anesthetized rat. *Synapse* **2007**, *61* (1), 37-39.
11. Venton, B. J.; Zhang, H.; Garris, P. A.; Phillips, P. E. M.; Sulzer, D.; Wightman, R. M. Real-time decoding of dopamine concentration changes in the caudate-putamen during tonic and phasic firing. *J. Neurochem.* **2003**, *87* (5), 1284-1295.
12. Baur, J. E.; Kristensen, E. W.; May, L. J.; Wiedemann, D. J.; Wightman, R. M. Fast-scan voltammetry of biogenic amines. *Anal. Chem.* **1988**, *60* (13), 1268-1272.

13. Heien, M. L.; Khan, A. S.; Ariansen, J. L.; Cheer, J. F.; Phillips, P. E.; Wassum, K. M.; Wightman, R. M. Real-time measurement of dopamine fluctuations after cocaine in the brain of behaving rats. *Proc. Natl. Acad. Sci. U. S. A* **2005**, *102* (29), 10023-10028.
14. Garris, P. A.; Wightman, R. M. In vivo voltammetric measurement of evoked extracellular dopamine in the rat basolateral amygdaloid nucleus. *J. Physiol* **1994**, *478* (Pt 2), 239-249.
15. Clark, J. J.; Sandberg, S. G.; Wanat, M. J.; Gan, J. O.; Horne, E. A.; Hart, A. S.; Akers, C. A.; Parker, J. G.; Willuhn, I.; Martinez, V.; Evans, S. B.; Stella, N.; Phillips, P. E. Chronic microsensors for longitudinal, subsecond dopamine detection in behaving animals. *Nat. Methods* **2010**, *7* (2), 126-129.
16. Jacobs, C. B.; Vickrey, T. L.; Venton, B. J. Functional groups modulate the sensitivity and electron transfer kinetics of neurochemicals at carbon nanotube modified microelectrodes. *Analyst* **2011**.
17. Swamy, B. E.; Venton, B. J. Carbon nanotube-modified microelectrodes for simultaneous detection of dopamine and serotonin in vivo. *Analyst* **2007**, *132* (9), 876-884.
18. Zachek, M. K.; Takmakov, P.; Park, J.; Wightman, R. M.; McCarty, G. S. Simultaneous monitoring of dopamine concentration at spatially different brain locations in vivo. *Biosensors & Bioelectronics* **2010**, *25* (5), 1179-1185.
19. Bath, B. D.; Michael, D. J.; Trafton, B. J.; Joseph, J. D.; Runnels, P. L.; Wightman, R. M. Subsecond adsorption and desorption of dopamine at carbon-fiber microelectrodes. *Anal. Chem.* **2000**, *72* (24), 5994-6002.
20. Heien, M. L. A. V.; Phillips, P. E. M.; Stuber, G. D.; Seipel, A. T.; Wightman, R. M. Overoxidation of carbon-fiber microelectrodes enhances dopamine adsorption and increases sensitivity. *Analyst* **2003**, *128*, 1413-1419.
21. Borue, X.; Cooper, S.; Hirsh, J.; Condrón, B.; Venton, B. J. Quantitative evaluation of serotonin release and clearance in *Drosophila*. *J. Neurosci. Methods* **2009**, *179* (2), 300-308.
22. Venton, B. J.; Wightman, R. M. Pharmacologically induced, subsecond dopamine transients in the caudate-putamen of the anesthetized rat. *Synapse* **2007**, *61* (1), 37-39.
23. Pajski, M. L.; Venton, B. J. Adenosine Release Evoked by Short Electrical Stimulations in Striatal Brain Slices Is Primarily Activity Dependent. *ACS Chemical Neuroscience* **2010**, *1* (12), 775-787.
24. Earl, S. D.; Sautter, J.; Xie, J. X.; Kruk, Z. L.; Kupsch, A.; Oertel, W. H. Pharmacological characterisation of dopamine overflow in the striatum of the normal and MPTP-treated common marmoset, studied in vivo using

- fast cyclic voltammetry, nomifensine and sulpiride. *J. Neurosci. Methods* **1998**, *85* (2), 201-209.
25. Kishida, K. T.; Sandberg, S. G.; Lohrenz, T.; Comair, Y. G.; Saez, I.; Phillips, P. E. M.; Montague, P. R. Sub-Second Dopamine Detection in Human Striatum. *Plos One* **2011**, *6* (8).
  26. Cahill, P. S.; Walker, Q. D.; Finnegan, J. M.; Mickelson, G. E.; Travis, E. R.; Wightman, R. M. Microelectrodes for the measurement of catecholamines in biological systems. *Anal. Chem.* **1996**, *68* (18), 3180-3186.
  27. What is Carbon Fiber? *Zoltek* **2011**.
  28. Budai, D. Carbon Fiber-based Microelectrodes and Microbiosensors. In *Intelligent and Biosensors*, Somerset, V. S., Ed.; 2010; pp 269-288.
  29. Garris, P. A.; Christensen, J. R.; Rebec, G. V.; Wightman, R. M. Real-time measurement of electrically evoked extracellular dopamine in the striatum of freely moving rats. *J. Neurochem.* **1997**, *68* (1), 152-161.
  30. Jacobs, C. B. Carbon Nanotube-based microelectrodes for enhanced detection of neurotransmitters. Dissertation . 2012.
  31. Zestos, A. G.; Nguyen, M. D.; Poe, B. L.; Jacobs, C. B.; Venton, B. J. Epoxy insulated carbon fiber and carbon nanotube fiber microelectrodes. *Sensors and Actuators B-Chemical* **2013**, *182*, 652-658.
  32. Morton, K. C.; Morris, C. A.; Derylo, M. A.; Thakar, R.; Baker, L. A. Carbon electrode fabrication from pyrolyzed parylene C. *Anal. Chem.* **2011**, *83* (13), 5447-5452.
  33. Lin, Y.; Trouillon, R.; Svensson, M. I.; Keighron, J. D.; Cans, A. S.; Ewing, A. G. Carbon-ring microelectrode arrays for electrochemical imaging of single cell exocytosis: fabrication and characterization. *Anal. Chem.* **2012**, *84* (6), 2949-2954.
  34. Kawagoe, K. T.; Jankowski, J. A.; Wightman, R. M. Etched carbon-fiber electrodes as amperometric detectors of catecholamine secretion from isolated biological cell. *Anal. Chem.* **1991**, *63* (15), 1589-1594.
  35. Strein, T. G.; Ewing, A. G. Characterization of submicron-sized carbon electrodes insulated with a phenol allylphenol copolymer. *Anal. Chem.* **1992**, *64* (13), 1368-1373.
  36. Schulte, A.; Chow, R. H. Cylindrically etched carbon-fiber microelectrodes for low-noise amperometric recording of cellular secretion. *Anal. Chem.* **1998**, *70* (5), 985-990.

37. Schulte, A.; Chow, R. H. A simple method for insulating carbon-fiber microelectrodes using anodic electrophoretic deposition of paint. *Anal. Chem.* **1996**, *68* (17), 3054-3058.
38. Hermans, A.; Wightman, R. M. Conical tungsten tips as substrates for the preparation of ultramicroelectrodes. *Langmuir* **2006**, *22* (25), 10348-10353.
39. Selimovic, A.; Johnson, A. S.; Kiss, I. Z.; Martin, R. S. Use of epoxy-embedded electrodes to integrate electrochemical detection with microchip-based analysis systems. *Electrophoresis* **2011**, *32* (8), 822-831.
40. Iijima, S. Helical Microtubules of Graphitic Carbon. *Nature* **1991**, *354* (6348), 56-58.
41. Iijima, S.; Ichihashi, T. Single-Shell Carbon Nanotubes of 1-Nm Diameter (Vol 363, Pg 603, 1993). *Nature* **1993**, *364* (6439), 737.
42. Iijima, S. Carbon nanotubes: past, present, and future. *Physica B-Condensed Matter* **2002**, *323* (1-4), 1-5.
43. Jacobs, C. B.; Peairs, M. J.; Venton, B. J. Review: Carbon nanotube based electrochemical sensors for biomolecules. *Anal. Chim. Acta* **2010**, *662* (2), 105-127.
44. Ali, S. R.; Parajuli, R. R.; Balogun, Y.; Ma, Y. F.; He, H. X. A Nonoxidative Electrochemical Sensor Based on a Self-Doped Polyaniline/Carbon Nanotube Composite for Sensitive and Selective Detection of the Neurotransmitter Dopamine: A Review. *Sensors* **2008**, *8* (12), 8423-8452.
45. Huang, F.; Jin, G. Y.; Liu, Y.; Kong, J. L. Sensitive determination of phenylephrine and chlorprothixene at poly(4-aminobenzene sulfonic acid) modified glassy carbon electrode. *Talanta* **2008**, *74* (5), 1435-1441.
46. Lucarelli, F.; Tombelli, S.; Minunni, M.; Marrazza, G.; Mascini, M. Electrochemical and piezoelectric DNA biosensors for hybridisation detection. *Analytica Chimica Acta* **2008**, *609* (2), 139-159.
47. Wang, M. K.; Shen, Y.; Liu, Y.; Wang, T.; Zhao, F.; Liu, B. F.; Dong, S. J. Direct electrochemistry of microperoxidase 11 using carbon nanotube modified electrodes. *J. Electroanal. Chem.* **2005**, *578* (1), 121-127.
48. Wang, J.; Musameh, M. Electrochemical detection of trace insulin at carbon-nanotube-modified electrodes. *Anal. Chim. Acta* **2004**, *511* (1), 33-36.
49. Zhou, X. J.; Moran-Mirabal, J. M.; Craighead, H. G.; Mceuen, P. L. Supported lipid bilayer/carbon nanotube hybrids. *Nature Nanotechnology* **2007**, *2* (3), 185-190.
50. Sebez, B.; Su, L.; Ogorevc, B.; Tong, Y.; Zhang, X. J. Aligned carbon nanotube modified carbon fibre coated with gold nanoparticles embedded in a

polymer film: Voltammetric microprobe for enzymeless glucose sensing. *Electrochemistry Communications* **2012**, *25*, 94-97.

51. Zhu, Z. G.; Garcia-Gancedo, L.; Flewitt, A. J.; Xie, H. Q.; Moussy, F.; Milne, W. I. A Critical Review of Glucose Biosensors Based on Carbon Nanomaterials: Carbon Nanotubes and Graphene. *Sensors* **2012**, *12* (5), 5996-6022.
52. Zhu, Z. G.; Garcia-Gancedo, L.; Flewitt, A. J.; Moussy, F.; Li, Y. L.; Milne, W. I. Design of carbon nanotube fiber microelectrode for glucose biosensing. *Journal of Chemical Technology and Biotechnology* **2012**, *87* (2), 256-262.
53. Wen, H.; Nallathambi, V.; Chakraborty, D.; Barton, S. C. Carbon fiber microelectrodes modified with carbon nanotubes as a new support for immobilization of glucose oxidase. *Microchimica Acta* **2011**, *175* (3-4), 283-289.
54. Gopalan, A. I.; Lee, K. P.; Ragupathy, D. Development of a stable cholesterol biosensor based on multi-walled carbon nanotubes-gold nanoparticles composite covered with a layer of chitosan-room-temperature ionic liquid network. *Biosensors & Bioelectronics* **2009**, *24* (7), 2211-2217.
55. Kim, J. H.; Kataoka, M.; Jung, Y. C.; Ko, Y. I.; Fujisawa, K.; Hayashi, T.; Kim, Y. A.; Endo, M. Mechanically Tough, Electrically Conductive Polyethylene Oxide Nanofiber Web Incorporating DNA-Wrapped Double-Walled Carbon Nanotubes. *Acs Applied Materials & Interfaces* **2013**, *5* (10), 4150-4154.
56. Ko, J. W.; Woo, J. M.; Ahn, J.; Cheon, J. H.; Lim, J. H.; Kim, S. H.; Chun, H.; Kim, E.; Park, Y. J. Multi-Order Dynamic Range DNA Sensor Using a Gold Decorated SWCNT Random Network. *Acs Nano* **2011**, *5* (6), 4365-4372.
57. Zhu, Z. G.; Song, W. H.; Burugapalli, K.; Moussy, F.; Li, Y. L.; Zhong, X. H. Nano-yarn carbon nanotube fiber based enzymatic glucose biosensor. *Nanotechnology* **2010**, *21* (16).
58. Britto, P. J.; Santhanam, K. S. V.; Ajayan, P. M. Carbon nanotube electrode for oxidation of dopamine. *Bioelectrochem. Bioenerg.* **1996**, *41* (1), 121-125.
59. Britto, P. J.; Santhanam, K. S. V.; Rubio, A.; Alonso, J. A.; Ajayan, P. M. Improved charge transfer at carbon nanotube electrodes. *Advanced Materials* **1999**, *11* (2), 154-157.
60. Swamy, B. E. K.; Venton, B. J. Carbon nanotube-modified microelectrodes for simultaneous detection of dopamine and serotonin in vivo. *Analyst* **2007**, *132*, 876-884.
61. Guell, A. G.; Meadows, K. E.; Unwin, P. R.; Macpherson, J. V. Trace voltammetric detection of serotonin at carbon electrodes: comparison of

- glassy carbon, boron doped diamond and carbon nanotube network electrodes. *Physical Chemistry Chemical Physics* **2010**, *12* (34), 10108-10114.
62. Harreither, W.; Trouillon, R.; Poulin, P.; Neri, W.; Ewing, A. G.; Safina, G. Carbon nanotube fiber microelectrodes show a higher resistance to dopamine fouling. *Anal. Chem.* **2013**, *85* (15), 7447-7453.
  63. Banks, C. E.; Compton, R. G. Exploring the electrocatalytic sites of carbon nanotubes for NADH detection: an edge plane pyrolytic graphite electrode study. *Analyst* **2005**, *130* (9), 1232-1239.
  64. Sekioka, N.; Kato, D.; Ueda, A.; Kamata, T.; Kurita, R.; Umemura, S.; Hirono, S.; Niwa, O. Controllable electrode activities of nano-carbon films while maintaining surface flatness by electrochemical pretreatment. *Carbon* **2008**, *46* (14), 1918-1926.
  65. Ross, A. E.; Venton, B. J. Nafion-CNT coated carbon-fiber microelectrodes for enhanced detection of adenosine. *Analyst* **2012**, *137* (13), 3045-3051.
  66. Peairs, M. J.; Ross, A. E.; Venton, B. J. Comparison of Nafion- and overoxidized polypyrrole-carbon nanotube electrodes for neurotransmitter detection. *Analytical Methods* **2011**, *3* (10), 2379-2386.
  67. Hashemi, P.; Dankoski, E. C.; Petrovic, J.; Keithley, R. B.; Wightman, R. M. Voltammetric Detection of 5-Hydroxytryptamine Release in the Rat Brain. *Analytical Chemistry* **2009**, *81* (22), 9462-9471.
  68. Singh, Y. S.; Sawarynski, L. E.; Dabiri, P. D.; Choi, W. R.; Andrews, A. M. Head-to-head comparisons of carbon fiber microelectrode coatings for sensitive and selective neurotransmitter detection by voltammetry. *Anal. Chem.* **2011**, *83* (17), 6658-6666.
  69. Xiao, N.; Venton, B. J. Rapid, Sensitive Detection of Neurotransmitters at Microelectrodes Modified with Self-assembled SWCNT Forests. *Analytical Chemistry* **2012**, *84* (18), 7816-7822.
  70. Vigolo, B.; Penicaud, A.; Coulon, C.; Sauder, C.; Pailler, R.; Journet, C.; Bernier, P.; Poulin, P. Macroscopic fibers and ribbons of oriented carbon nanotubes. *Science* **2000**, *290* (5495), 1331-1334.
  71. Ko, F. K.; Lam, H.; Titchenal, N.; Ye, H. H.; Gogotsi, Y. Coelectrospinning of carbon nanotube reinforced nanocomposite fibrils. *Polymeric Nanofibers* **2006**, *918*, 231-245.
  72. Ko, F.; Foedinger, R.; Chung, S.; Chatterjee, S.; Roberts, K.; Titchenal, N. L. Structures and properties of carbon nanotube based continuous nanocomposite yarns. *Abstracts of Papers of the American Chemical Society* **2006**, 231.

73. Liao, Y.; Zhang, C.; Zhang, Y.; Strong, V.; Tang, J.; Li, X. G.; Kalantar-Zadeh, K.; Hoek, E. M.; Wang, K. L.; Kaner, R. B. Carbon nanotube/polyaniline composite nanofibers: facile synthesis and chemosensors. *Nano. Lett.* **2011**, *11* (3), 954-959.
74. Wang, J.; Deo, R. P.; Poulin, P.; Mangey, M. Carbon nanotube fiber microelectrodes. *J. Am. Chem. Soc.* **2003**, *125* (48), 14706-14707.
75. Munoz, E.; Suh, D. S.; Collins, S.; Selvidge, M.; Dalton, A. B.; Kim, B. G.; Razal, J. M.; Ussery, G.; Rinzler, A. G.; Martinez, M. T.; Baughman, R. H. Highly conducting carbon nanotube/polyethyleneimine composite fibers. *Advanced Materials* **2005**, *17* (8), 1064-+.
76. Viry, L.; Derre, A.; Poulin, P.; Kuhn, A. Discrimination of dopamine and ascorbic acid using carbon nanotube fiber microelectrodes. *Physical Chemistry Chemical Physics* **2010**, *12* (34), 9993-9995.
77. Viry, L.; Derre, A.; Garrigue, P.; Sojic, N.; Poulin, P.; Kuhn, A. Carbon nanotube fiber microelectrodes: Design, characterization, and optimization. *Journal of Nanoscience and Nanotechnology* **2007**, *7* (10), 3373-3377.
78. Viry, L.; Derre, A.; Garrigue, P.; Sojic, N.; Poulin, P.; Kuhn, A. Optimized carbon nanotube fiber microelectrodes as potential analytical tools. *Analytical and Bioanalytical Chemistry* **2007**, *389* (2), 499-505.
79. Inoue, Y.; Kakihata, K.; Hirono, Y.; Horie, T.; Ishida, A.; Mimura, H. One-step grown aligned bulk carbon nanotubes by chloride mediated chemical vapor deposition. *Applied Physics Letters* **2008**, *92* (21).
80. Schmidt, A. C.; Wang, X.; Zhu, Y.; Sombers, L. A. Carbon Nanotube Yarn Electrodes for Enhanced Detection of Neurotransmitter Dynamics in Live Brain Tissue. *ACS Nano* **2013**.
81. Ericson, L. M.; Fan, H.; Peng, H.; Davis, V. A.; Zhou, W.; Sulpizio, J.; Wang, Y.; Booker, R.; Vavro, J.; Guthy, C.; Parra-Vasquez, A. N.; Kim, M. J.; Ramesh, S.; Saini, R. K.; Kittrell, C.; Lavin, G.; Schmidt, H.; Adams, W. W.; Billups, W. E.; Pasquali, M.; Hwang, W. F.; Hauge, R. H.; Fischer, J. E.; Smalley, R. E. Macroscopic, neat, single-walled carbon nanotube fibers. *Science* **2004**, *305* (5689), 1447-1450.
82. Behabtu, N.; Young, C. C.; Tsentelovich, D. E.; Kleinerman, O.; Wang, X.; Ma, A. W.; Bengio, E. A.; ter Waarbeek, R. F.; de Jong, J. J.; Hoogerwerf, R. E.; Fairchild, S. B.; Ferguson, J. B.; Maruyama, B.; Kono, J.; Talmon, Y.; Cohen, Y.; Otto, M. J.; Pasquali, M. Strong, light, multifunctional fibers of carbon nanotubes with ultrahigh conductivity. *Science* **2013**, *339* (6116), 182-186.
83. Koehne, J.; Chen, H.; Li, J.; Cassell, A. M.; Ye, Q.; Ng, H. T.; Han, J.; Meyyappan, M. Ultrasensitive label-free DNA analysis using an electronic chip based on carbon nanotube nanoelectrode arrays. *Nanotechnology* **2003**, *14* (12), 1239-1245.

84. McKnight, T. E.; Melechko, A. V.; Fletcher, B. L.; Jones, S. W.; Hensley, D. K.; Peckys, D. B.; Griffin, G. D.; Simpson, M. L.; Ericson, M. N. Resident neuroelectrochemical interfacing using carbon nanofiber arrays. *J. Phys. Chem. B* **2006**, *110* (31), 15317-15327.
85. Yu, Z.; McKnight, T. E.; Ericson, M. N.; Melechko, A. V.; Simpson, M. L.; Morrison, B., III Vertically aligned carbon nanofiber arrays record electrophysiological signals from hippocampal slices. *Nano Lett.* **2007**, *7* (8), 2188-2195.
86. Yu, Z.; McKnight, T. E.; Ericson, M. N.; Melechko, A. V.; Simpson, M. L.; Morrison, B., III Vertically aligned carbon nanofiber as nano-neuron interface for monitoring neural function. *Nanomedicine* **2012**, *8* (4), 419-423.
87. Koehne, J. E.; Marsh, M.; Boakye, A.; Douglas, B.; Kim, I. Y.; Chang, S. Y.; Jang, D. P.; Bennet, K. E.; Kimble, C.; Andrews, R.; Meyyappan, M.; Lee, K. H. Carbon nanofiber electrode array for electrochemical detection of dopamine using fast scan cyclic voltammetry. *Analyst* **2011**, *136* (9), 1802-1805.

# Chapter 2: Epoxy insulated carbon fiber and carbon nanotube fiber microelectrodes

---

Abbreviations:

CFME – carbon-fiber microelectrode, CNT – carbon nanotube, FSCV – fast scan cyclic voltammetry,

PVA – poly(vinyl alcohol), CV – cyclic voltammogram

## 2.1 Abstract

Carbon-fiber microelectrodes (CFMEs) are typically constructed from glass capillaries pulled to a fine taper or from a polyimide-coated capillary that is 90  $\mu\text{m}$  in outer diameter. Here, a new fabrication method is developed to insulate carbon-fiber microelectrodes with a thin epoxy coating. A polytetrafluoroethylene (Teflon) mold was laser etched with channels 30-40  $\mu\text{m}$  deep and wide and each channel filled with Armstrong C7 epoxy. A carbon fiber was laid into each channel so that the fiber extended past the mold, and the epoxy cured in an oven. One end of the fiber was trimmed to about 100  $\mu\text{m}$  to form a cylindrical carbon-fiber microelectrode, while the other end was attached to a pin and connected to a potentiostat. Epoxy-insulated electrodes were tested with fast-scan cyclic voltammetry. For dopamine, the sensitivity is similar to glass and polyimide-coated capillary electrodes with a linear range of 0.1 to 10  $\mu\text{M}$  and a LOD of 24 nM. SU-8 epoxy was tested as an alternative insulator because it cures at a lower temperature using light, but it was more brittle. Carbon nanotube fibers were also successfully insulated with epoxy. Epoxy-insulated CFMEs were used to detect stimulated dopamine release *in vivo*. Epoxy-insulated electrodes are smaller in diameter than polyimide-coated capillary electrodes and amenable to mass production. They are advantageous for use in higher order mammals, where glass is not permitted, and with alternative electrode materials, such as carbon nanotube fibers, that cannot be fabricated in a capillary puller. This paper was published in *Sensors and Actuators B: Chemical*. (Zestos, A.G. et. al. *Sensors and Actuators B-Chemical* **2013**, 182, 652-658.)

## 2.2 Introduction

Carbon-fiber microelectrodes (CFMEs) have been extensively used to detect neurotransmitters *in vivo*<sup>1</sup>. CFMEs are traditionally insulated in glass capillary tubes pulled to a fine taper using a vertical capillary puller<sup>1,2</sup>. Recently, many alternatives to carbon fibers have been investigated, including diamond microelectrodes<sup>3</sup>, carbon nanotube fibers<sup>4,5</sup> and carbon nanotube coated microelectrodes<sup>6</sup>. Although glass insulation has been used for over twenty years, it has certain drawbacks. First, the electrode material must withstand the heat and force of the puller and some alternative electrode materials such as carbon nanotube fibers<sup>4</sup> break in the puller. Second, in the puller, electrodes are formed from the middle of a long carbon fiber that is aspirated into a glass capillary. If material is sparse or the electroactive surface was fabricated on the end of a wire, then making electrodes directly in the puller is not possible. Instead, the material must be threaded into a glass capillary that has already been pulled, which is a time consuming process. Third, glass electrodes can potentially shatter in the brain, so they are not allowed for the *in vivo* testing of higher order non-human primates, which must be used for years of experiments<sup>7</sup>. An alternative electrode fabrication method is needed that avoids using a capillary puller and is not made from glass. Previous studies show that electrodes have been manufactured and show advantageously long stability and lifetimes as seen in lead sensors<sup>8,9</sup>. Additionally, mass production of CFMEs is preferred because most electrodes are used only once.

Alternative insulations instead of glass have been studied for carbon-fiber microelectrodes. Polymer insulations, including poly(oxyphenylene) and a

copolymer of 2-allylphenol and phenol, have been electropolymerized onto the surface of the carbon fiber<sup>10,11</sup>. This procedure provides a thin (1-3  $\mu\text{m}$ ) insulation; however, it is not reproducible, and the tip of the fiber must be masked to preserve the electroactive region of the fiber. Another alternative insulation of carbon-fiber microelectrodes is electrodeposition of an anodic paint, which takes a shorter time and utilizes lower toxicity reagents compared with phenolic polymers<sup>12,13</sup>. However, with anodic paints, the electroactive area must still be masked creating problems for reproducibility and mass production. The Phillips group has developed an alternative insulation for chronically implanted electrodes by inserting carbon fibers into polyimide-coated, fused silica capillaries and sealing the end with epoxy<sup>14</sup>. These electrodes are suitable for long term implantation, and their microelectrodes are the first to detect dopamine in rats over a period spanning several months. However, manually inserting carbon-fibers into fused silica capillaries is tedious and not amenable to mass production. In addition, the diameter of the resulting electrode is 90  $\mu\text{m}$ , much larger than the traditional glass insulation.

Epoxy is attractive as an insulator for electrodes because it is non-conductive, can be poured into molds of any shape, and cures quickly. Wightman's group used epoxy insulation to insulate conical tungsten wire tips that were substrates for the preparation of platinum and gold ultramicroelectrodes<sup>15</sup>. Electrodes were dipped into epoxy so the electroactive area had to be protected from the epoxy insulation with a masking agent such as paraffin wax. Another strategy is to pour epoxy into a mold. Selimovic et al

utilized non-stick Teflon molds to coat 0.1 cm electrodes for integration into microchips as electrochemical detectors<sup>16</sup>. Fabricating microelectrodes in a mold with epoxy insulation would provide an easy method for insulation that would not require masking of the electrochemical surface.

In this work, we develop a novel fabrication method for carbon-fiber microelectrodes using epoxy insulation. A Teflon mold was laser etched with channels, which were filled with epoxy and carbon fibers. These epoxy-insulated CFMEs have comparable sensitivity (LOD ~ 20 nM), stability, and temporal resolution to glass-insulated CFMEs. The method of construction is facile, amenable to mass production, and relatively fast. Epoxy-insulated CFMEs are shown to be suitable for *in vivo* measurements. The epoxy insulation is advantageous because it does not require a vertical capillary puller, uses small amounts of materials, and is more durable. Epoxy coatings will be useful for the insulation of alternative nanomaterials such as carbon nanotube fiber microelectrodes and for making electrodes for long-term measurements in non-human primates, where glass electrodes are not suitable.

## **2.3 Methods and Materials**

### **2.3.1. Chemicals and Materials**

Dopamine was purchased from Sigma (St. Louis, MO). A 10 mM stock solution was prepared in 0.1 M perchloric acid and diluted to 1.0  $\mu$ M daily with phosphate-buffered saline (PBS) (131.5 mM NaCl, 3.25 mM KCl, 1.2 mM CaCl<sub>2</sub>, 1.25 mM NaH<sub>2</sub>PO<sub>4</sub>, 1.2 mM MgCl<sub>2</sub>, and 2.0 mM Na<sub>2</sub>SO<sub>4</sub> with the pH adjusted to 7.4). All aqueous solutions were made with deionized water (Millipore, Billerica,

MA). Armstrong C7 Resin and Armstrong A2 Activator were obtained from Ellsworth Adhesives (Germantown, WI) and SU-8 from MicroChem (Newton, MA). Diethylenetriamine hardener was used as received from Fisher Scientific (Waltham, MA).

### **2.3.2. Instrumentation**

Fast Scan Cyclic Voltammetry (FSCV) was performed using a ChemClamp potentiostat (Dagan, Minneapolis, MN). Data were collected and analyzed with Tarheel CV software (gift of Mark Wightman, UNC) using custom data acquisition hardware previously described<sup>17</sup>. A triangle waveform was applied to the electrode from a holding potential of -0.4 V to 1.3 V and back at a scan rate of 400 V/s and a frequency of 10 Hz unless otherwise noted. A silver-silver chloride wire was used as the reference electrode. Samples were tested in a flow injection analysis system consisting of a six-port, stainless steel HPLC loop injector mounted on a two-position air actuator (Valco Instruments, Co., Houston, TX). Buffer and samples were pumped through the flow cell at 2 mL/min unless otherwise noted using a syringe pump (Harvard Apparatus, Holliston, MA).

### **2.3.3. Electrode Construction**

A 2 cm thick teflon block (McMaster Carr, Atlanta GA) was cut into rectangles using a band saw. Channels in the teflon mold (~30-40  $\mu\text{m}$  thick, ~30-40  $\mu\text{m}$  deep, and 2-6 cm long) were laser etched using a CO<sub>2</sub> engraving machine (Versa Laser® 350 with High Power Density Focusing Optic lens unit, Universal

Laser Systems, Scottsdale, AZ, USA). Depth and width measurements were determined with a Dektak 3030 profilometer (Veeco Technologies, Santa Barbara, CA). Under a stereoscope, epoxy (Armstrong Resin C7 and 0.8% Activator A2) was syringed into each channel using a 30 gauge needle. Individual carbon fibers (T-650, Cytec Engineering Materials, West Patterson, NJ) were laid manually into each channel, and the epoxy was allowed to cure for three hours at 165°C. The electrodes were pried out of the channels using a 30 gauge needle tip. Fibers were cut using scissors to approximately 100  $\mu\text{m}$  protruding length. Silver epoxy (H20E, equal portions of Parts A and B, Epoxy Technology, Billerica, MA) was applied with a syringe to the other end of the epoxied carbon fiber to connect it to a gold pin (0.035" x 0.249", Digikey, Thief River Falls, MN) that connects to the potentiostat. The silver epoxy was cured for 1 hour at 150°C.

SU-8 was stored away from light to prevent premature photocuring. It was syringed into each channel using the 30 gauge needle, the carbon fiber added, and then baked pre-exposure at 90°C for 10 minutes. In a dark room, it was then exposed to UV-light (365 nm, Contact UV Lamp: UVGL-15, UVP, Upland, CA) for two minutes. Finally, the SU-8 was cured post-exposure at 90°C for 10 minutes. Glass insulated cylindrical carbon-fiber microelectrodes were made by aspirating a single carbon fiber into a glass capillary (1.2 mm by 0.68 mm, A-M Systems, Inc., Carlsborg, WA). The capillary was pulled to form two electrodes on a vertical pipette puller (Narishige, model PE-21, Tokyo, Japan), and the fiber cut to length. Glass insulated electrodes were epoxied with Epon 828 epoxy and phenylenediamine hardener (Miller-Stephenson, Morton Grove, IL). To

construct polyimide coated fused silica capillary electrodes, carbon fibers were manually floated into the capillaries (10-15 mm length, Polymicro Technologies, Phoenix, AZ) in methanol under a stereoscope. They were epoxied with Devcon two-component epoxy (31345, IWT Performance Polymers, Riviera, FL).

Carbon nanotube (CNT) fibers were prepared as previously described<sup>6</sup>. A suspension of 0.35% HiPCo (High Pressure Carbon Monoxide) CNTs in 1% sodium dodecylbenzenesulfonic acid (SDBS) in water was pumped through a luer lock syringe (flow rate 0.5 mL/minute) into a 4% solution of poly(vinyl alcohol) (PVA) (Aqua Solutions, Deer Park, TX, MW = 124,000-186,000) in water. The PVA solution was rotated on a rotating stage. CNT ribbons were subsequently purified and rinsed in water and then methanol, which washed away the excess polymer. Ribbons collapsed into fibers upon being allowed to dry in air. CNT fibers were epoxy insulated in the same manner as carbon fibers.

#### **2.3.4. Animals**

Male Sprague-Dawley rats (250-350 g) purchased from Charles River were housed in a vivarium and given food and water *ab libitum*. All experiments were approved by the Animal Care and Use Committee of the University of Virginia. The rat was anesthetized with urethane (1.5 mg/kg i.p.), the scalp shaved, and 0.25 mL bupivacaine (0.25% solution) given subcutaneously. The working electrode was implanted in the caudate putamen (in mm from bregma: AP + 1.2, ML + 2.0, and DV - 4.5 to 5.0), the stimulating electrode in the substantia nigra (AP -5.4, ML + 1.2, and DV - 7.5), and the Ag/AgCl reference

electrode in the contralateral side of the brain. The DV placement of the stimulating electrode was adjusted downward until a robust dopamine signal was measured. The epoxy-insulated carbon-fiber electrode was inserted into the brain and the FSCV waveform applied for 30 min to allow the electrode to stabilize. Stimulated release was electrically evoked using biphasic stimulation pulses (300  $\mu$ A, 4-60 pulses, 60 Hz).

## **2.4 Results**

### **2.4.1. *Electrode Construction***

Epoxy-insulated carbon-fiber microelectrodes were constructed in a Teflon mold due to its non-stick properties. The mold was made by laser etching channels with a Versa® Laser and channels were on average 30-40  $\mu$ m wide and deep. Channels were filled with Armstrong C7 epoxy, then a carbon fiber laid in the channel extending past both ends of the mold. Figure 2.1A is a photograph of a CFME epoxied in a teflon mold, while Figure 2.1B shows the epoxied CFME removed from the Teflon mold. It takes about 15 minutes to fill 15 channels with epoxy and carbon fiber. Epoxy curing takes about 3 hours, then the electrodes are removed from the mold and one end attached to a gold pin with silver epoxy, which requires an additional 1 hour to cure. The protruding carbon fiber on the other end is trimmed to make a cylindrical working electrode. Thus, it only requires about 45 minutes of time from the investigator to make 30 electrodes, and electrodes are ready in half a day. The Teflon mold can be reused, and we have made over 30 batches of electrodes using the same mold. The average cost of consumables for each electrode was only \$ 0.33; thus,

fabrication is very economical. In the future, the process could be automated to fill the channels robotically and molds used with more channels.

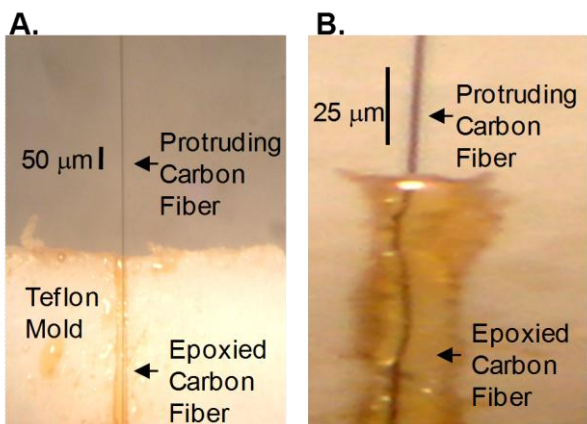


**Figure 2.1:** Pictures of epoxy coated electrodes. A. Epoxyed CFME in the Teflon mold. B. Epoxyed CFME after removal from the Teflon mold.

#### **2.4.2. Comparison of epoxy, glass, and polyimide capillary insulations**

We compared epoxy-insulated CFMEs to more common insulations: glass capillaries and polyimide-coated capillaries. For the glass insulation, a capillary containing a carbon fiber is pulled in a vertical capillary puller, which applies heat and force to form a fine taper on the glass. The seal is reinforced with Epon 828 epoxy. Polyimide-coated fused silica capillaries are made by floating the fiber into the capillary and then applying epoxy on the seal by hand<sup>14</sup>. This method of construction is tedious, requiring 5-10 minutes to make one electrode by a skilled researcher, and it can require months to become skilled. The yield of successful electrodes is relatively low and the curing of the 5 minute epoxy used to seal the fibers in the polyimide capillary is variable. Constructing CFMEs with polyimide

coated fused silica capillaries is advantageous because it does not require the vertical capillary puller and is amenable to alternative electrode materials.

Figure 2.2A shows example background-subtracted cyclic voltammograms (CVs) of 100  $\mu\text{m}$  long cylindrical CFMEs made with each of the different insulations. The three different electrode insulations produce electrodes with similar sensitivities, and the slight variation is likely due to slight differences in fiber length and exposed surface area. The similarities in the background charging currents show that the fibers were all approximately the same area (Fig 2.2B). Average peak oxidative currents for 1  $\mu\text{M}$  dopamine were not significantly different and were  $13.5 \pm 1.2$ ,  $13.7 \pm 1.0$ , and  $13.9 \pm 1.2$  nA for 100  $\mu\text{m}$  long glass-, polyimide capillary-, and epoxy-insulated CFMEs, respectively ( $n = 4$ ,  $p = 0.9708$ , 1-way ANOVA). Therefore, the sensitivity of the electrodes is not dependent on the type of insulation, as expected. Figure 2.2C shows that there is no effect of insulation on the temporal response of the CFMEs. This shows that the epoxy-insulated microelectrodes are well insulated and that the epoxy does not trap dopamine near the surface of the electrode.

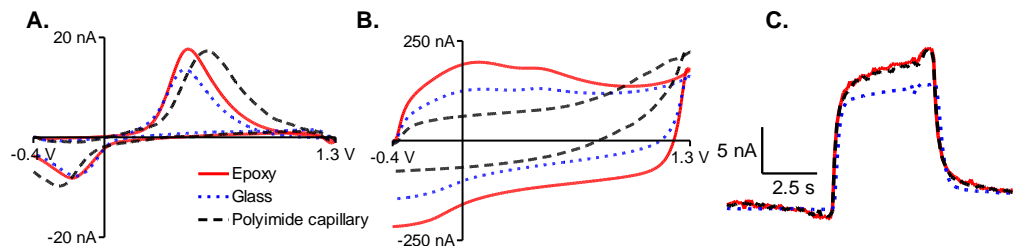


**Figure 2.2:** Example FSCV data for different electrode insulations. Epoxy-insulated CFMEs (Armstrong C7, solid red line), glass-insulated (blue dotted line), and polyimide-coated capillary insulated microelectrodes (black dashed line) are compared. A. Example cyclic voltammograms for 1  $\mu\text{M}$  dopamine for cylindrical electrodes approximately 100  $\mu\text{m}$  long. B. Background charging currents for the same electrodes. C. Current vs time plots at the dopamine oxidation potential during a flow injection analysis experiment.

### 2.4.3. Epoxy-insulated electrode characterization

To compare the adsorption properties of epoxy-insulated to glass-insulated carbon-fiber microelectrodes, the scan rate was varied from 20 to 1,000 V/s. A 5  $\mu\text{M}$  dopamine solution was tested and the waveform frequency was kept constant at 1 Hz to allow measurements with the slower scan rates. Figure 2.3A shows that current for dopamine increases linearly with respect to scan rate. Therefore, dopamine is adsorption controlled and not diffusion controlled. Adsorption control was expected because previous studies of glass-insulated carbon-fiber microelectrodes have found that dopamine is adsorption controlled at physiological pH<sup>18</sup>. Therefore, the epoxy insulation does not alter the fundamental properties of dopamine detection at the electrode.

Epoxy-insulated CFMEs were used to detect dopamine concentrations from 100 nM to 100  $\mu\text{M}$  (Fig. 2.3B). As expected, current was directly proportional to concentration up to 10  $\mu\text{M}$  dopamine<sup>18</sup>. At concentrations higher than 10  $\mu\text{M}$ , the adsorption sites on the surface of the carbon fiber become

saturated and the behavior is more diffusion controlled, which explains the deviation from linearity (Figure 2.4)<sup>18</sup>. Average limits of detection, calculated for a S/N of 3 for the 100 nM samples, were  $24 \pm 4$  nM for epoxy insulation and  $27 \pm 3$  nM for glass insulation and were not significantly different ( $n = 3$ ,  $p = 0.8449$ , t-test).

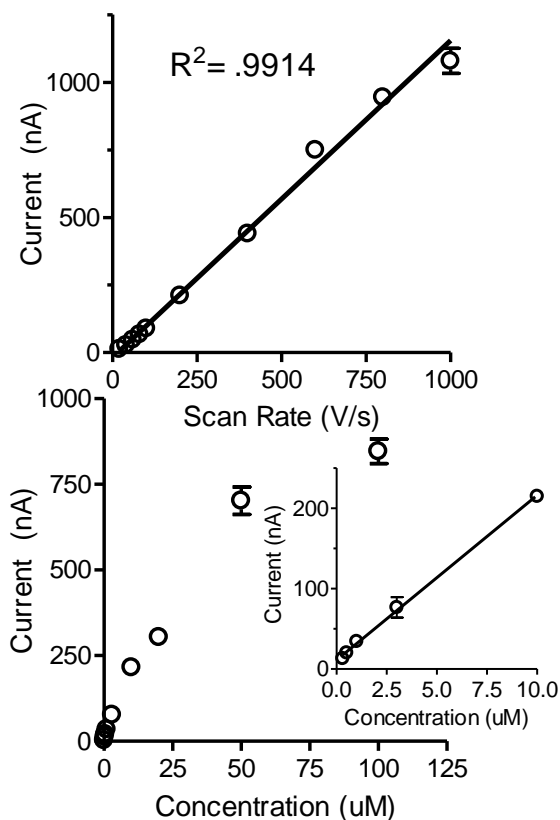


**Figure 2.3:** Characterization of epoxy-insulated electrodes (Armstrong C7 epoxy). A. Current vs. scan rate for 5 μM dopamine is linear with scan rate, so the kinetics are adsorption controlled ( $n = 3$ ). B. Concentration study. Concentration was varied and the current is linear with concentration up to 10 μM for 100 μm long epoxy-insulated CFMEs (inset). Error bars are SEM, ( $n = 3$ ).

#### **2.4.4. Optimization: Armstrong Epoxy vs. SU-8**

We also tested SU-8 as an alternative epoxy insulator. SU-8 is a negative photoresist used for microfluidic devices, microchannels, electrochemical detectors, soft lithography, and other applications<sup>19-23</sup>. SU-8 is cured photochemically and the exposure to UV-light crosslinks the SU-8 molecule, forming a polymer through a free radical polymerization and hardening of the material. SU-8 is baked in an oven pre or post UV curing but the temperature is much lower than with the Armstrong epoxy, so SU-8 could be used in the future with molds other than Teflon that might not withstand the higher temperatures for curing.

As shown in Figure 2.4, there is no effect of Armstrong vs. SU-8 epoxy insulation on sensitivity for detection of 1  $\mu\text{M}$  dopamine. Average currents for 1  $\mu\text{M}$  dopamine at approximately 120  $\mu\text{m}$  long electrodes were  $17.8 \pm 0.9$  for SU-8 epoxy insulated electrodes and  $17.3 \pm 0.2$  for Armstrong epoxy insulated electrodes and were not statistically different ( $n = 4$ ,  $p = 0.5917$ , t-test). The SU-8-insulated CFMEs have a slower temporal response compared to the Armstrong epoxy insulated CFMEs (Fig. 2.4B). This can be explained by the process of restricted diffusion where the small holes in SU-8 epoxy create pockets where dopamine can be trapped at the surface of the carbon fiber, which accounts for the slower time response.

The SU-8 electrodes were more brittle, and therefore, more difficult to remove from the Teflon mold. Only 50 % of electrodes made with SU-8 could be removed intact from the mold. With Armstrong Epoxy, the success rate is

approximately 70%. Approximately 15% percent fail because they break upon removal from the mold, while 15 % fail because of incomplete insulation (bubbles in the epoxy) at the tip. This overall failure rate is similar to glass insulated electrodes, where failures occur when the glass pulls unevenly or the glass seal cracks when trimming the fiber. Reproducibility between Armstrong epoxy-insulated electrodes is good and differences in sensitivity depend on the length of protruding fiber, similar to glass-insulated electrodes. Therefore, Armstrong epoxy was preferred due to its robustness and the relative ease of its removal from the Teflon mold.

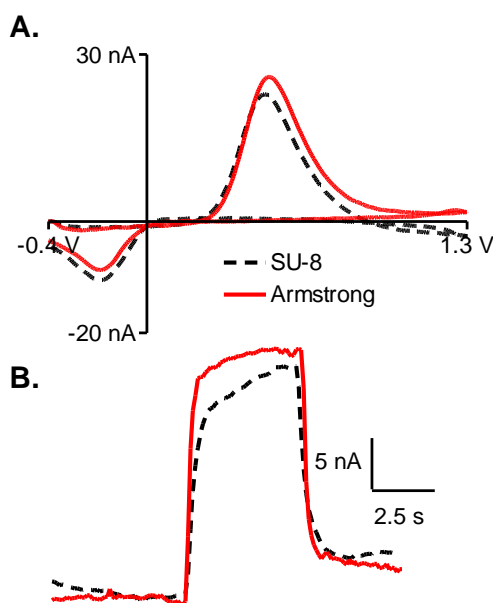


**Figure 2.4:** Comparison of SU-8 vs. Armstrong C7 epoxy insulation. A. The cyclic voltammograms for 1  $\mu\text{M}$  dopamine are comparable. B. The time response of the electrodes is similar, although the SU-8 electrodes have a slower rise time.

#### **2.4.5. Stability Experiment**

Carbon-fiber microelectrodes are used to monitor neurotransmitters *in vivo* for hours at a time to monitor dopamine transients elicited by electrical stimulation, behavior, or pharmacological agents<sup>24-26</sup>. Therefore, electrodes must have a stable current for several hours. Stability was tested by continuously applying the waveform to the electrode immersed in a buffer solution and then performing a flow injection analysis experiment to detect dopamine over a 10 hour period. When the epoxy insulated electrode was scanned from -0.4 to 1.0 V at 400 V/s, there was no significant change in peak oxidative current over the ten hour time period with measurements taken every two hours (Fig. 2.5). This is longer than a typical *in vivo* experiment, which lasts only a few hours. When the electrodes were scanned to 1.3 V, the current rose in the first hour (data not shown) due to oxidation of the electrode surface and surface roughness increases<sup>17</sup>. For electrodes scanned to 1.3 V, the current was stable after the first hour, indicating that this waveform is suitable for *in vivo* use after the surface has stabilized.

The lifetime of the electrode is thought to be perpetual out of solution. According to documentation in laboratory notebooks, electrodes have been used up to two months after the date of their manufacture for *in vivo* and *in vitro* experiments. No change in sensitivity or temporal resolution has been seen through this two month period (data not shown).

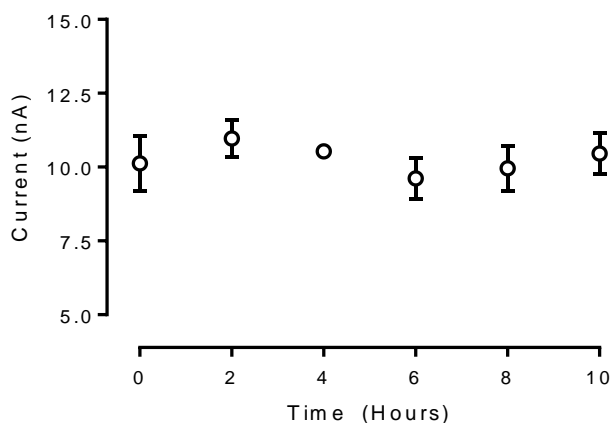


**Figure 2.5:** Stability Experiment. Measurements of 1  $\mu\text{M}$  dopamine were taken over a ten hour time period at epoxy-insulated CFMEs. When the switching potential was 1.0 V (open circles), the signal was stable over ten hours. All other parameters were held constant.

#### **2.4.6. Stimulated Dopamine Release In vivo**

To determine the applicability of an epoxy insulated CFME as a novel in vivo sensor, stimulated dopamine release was measured in anesthetized, male Sprague-Dawley rats. The working electrode, an Armstrong C7 epoxy-insulated CFME, was placed in the caudate putamen. The electrode was allowed to equilibrate for one hour before stimulated dopamine release was measured. A biphasic stimulating electrode was placed in the substantia nigra to stimulate the dopaminergic cell bodies. Stimulation pulse trains were applied (300  $\mu\text{A}$ , 4-60  $\mu\text{s}$ , 60 Hz) and the dopamine response recorded. Figure 2.6 shows an example of dopamine detection in vivo for a variety of pulse trains. Current increase during the stimulation, as dopamine is released and decreases after the stimulation due to uptake. The cyclic voltammogram confirms that dopamine is detected and is similar to those observed in previous studies with glass insulated CFMEs.

Current can be converted to dopamine concentration using an *in vitro* calibration and a 60 pulse stimulation results in a maximum dopamine change of 185 nM. Dopamine can be detected with as little as 4 stimulation pulses, which is a short stimulation that elicited only 31 nM of dopamine. It is not possible to obtain an exact comparison between epoxy-insulated and glass-insulated CFMEs in the same animal because dopamine release varies considerably with electrode placement and the exact same placement cannot be obtained<sup>27</sup>. However, these studies show that epoxy-coated electrodes are promising for *in vivo* studies

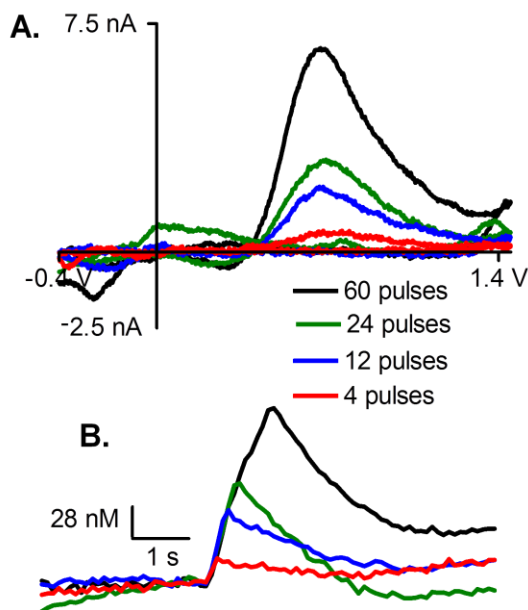


**Figure 2.6:** Dopamine detection *in vivo* at an epoxy-insulated microelectrode. A. Example CVs depicting stimulated dopamine release detected from an Armstrong epoxy-insulated CFME placed in the caudate putamen with a stimulation pulse train of 60, 24, 12, and 4 pulses, respectively. B. The associated current vs concentration plots. The electrode was scanned from -0.4 to 1.45 V and back at 400 V/s at 10 Hz.

#### **2.4.7. Carbon Nanotube-Fiber Microelectrodes**

This alternative epoxy insulation method allows for the easy construction of carbon nanotube fiber electrodes. Electrodes made from CNTs have been proposed as alternatives to traditional carbon-fiber microelectrodes because the CNTs should increase sensitivity through a larger electroactive surface area<sup>28</sup>, increased conductivity and electron transfer kinetics<sup>29</sup>, and a resistance to surface fouling<sup>29</sup>. CNT fibers have also been made using polyaniline composites<sup>30</sup>. CNT fibers were formed as previously described using a particle coagulation spinning method<sup>6</sup>. HiPCo CNTs are suspended in a charged surfactant in an aqueous solution to prevent aggregates from forming. The suspended CNTs were pumped through a syringe into a 4 % solution of poly(vinyl alcohol) (PVA) that displaced the charged surfactant and caused the formation of CNT ribbons. Ribbons were purified and then stretched and dried to form macroscale fibers with diameters around ~15  $\mu\text{m}$ . PVA-CNT fibers have been used to differentiate dopamine and ascorbic acid using differential pulse voltammetry<sup>31</sup>, detect dopamine and hydrogen peroxide with chronoamperometry<sup>32</sup>, and measure potassium ferricyanide and NADH using cyclic voltammetry<sup>33</sup>. CNT fiber microelectrodes had not been characterized with FSCV. However, due to variations in fiber thickness, CNT fibers cannot be pulled in a vertical capillary puller because they snap. Threading the CNT fiber through the capillary is tedious and not amenable to mass production. Therefore, epoxy insulation would be a valuable alternative to threading the fibers into an already pulled capillary or polyimide coated capillary.

Epoxy-insulated CNT fibers were fabricated and used to detect 1  $\mu\text{M}$  dopamine *in vitro* (Fig. 2.7). Previous studies have shown that CNTs are concentrated in the middle of the fiber while the carbonaceous impurities and excess PVA polymer are on the outside. Thus, short ( $\sim 10 \mu\text{m}$  long) cylinder electrodes were made because we expect the end, where the middle of the fiber is exposed, to be the most electroactive. Epoxy-insulated CNT fiber microelectrodes yielded currents of  $1.7 \pm 0.2 \text{ nA}$  for 1  $\mu\text{M}$  dopamine ( $n = 3$ ). The sensitivity of the CNT fiber is not as high as for CFMEs, but we expect that disk electrodes might show improved sensitivity. The  $\Delta E_p$  for PVA CNT-fiber electrodes at a scan rate of 400 V/s was  $0.945 \text{ V} \pm 0.004$  ( $n=3$ ) as opposed to  $0.70 \text{ V} \pm 0.01$  for CFMEs ( $n = 8$ ), which is significantly different (t-test,  $p < 0.0001$ ). Our hypothesis is that non-conductive carbonaceous impurities and excess PVA on the surface may lead to slower electron transfer and that better purification of the CNT fiber or use of disk electrodes might increase electron transfer kinetics. The background charging current (Fig. 2.7B) also has some different features than the carbon fiber, indicating there may be different surface functional groups, which affect electron transfer. These results show proof of concept that epoxy insulation facilitates easy fabrication of CNT fiber microelectrodes, which will facilitate future characterization and applications of these electrodes as rapid sensors for neurotransmitters.

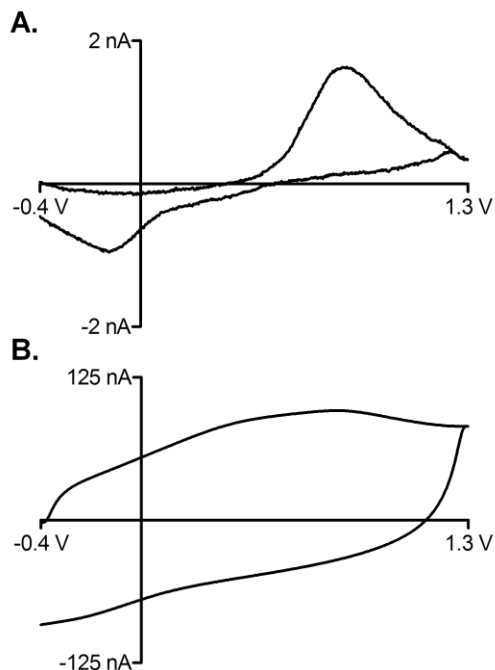


**Figure 2.7:** Epoxy-insulated CNT fiber microelectrode. A. Cyclic Voltammogram of 1  $\mu\text{M}$  dopamine *in vitro* using a PVA formed CNT fiber microelectrode. B. Background charging current of electrode.

## 2.5 Conclusions

Epoxy insulation is a fast, easy method to fabricate carbon-fiber microelectrodes for *in vivo* use. The LOD, time response, and adsorption characteristics were similar for epoxy insulated electrodes, glass-insulated electrodes, and polyimide-coated capillary electrodes. The electrodes fabricated with SU-8 epoxy had a similar sensitivity to the electrodes made with Armstrong epoxy, but they were more brittle and difficult to remove from the mold. Epoxy-insulated electrodes were constructed in a relatively short time in a reproducible process that is amenable to mass production. Epoxy insulation offers a method of construction for novel electrodes made from nanomaterials such as carbon

nanotube fibers and aligned carbon nanotube array microelectrodes<sup>34</sup>. Due to the altered tensile strengths, some of these materials cannot withstand the force of the vertical capillary puller. Threading these materials into a pulled glass or fused silica capillary is challenging and tedious, so epoxy insulation is a viable alternative. Additionally, glass insulated electrodes cannot be used for *in vivo* testing in non-human primates<sup>35</sup> for chronic periods due to the possibility of glass breaking in their brain. Epoxy-insulated electrodes provide a viable alternative for constructing electrodes for this purpose.

**Acknowledgments.** This work was funded by NSF (CHE0645587522).

## Reference List

1. Baur, J. E.; Kristensen, E. W.; May, L. J.; Wiedemann, D. J.; Wightman, R. M. Fast-scan voltammetry of biogenic amines. *Anal. Chem.* **1988**, *60* (13), 1268-1272.
2. Cahill, P. S.; Walker, Q. D.; Finnegan, J. M.; Mickelson, G. E.; Travis, E. R.; Wightman, R. M. Microelectrodes for the measurement of catecholamines in biological systems. *Anal. Chem.* **1996**, *68* (18), 3180-3186.
3. Cvacka, J.; Quaiserova, V.; Park, J.; Show, Y.; Muck, A., Jr.; Swain, G. M. Boron-doped diamond microelectrodes for use in capillary electrophoresis with electrochemical detection. *Anal. Chem.* **2003**, *75* (11), 2678-2687.
4. Viry, L.; Derre, A.; Garrigue, P.; Sojic, N.; Poulin, P.; Kuhn, A. Carbon nanotube fiber microelectrodes: design, characterization, and optimization. *J. Nanosci. Nanotechnol.* **2007**, *7* (10), 3373-3377.
5. Vigolo, B.; Penicaud, A.; Coulon, C.; Sauder, C.; Pailler, R.; Journet, C.; Bernier, P.; Poulin, P. Macroscopic fibers and ribbons of oriented carbon nanotubes. *Science* **2000**, *290* (5495), 1331-1334.
6. Xiao, N.; Venton, B. J. Rapid, sensitive detection of neurotransmitters at microelectrodes modified with self-assembled SWCNT forests. *Anal. Chem.* **2012**, *84* (18), 7816-7822.
7. Earl, C. D.; Sautter, J.; Xie, J.; Kruk, Z. L.; Kupsch, A.; Oertel, W. H. Pharmacological characterisation of dopamine overflow in the striatum of the normal and MPTP-treated common marmoset, studied in vivo using fast cyclic voltammetry, nomifensine and sulpiride. *J. Neurosci. Methods* **1998**, *85* (2), 201-209.
8. Huang, M. R.; Rao, X. W.; Li, X. G.; Ding, Y. B. Lead ion-selective electrodes based on polyphenylenediamine as unique solid ionophores. *Talanta* **2011**, *85* (3), 1575-1584.
9. Li, X. G.; Feng, H.; Huang, M. R.; Gu, G. L.; Moloney, M. G. Ultrasensitive Pb(II) potentiometric sensor based on copolyaniline nanoparticles in a plasticizer-free membrane with a long lifetime. *Anal. Chem.* **2012**, *84* (1), 134-140.
10. Strein, T. G.; Ewing, A. G. Characterization of submicron-sized carbon electrodes insulated with a phenol allylphenol copolymer. *Anal. Chem.* **1992**, *64* (13), 1368-1373.
11. Kawagoe, K. T.; Jankowski, J. A.; Wightman, R. M. Etched carbon-fiber electrodes as amperometric detectors of catecholamine secretion from isolated biological cell. *Anal. Chem.* **1991**, *63* (15), 1589-1594.

12. Schulte, A.; Chow, R. H. A simple method for insulating carbon-fiber microelectrodes using anodic electrophoretic deposition of paint. *Anal. Chem.* **1996**, *68* (17), 3054-3058.
13. Schulte, A.; Chow, R. H. Cylindrically etched carbon-fiber microelectrodes for low-noise amperometric recording of cellular secretion. *Anal. Chem.* **1998**, *70* (5), 985-990.
14. Clark, J. J.; Sandberg, S. G.; Wanat, M. J.; Gan, J. O.; Horne, E. A.; Hart, A. S.; Akers, C. A.; Parker, J. G.; Willuhn, I.; Martinez, V.; Evans, S. B.; Stella, N.; Phillips, P. E. Chronic microsensors for longitudinal, subsecond dopamine detection in behaving animals. *Nat. Methods* **2010**, *7* (2), 126-129.
15. Hermans, A.; Wightman, R. M. Conical tungsten tips as substrates for the preparation of ultramicroelectrodes. *Langmuir* **2006**, *22* (25), 10348-10353.
16. Selimovic, A.; Johnson, A. S.; Kiss, I. Z.; Martin, R. S. Use of epoxy-embedded electrodes to integrate electrochemical detection with microchip-based analysis systems. *Electrophoresis* **2011**, *32* (8), 822-831.
17. Heien, M. L. A. V.; Phillips, P. E. M.; Stuber, G. D.; Seipel, A. T.; Wightman, R. M. Overoxidation of carbon-fiber microelectrodes enhances dopamine adsorption and increases sensitivity. *Analyst* **2003**, *128*, 1413-1419.
18. Bath, B. D.; Michael, D. J.; Trafton, B. J.; Joseph, J. D.; Runnels, P. L.; Wightman, R. M. Subsecond adsorption and desorption of dopamine at carbon-fiber microelectrodes. *Anal. Chem.* **2000**, *72* (24), 5994-6002.
19. Chen, K. N.; Cheng, C. A.; Huang, W. C.; Ko, C. T. Bonding temperature optimization and property evolution of SU-8 material in metal/adhesive hybrid wafer bonding. *J. Nanosci. Nanotechnol.* **2011**, *11* (8), 6969-6972.
20. Kuo, S. M.; Huang, Y. W.; Yeh, S. M.; Cheng, W. H.; Lin, C. H. Liquid crystal modified photonic crystal fiber (LC-PCF) fabricated with an un-cured SU-8 photoresist sealing technique for electrical flux measurement. *Opt. Express* **2011**, *19* (19), 18372-18379.
21. Nemani, K.; Kwon, J.; Trivedi, K.; Hu, W.; Lee, J. B.; Gimi, B. Biofriendly bonding processes for nanoporous implantable SU-8 microcapsules for encapsulated cell therapy. *J. Microencapsul.* **2011**, *28* (8), 771-782.
22. Nordman, N.; Sikanen, T.; Aura, S.; Tuomikoski, S.; Vuorensola, K.; Kotiaho, T.; Franssila, S.; Kostianen, R. Feasibility of SU-8-based capillary electrophoresis-electrospray ionization mass spectrometry microfluidic chips for the analysis of human cell lysates. *Electrophoresis* **2010**, *31* (22), 3745-3753.
23. Psoma, S. D.; van der Wal, P. D.; Frey, O.; de Rooij, N. F.; Turner, A. P. A novel enzyme entrapment in SU-8 microfabricated films for glucose microbiosensors. *Biosens. Bioelectron.* **2010**, *26* (4), 1582-1587.

24. Zachek, M. K.; Takmakov, P.; Park, J.; Wightman, R. M.; McCarty, G. S. Simultaneous monitoring of dopamine concentration at spatially different brain locations in vivo. *Biosensors & Bioelectronics* **2010**, *25* (5), 1179-1185.
25. Phillips, P. E. M.; Wightman, R. M. Critical guidelines for validation of the selectivity of in-vivo chemical microsensors. *Trac-Trends in Analytical Chemistry* **2003**, *22* (9), 509-514.
26. Williams, J. E.; Wieczorek, W.; Willner, P.; Kruk, Z. L. Parametric analysis of the effects of cocaine and cocaine pretreatment on dopamine release in the nucleus accumbens measured by fast cyclic voltammetry. *Brain Res.* **1995**, *678* (1-2), 225-232.
27. Robinson, D. L.; Venton, B. J.; Heien, M. L. A. V.; Wightman, R. M. Detecting subsecond dopamine release with fast-scan cyclic voltammetry in vivo. *Clinical Chemistry* **2003**, *49* (10), 1763-1773.
28. Jacobs, C. B.; Vickrey, T. L.; Venton, B. J. Functional groups modulate the sensitivity and electron transfer kinetics of neurochemicals at carbon nanotube modified microelectrodes. *Analyst* **2011**.
29. Jacobs, C. B.; Peairs, M. J.; Venton, B. J. Review: Carbon nanotube based electrochemical sensors for biomolecules. *Anal. Chim. Acta* **2010**, *662* (2), 105-127.
30. Liao, Y.; Zhang, C.; Zhang, Y.; Strong, V.; Tang, J.; Li, X. G.; Kalantar-Zadeh, K.; Hoek, E. M.; Wang, K. L.; Kaner, R. B. Carbon nanotube/polyaniline composite nanofibers: facile synthesis and chemosensors. *Nano. Lett.* **2011**, *11* (3), 954-959.
31. Viry, L.; Derre, A.; Poulin, P.; Kuhn, A. Discrimination of dopamine and ascorbic acid using carbon nanotube fiber microelectrodes. *Phys. Chem. Chem. Phys.* **2010**, *12* (34), 9993-9995.
32. Wang, J.; Deo, R. P.; Poulin, P.; Mangey, M. Carbon nanotube fiber microelectrodes. *J. Am. Chem. Soc.* **2003**, *125* (48), 14706-14707.
33. Viry, L.; Derre, A.; Garrigue, P.; Sojic, N.; Poulin, P.; Kuhn, A. Optimized carbon nanotube fiber microelectrodes as potential analytical tools. *Anal. Bioanal. Chem.* **2007**, *389* (2), 499-505.
34. Koehne, J. E.; Marsh, M.; Boakye, A.; Douglas, B.; Kim, I. Y.; Chang, S. Y.; Jang, D. P.; Bennet, K. E.; Kimble, C.; Andrews, R.; Meyyappan, M.; Lee, K. H. Carbon nanofiber electrode array for electrochemical detection of dopamine using fast scan cyclic voltammetry. *Analyst* **2011**, *136* (9), 1802-1805.
35. Ariansen, J. L.; Heien, M. L.; Hermans, A.; Phillips, P. E.; Hernadi, I.; Bermudez, M. A.; Schultz, W.; Wightman, R. M. Monitoring extracellular pH, oxygen, and dopamine during reward delivery in the striatum of primates. *Front Behav. Neurosci.* **2012**, *6*, 36.

# Chapter 3: Polyethyleneimine Carbon Nanotube Fiber Electrodes For Enhanced Detection of Neurotransmitters

---

### 3.1 Abstract

Carbon nanotube (CNT) based microelectrodes have been investigated as *in vivo* alternatives to carbon-fiber microelectrodes (CFMEs) for the detection of neurotransmitters because they are sensitive, exhibit fast electron transfer kinetics, and are more resistant to surface fouling. Wet spinning CNTs into fibers using a coagulating polymer produces a thin, uniform fiber that can be fabricated into an electrode. CNT fibers formed in poly(vinyl alcohol) (PVA) have been used as microelectrodes to detect dopamine, serotonin, and hydrogen peroxide. In this study, we characterize microelectrodes fabricated with CNT fibers made in polyethyleneimine (PEI), which have much higher conductivity than PVA-CNT fibers. PEI-CNT fibers have lower overpotentials and higher sensitivities than PVA-CNT fiber microelectrodes, with a limit of detection of 5 nM for dopamine. Similar to CFMEs, the oxidation kinetics for dopamine were adsorption controlled at PEI-CNT and stable for over ten hours. PEI-CNT fiber microelectrodes were resistant to surface fouling by serotonin and the metabolite interferant 5-hydroxyindoleacetic acid (5-HIAA). No change in sensitivity was observed for detection of serotonin after 30 flow injection experiments or after 2 hours in 5-HIAA for PEI-CNT electrodes. Thus, PEI-CNT fiber electrodes could be useful for the *in vivo* monitoring of neurochemicals.

### 3.2 Introduction

Carbon nanotubes (CNTs) were identified in 1991<sup>1</sup> and have been used extensively in electrochemistry to enhance sensitivity and electron transfer kinetics of electrodes.<sup>2,3</sup> Britto et. al developed the first carbon nanotube paste electrode, which had perfect, Nernstian reversible kinetics for dopamine detection (~30 mV peak separation).<sup>4</sup> The CNT-based electrode displayed faster electron transfer kinetics than typical carbon electrodes because the  $sp^2$  hybridized CNT structure is highly conductive due to the delocalization of electrons and the ends of CNTs have reactive edge plane sites.<sup>5</sup> CNTs are especially attractive for making smaller electrodes because the high surface area to volume ratio allows for a large electroactive surface area for the adsorption of biomolecules. Many different strategies have been developed to modify microelectrode surfaces with CNTs and, consequently, improve the electrochemical detection properties. Dip-coating carbon nanotubes onto carbon-fiber microelectrodes (CFMEs) results in an increase in sensitivity, faster electron transfer kinetics, and a resistance to serotonin fouling, but the electrodes are difficult to make reproducibly.<sup>6,7</sup> Polymer coatings, such as Nafion or overoxidized polypyrrole, can be used to immobilize CNTs and increase sensitivity for dopamine while repelling anionic interferants such as ascorbic acid.<sup>8-10</sup> The most sensitive CNT-modified CFMEs have aligned CNT forests self-assembled onto the surface, suggesting that CNT alignment is key.<sup>11</sup> However, all of these methods are difficult to fabricate reproducibly, and the carbon fiber core may convolute the electrochemical properties.

Fibers made from CNTs would be an ideal microelectrode material because they could be directly fabricated into electrodes in a manner similar to carbon fibers, rather than coating an existing electrode with CNTs. CNT fibers grown via chemical vapor deposition and twisted into yarns have faster electron transfer kinetics than CFMEs and have been used to measure stimulated dopamine release in brain slices.<sup>12</sup> However, synthesis of the CNT yarn requires specialized equipment.<sup>12</sup> The Poulin group developed a method of making carbon nanotube fibers through polymer wet spinning.<sup>13</sup> They separated carbon nanotube bundles in an aqueous surfactant solution to overcome van der Waals forces of attraction and aggregation. The suspended nanotubes were then pushed into a streaming solution of poly(vinyl alcohol) (PVA) which displaced the surfactant and arranged the nanotubes into ribbons which subsequently collapsed into fibers.<sup>13</sup> Wang's group examined these PVA-CNT fibers as electrodes for the detection of NADH, peroxide, and dopamine using hydrodynamic voltammetry and amperometry; however, the concentrations tested were much higher than those found physiologically.<sup>14</sup> PVA-CNT fiber electrodes have been used to co-detect complex mixtures of dopamine and ascorbic acid,<sup>8</sup> electrocatalytically oxidize NADH,<sup>15,16</sup> detect glucose in enzymatic sensors,<sup>15</sup> and reduce electrode fouling from large concentrations of dopamine.<sup>17</sup>

Polymer wet spinning is a common technique in the textile industry and other polymer-CNT fibers have been developed but not been tested as microelectrode materials. Polymer-CNT fibers wet-spun with polyethyleneimine

(PEI), for example, are 100-times more conductive than PVA-CNT fibers because of the physisorption of the amine to the CNT wall.<sup>18</sup> The amine intercalates into bundles of SWCNTs and initiates a charge transfer. In this study, we compare the electrochemical properties of PEI-CNT fiber microelectrodes to PVA-CNT fiber microelectrodes and carbon-fiber microelectrodes. PEI-CNT fibers have lower limits of detection and better electron transfer kinetics than PVA-CNT fibers. Dopamine detection is adsorption controlled and the signal is stable for up to 10 hours. The PEI-CNT fibers are resistant to fouling by serotonin and 5-hydroxyindoleacetic acid (5-HIAA), a serotonin metabolism product, which will make them useful for the detection of neurotransmitters *in vivo*.

### **3.3 Methods and Materials**

#### **3.3.1. Chemicals and Materials**

Dopamine was purchased from Sigma (St. Louis, MO, U.S.). A 10 mM stock solution was prepared in 0.1 M perchloric acid and diluted to 1.0  $\mu$ M daily with phosphate-buffered saline (PBS) (131.5 mM NaCl, 3.25 mM KCl, 1.2 mM CaCl<sub>2</sub>, 1.25 mM NaH<sub>2</sub>PO<sub>4</sub>, 1.2 mM MgCl<sub>2</sub>, and 2.0 mM Na<sub>2</sub>SO<sub>4</sub> with the pH adjusted to 7.4) (all from Fisher Scientific, Fair Lawn, New Jersey, U.S.). All aqueous solutions were made with deionized water (EMD Millipore, Billerica, MA, U.S.). Armstrong C7 Resin and Armstrong A2 Activator were obtained from Ellsworth Adhesives (Germantown, WI, U.S.). Diethylenetriamine hardener (DETA) was used as received from Fisher Scientific.

### **3.3.2. Instrumentation**

Fast scan cyclic voltammetry (FSCV) was performed using a ChemClamp potentiostat (Dagan, Minneapolis, MN, U.S.). Data were collected and analyzed with Tarheel CV software (gift of Mark Wightman, UNC, Chapel Hill, NC, U.S.) using custom data acquisition hardware previously described.<sup>19</sup> A triangle waveform was applied to the electrode from a holding potential of -0.4 V to 1.3 V and back at a scan rate of 400 V/sec and a frequency of 10 Hz unless otherwise noted. A silver-silver chloride wire was used as the reference electrode. Samples were tested in a flow injection analysis system consisting of a six-port, stainless steel HPLC loop injector mounted on a two-position air actuator (VICI Valco Instruments, Co., Houston, TX, U.S.). Buffer and samples were pumped through the flow cell at 2 mL/min using a syringe pump (Harvard Apparatus, Holliston, MA, U.S.).

### **3.3.3. Scanning electron microscopy**

Scanning electron microscope (SEM) images were collected on a FEI Quanta 650 microscope with a secondary electron detector using an accelerating voltage of 5 kV and a working distance of 5.6 mm.

### **3.3.4. Electrode Construction**

All carbon nanotube fiber microelectrodes were made with epoxy insulation.<sup>20</sup> A mold was made in Teflon with 30-40  $\mu\text{m}$  wide and deep

channels.<sup>20</sup> Under a stereoscope, Armstrong Resin C7 and 0.8% Armstrong Activator A2 filled each channel using a 30 gauge needle. A single carbon nanotube fiber or carbon fiber was manually inserted into each channel, and the epoxy was allowed to cure for three hours at 165°C before being removed from the mold. Silver epoxy (H20E, equal portions of Parts A and B, Epoxy Technology, Billerica, MA, U.S.) was applied with a syringe to the other end of the epoxied carbon fiber and connected to a gold pin (0.035" x 0.249", Digikey, Thief River Falls, MN, U.S.) to connect to the potentiostat. The silver epoxy was cured for one hour at 150°C. CNT fibers were cut at the surface at an angle of 90° to form "disk-like" electrodes. Carbon-fibers were cut at 100 µm to give them more surface area.

Glass insulated cylindrical carbon-fiber microelectrodes were made for the comparison serotonin fouling experiment by aspirating a single carbon fiber into a glass capillary (1.2 mm by 0.68 mm, A-M Systems, Inc., Carlsborg, WA, U.S.). The capillary was pulled to form two electrodes on a vertical pipette puller (Narishige, model PE-21, Tokyo, Japan), and the fiber cut to length. Glass electrodes were epoxied with Epon 828 resin and phenylenediamine hardener (Miller-Stephenson, Morton Grove, IL, U.S.).

Poly (vinyl alcohol) (PVA) carbon nanotube (CNT) fibers were prepared as previously described.<sup>13</sup> Gloves and glasses are recommended to be worn when handling raw powders of nanotubes. A suspension of 0.35% HiPCo CNTs (high pressure carbon monoxide, Unidym, Sunnyvale, CA) in 1.2% sodium dodecylbenzenesulfonic acid (SDBS, Sigma) in water was pumped through a 30

G syringe needle (flow rate 0.5 mL/minute) into a 4% aqueous solution of poly(vinyl alcohol) (PVA) (Aqua Solutions, Deer Park, TX, MW = 124,000-186,000). The PVA solution was revolved using a custom built rotating stage. CNT ribbons were subsequently purified and rinsed in water and then methanol, which washed away the excess polymer. Ribbons collapsed into fibers upon being allowed to dry in air and then in the oven for 1 hour at 180°C.

Polyethyleneimine (PEI) CNT fibers were formed as previously described.<sup>18</sup> HiPCo CNTs (0.4%) were suspended in water with SDBS (1.2%) and were syringed into a streaming solution of 40% PEI (branched, MW = 50,000 – 100,000, MP Biomedicals, LLC, Santa Ana, CA) in methanol. The CNT ribbons were subsequently purified in methanol. CNT fibers were dried in the oven for approximately one hour at 180°C to remove any excess impurities. All CNT fiber microelectrodes were equilibrated in the flow cell by scanning with the applied waveform for 1 hour before testing with the exception of electrodes tested using the serotonin waveform (.2 to 1.0 to -0.1 to .2 V at 1000 V/sec)<sup>21</sup> or for stability experiments (upper limit = 1.0 V) that were equilibrated with their aforementioned waveforms for ten minutes. The limit of detection (LOD) was calculated using a S/N ratio of 3 from 1 μM measurements for serotonin and 100 nM measurements for dopamine.

### **3.4 Results**

#### **3.4.1. Synthesis and Characterization of PEI-CNT Fibers**

Polyethyleneimine (PEI) CNT fibers were constructed by a wet spinning procedure, in a manner similar to that of PVA-CNT fibers.<sup>18</sup> SWCNTs were

suspended in water using a charged surfactant, SDBS, and sonication. PEI, similar to other amines, physisorbs to the sidewall of single-wall carbon nanotubes and can facilitate electron transfer by intercalating between adjacent CNT bundles.<sup>18</sup> The conductivity of the fiber is expected to be greatly increased when replacing PVA with PEI in polymer-CNT fibers because of the electron donation from the amine group of PEI to SWNT sidewalls.

Scanning electron microscope images show PEI-CNT fibers have diameters of 15 to 25  $\mu\text{m}$ . The diameter is dependent on the flow rate of the syringe pump and the rotation speed of the stage and can be controlled by varying these two parameters. Fig. 3.1A shows the side of a fiber. The surface of the fiber is primarily comprised of SWCNTs with distinct regions of PEI that were not fully removed during the rinse. Fewer regions of polymer impurities are observed on the outside of the CNT fiber walls for PEI-CNT fibers than for PVA-CNT fibers.<sup>13</sup> Fig. 3.1B shows an end of a CNT fiber. The CNTs appear to be in thick bundles and thin CNT bundles are seen protruding from the surface.

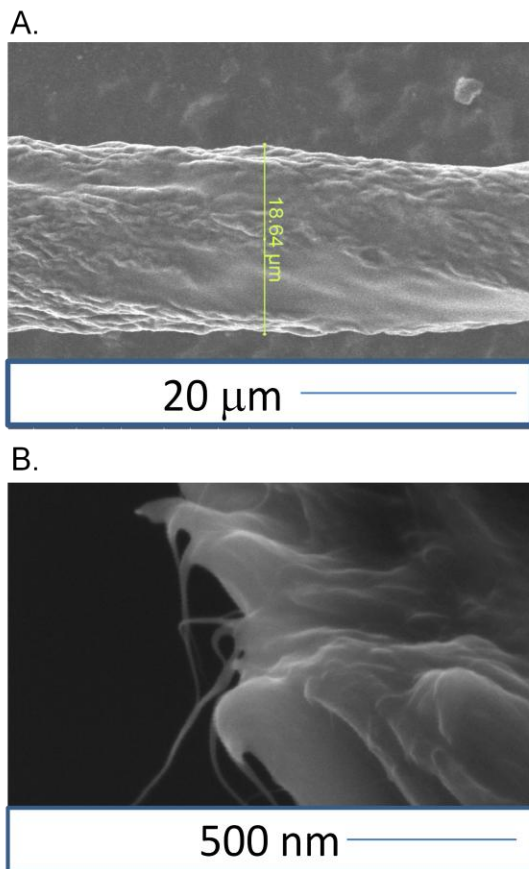


**Figure 3.1:** SEM Image of PEI-CNT Fiber **A.** SEM Image of a CNT fiber with darker regions containing more conductive CNTs. **B.** SEM image of a CNT fiber end. Thin whiskers of individual CNTs protrude from the bundles in the cross-section.

### 3.4.2. Comparison of PVA-CNT and PEI-CNT Fiber Electrodes

As an initial comparison, the electrochemical detection of 1  $\mu\text{M}$  dopamine was compared at PVA-CNT and PEI-CNT fiber microelectrodes. Our lab and the Ewing lab have previously used PVA-CNT fiber microelectrodes to detect dopamine using fast-scan cyclic voltammetry,<sup>17,20</sup> and others have characterized their performance with other analytes and electrochemical techniques.<sup>8,14-16</sup> Disk electrodes were used and the potential was scanned from -0.4 V to 1.3 V at a

scan rate of 400 V/s and a repetition frequency of 10 Hz. The example cyclic voltammograms (CVs), Figure 3.2A, show that the PEI-CNT fiber microelectrode has a higher oxidation current for dopamine as well as a smaller potential separation between the peaks ( $\Delta E_p$ ) than PVA-CNT microelectrodes. The background CVs in Fig. 3.2B show a larger background current at the PEI-CNT fiber microelectrode compared to the PVA-CNT fiber microelectrode, even though the microelectrodes had a similar diameter (about 15  $\mu\text{m}$ ). The larger capacitive current indicates that the PEI-CNT fiber microelectrodes have a larger electroactive surface area or greater surface roughness than PVA-CNT microelectrodes. On average, PEI-CNT fiber microelectrodes have a 6-fold greater oxidation current for 1  $\mu\text{M}$  dopamine compared to PVA-CNT fiber microelectrodes (Fig. 3.2C,  $n=6$  each,  $p < 0.0001$ , t-test). Figure 3.2D shows a significant difference in  $\Delta E_p$  between the two CNT fibers with the peak separation of PEI-CNT microelectrodes about 300 mV less than PVA-CNT microelectrodes ( $n=6$  each,  $p < 0.0001$ , t-test). This suggests that the electron transfer kinetics may be faster at PEI-CNT fiber microelectrodes, and PVA may slow the kinetics. Since the PEI-CNT fibers are reported to be 100-fold more conductive than PVA-CNT fibers, faster charge transfer is not a surprise.<sup>18</sup>

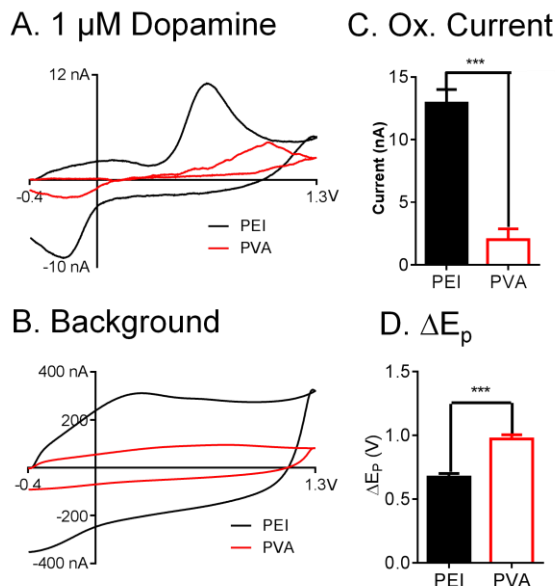


**Figure 3.2:** Comparison of PEI-CNT and PVA-CNT fiber microelectrodes. All electrodes were scanned from -0.4 to 1.3 V and back at 400 V/s at 10 Hz. **A.** Example cyclic voltammograms of 1  $\mu\text{M}$  dopamine for PEI-CNT (black) and PVA-CNT (red) fiber electrodes of about 15 microns in diameter. **B.** Example background charging current for the same electrodes. **C.** Average peak oxidative currents (nA) for 1  $\mu\text{M}$  dopamine are significantly different ( $n=6$  each,  $p < 0.0001$ , t-test, error bars SEM). **D.** The  $\Delta E_p$  values of the electrodes are significantly different ( $n=6$  each,  $p < 0.0001$ , t-test, error bars SEM).

In this study, we used untreated CNT fibers, but post-treatments have been developed. For PVA-CNT fibers, acid treatment, oxidizing with polyoxymolybdate agents, or heating to high temperatures above 1000 K have been used to remove PVA as well as to oxidize the surface and increase conductivity of the fiber.<sup>8,15,16</sup> However, these procedures are often tedious and lack reproducibility.<sup>16</sup> At high temperatures, the carbon nanotube fibers become more conductive as non-graphitic carbon is either removed or graphitized, but heat treatment must be carried out in either inert-atmosphere or under vacuum to avoid excessive oxidation and combustion of the carbon in the fiber.<sup>22</sup> While heat treatment may further improve PEI-CNT microelectrodes, the FSCV data

show that as fabricated PEI-CNT fibers are suitable for dopamine detection, and heat treatment is not necessary.<sup>18</sup> Thus, untreated PEI-CNT fiber microelectrodes are simple to use and have enhanced performance for dopamine detection compared to untreated PVA-CNT fibers.

### **3.4.3. Characterization of dopamine detection at PEI-CNT fiber microelectrodes**

To characterize the properties of PEI-CNT fiber microelectrodes, the scan rate was varied from 100 to 1000 V/s. Figure 3.3A shows that current for 1  $\mu\text{M}$  dopamine increases linearly with respect to scan rate. This indicates that dopamine oxidation at PEI-CNT microelectrodes is an adsorption controlled process, similar to dopamine oxidation at CFMEs, and is likely to be dependent upon oxide groups at the surface of the microelectrode.<sup>23</sup>

PEI-CNT fiber electrodes were used to detect from 100 nM to 100  $\mu\text{M}$  dopamine (Figure 3.3B). The current for PEI-CNT fiber microelectrodes was linear up to 10  $\mu\text{M}$  dopamine, similar to carbon-fiber microelectrodes (Fig. 3.3C).<sup>23</sup> At concentrations higher than 10  $\mu\text{M}$ , the adsorption sites on the surface of the PEI-CNT fiber microelectrode become saturated, and the behavior is more diffusion controlled, which explains the deviation from linearity (Figure 3.3B).<sup>23</sup> The limit of detection for dopamine was  $4.7 \pm 0.2$  nM ( $n = 6$ ) for PEI-CNT fiber electrodes as opposed to a 24 nM for epoxy-insulated CFMEs found in our previous work.<sup>20</sup>

Microelectrodes are typically used *in vivo* for hours at a time to measure neurotransmission in behavioral or pharmacological experiments.<sup>24-26</sup> Therefore, electrodes must have a stable electrochemical response for several hours. The stability of PEI-CNT fiber microelectrodes was investigated by continuously applying the potential waveform to the microelectrode for an extended period of time and injecting a bolus of dopamine every 2 hours. Over a 10 hour period, there was no significant change in peak oxidative current at PEI-CNT fiber microelectrodes with a potential waveform of -0.4 to 1.0 V at a scan rate of 400 V/s as seen in Figure 3.4A. Both the sensitivity and the stability of PEI-CNT microelectrodes indicate that these microelectrodes are suitable for *in vivo* experimentation.

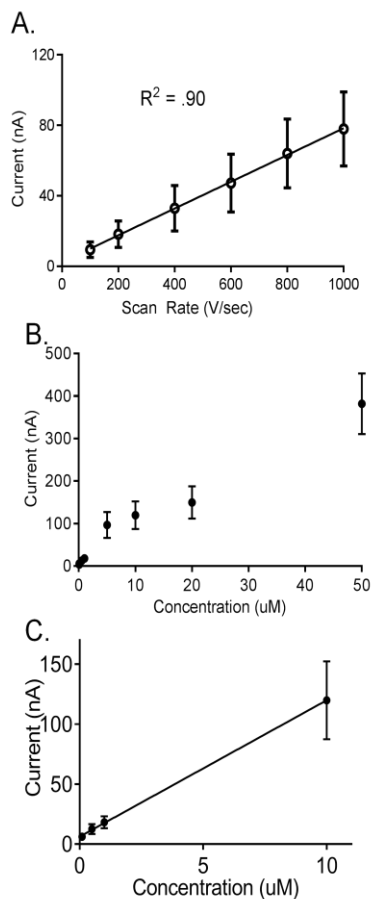


**Figure 3.3: Adsorption Studies** **A.** Effect of Scan Rate. A linear relationship was observed between scan rate and peak oxidative current for 1  $\mu\text{M}$  dopamine denoting adsorption control ( $n = 3$ ,  $R^2 = 0.80$ ). **B.** Concentration Study. Dopamine concentrations were varied from 100 nM to 50  $\mu\text{M}$ . After 10  $\mu\text{M}$ , dopamine is saturated at the surface of the electrode and is diffusion controlled. Error bars are SEM ( $n = 3$ ). **C.** Dopamine concentrations are linear up to 10  $\mu\text{M}$  ( $R^2 = 0.90$ ).

To optimize dopamine detection, the effect of increasing the switching potential was tested. Large positive potentials can cause oxidation of the surface carbons and can modify the electrochemical properties of carbon electrodes.<sup>27,28</sup>

At CFMEs, overoxidation of the electrode surface occurs past 1.3 V, where

carbons are functionalized with electron rich oxide groups, resulting in an increase in the sensitivity towards dopamine.<sup>27</sup> Higher switching potentials can also break carbon-carbon bonds, which alters surface roughness and electroactive surface area and is thought to increase adsorption sites for dopamine.<sup>27,28</sup> Figure 3.4B shows that the measured oxidation current at PEI-CNT microelectrodes increases with increased switching potentials, and potentials of 1.2 V and below result in lower currents. While larger peak currents are observed at switching potentials of 1.4 V and 1.5 V, the signal to noise ratio decreased at potentials above 1.3 V. At higher switching potentials, water oxidation likely causes an unstable background, and background subtraction errors result in a greater increase in noise than in signal. Thus, the overoxidation behavior of PEI-CNT fibers is similar to carbon fibers, and the optimal switching potential for improved sensitivity is 1.3 V. A 1.3 V switching potential was chosen for most experiments because it provided some surface activation and was away from the potential for water oxidation.

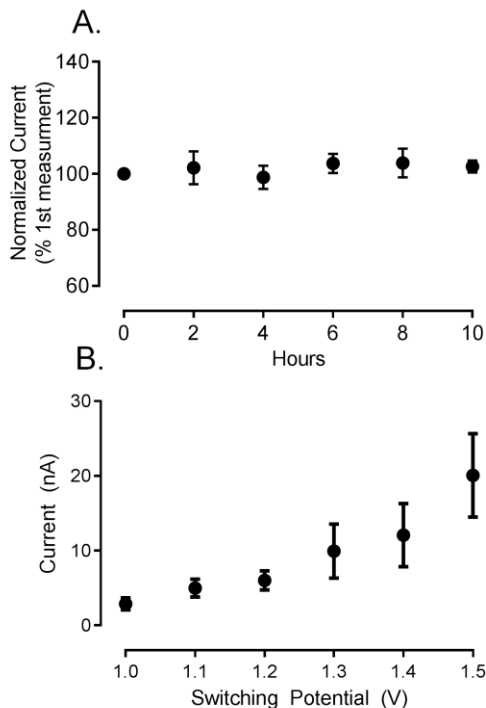


**Figure 3.4:** Stability and Switching Potential Studies. **A.** A stability experiment was performed by testing the response of a PEI-CNT to 1 μM dopamine every 2 hours for 10 hours. There was no change in sensitivity over 10 hours. The electrodes were scanned from -0.4 V to 1.0 V at 400 V/sec at 10 Hz. Error bars are SEM (n = 3). **B.** The switching potential was varied from 1.0 to 1.5 V, and the response to 1 μM dopamine measured. Each waveform was applied for 10 minutes before dopamine was measured. Over-oxidation occurs at higher switching potentials, which greatly increases sensitivity towards dopamine. Error bars are SEM (n = 6).

#### 3.4.4. Characterization of serotonin and 5-HIAA detection at PEI-CNT fiber microelectrodes

Serotonin (5-HT) is an important electroactive indolamine neurotransmitter in the brain. Serotonin levels are monitored because they are important for neurological disorders such as anxiety and depression.<sup>29</sup> The serotonin oxidation peak at CFMEs is typically around 0.6 V with FSCV, and the reduction peak is

around 0 V. With the waveform scanning from -0.4 to 1.3 V and back with a scan rate of 400 V/s, PEI-CNT fiber electrodes were more sensitive for serotonin than CFMEs, with a limit of detection of  $15 \pm 2$  nM compared to  $24 \pm 2$  nM ( $p < 0.05$ , t-test,  $n = 3$ ).

With the standard FSCV waveform, oxidative products of serotonin can passivate the CFME surface and block serotonin adsorption sites, resulting in serotonin fouling of the CFME surface.<sup>21</sup> Alternative waveforms exist to reduce serotonin fouling; however, these waveforms do not detect a reduction potential for dopamine, and, thus, cannot codetect both dopamine and serotonin.<sup>6</sup> To determine if PEI-CNT microelectrodes are fouled by serotonin in a manner similar to that of CFMEs, 25 consecutive flow injection experiments of serotonin were run using the same waveform we used for dopamine analysis, -0.4 V to 1.3 V and back at 400 V/s. In each experiment, the electrode was exposed to a flowing 5 second bolus of 1  $\mu$ M serotonin, followed by 10 seconds of flowing buffer and then a subsequent serotonin injection performed. Figure 3.5A compares oxidative currents for serotonin, normalized to the first injection, at CFMEs and PEI-CNT microelectrodes. Over the 25 serotonin injections, the oxidation current of serotonin decreased by 50% at CFMEs, indicating passivation of the electrode surface. In contrast, the oxidation current at PEI-CNT microelectrodes remained at 100% throughout the experiment, demonstrating there is no signal decrease due to serotonin fouling. The CVs in Figure 3.5B confirm that there is very little change in the serotonin CV between

the first and last run at PEI-CNT microelectrodes as opposed to CFMEs where there is a greater than 50% decrease (Figure 3.5C).

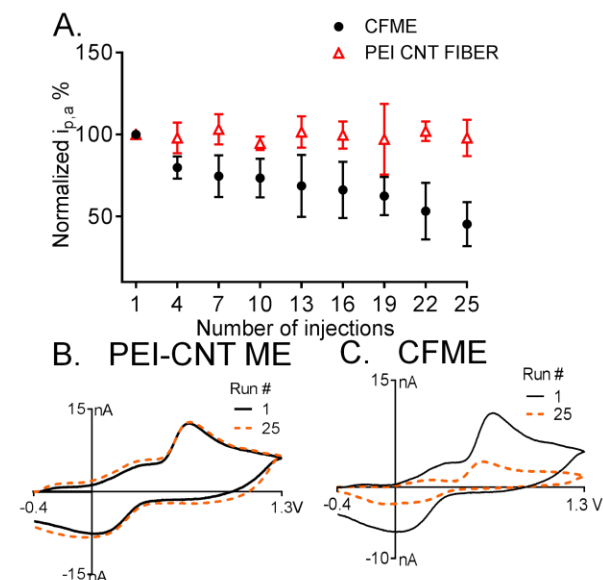


**Figure 3.5:** Serotonin Fouling. **A**  $1 \mu\text{M}$  serotonin solution was tested in the flow cell for 25 consecutive injections of serotonin. The electrodes were scanned from  $-0.4 \text{ V}$  to  $1.3 \text{ V}$  at  $400 \text{ V/sec}$  at  $10 \text{ Hz}$ . Dopamine was injected for 5 seconds every 15 seconds. There was no decrease in sensitivity for serotonin for PEI CNT fiber electrodes (red) as opposed to the 50% decrease in sensitivity for CFMEs (black). Both CFMEs and PEI CNT fibers were normalized to the first electrode to account for electrode to electrode differences. Error bars are SEM ( $n = 3$ ). **B.** Example cyclic voltammograms of  $1 \mu\text{M}$  serotonin for PEI-CNT Fiber microelectrodes (PEI-CNT MEs) at the 1<sup>st</sup> and 25<sup>th</sup> injection (approximately 6.25 minutes apart). This indicates that serotonin fouling does not occur at the surface of the PEI-CNT fiber electrode. **C.** Example cyclic voltammograms of  $1 \mu\text{M}$  serotonin for CFMEs at the 1<sup>st</sup> and 25<sup>th</sup> injection, indicating serotonin fouling does occur at the surface of the CFME.

A recent study found that a metabolite of serotonin, 5-hydroxyindoleacetic acid (5-HIAA), is the main cause of fouling at the CFME surface during *in vivo* serotonin detection.<sup>30</sup> 5-HIAA fouling is similar to serotonin fouling because it also blocks serotonin adsorption sites on the surface of the electrode and results

in decreased sensitivity. Physiological concentrations of 5-HIAA are approximately 10-times greater than serotonin, and the fouling of 5-HIAA occurs even with the waveforms developed specifically to reduce serotonin fouling.<sup>21</sup> Physical or electrochemical deposition of Nafion coatings can be used to repel the negatively charged 5-HIAA, but the electrode preparation methods are time consuming and the thickness of the Nafion layer is difficult to control reproducibly.<sup>30</sup> Since both polymer coatings and electrochemical pretreatments are known to slow the time response of electrodes, it is advantageous to avoid them if possible.<sup>30</sup>

The effect of 5-HIAA fouling was tested at PEI-CNT fiber microelectrodes by comparing the response to 1  $\mu\text{M}$  serotonin before and after the microelectrode was soaked in 10  $\mu\text{M}$  5-HIAA for two hours while the serotonin waveform was applied.<sup>21</sup> At the PEI-CNT microelectrode, there was almost no change in oxidation or reduction current for serotonin before and after 5-HIAA immersion (Figure 3.6A). However, for CFMEs, both the oxidation and reduction peaks of serotonin are distorted and barely visible after 2 hours in 5-HIAA (Figure 3.6B). The serotonin oxidation peak is not significantly different for PEI-CNT fiber microelectrodes ( $n=4$ ,  $p=.6270$ , t-test) after soaking in 5-HIAA. For CFMEs, the signal decreases 95 % after 5-HIAA (Fig. 3.6C,  $n=4$ ,  $p < 0.0001$ , t-test).

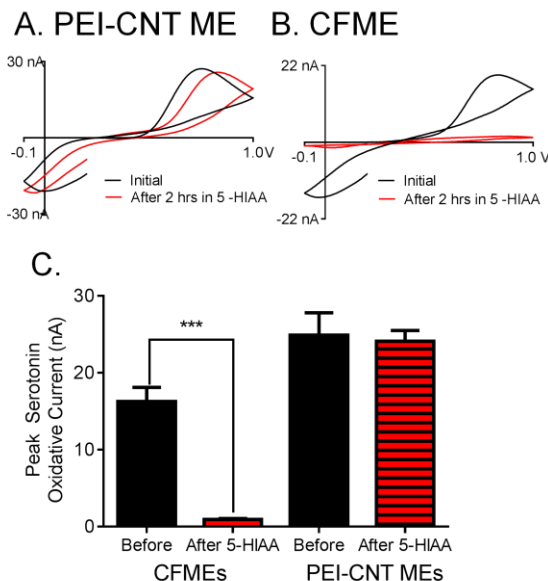


**Figure 3.6: 5-HIAA Fouling. A.** 1  $\mu\text{M}$  serotonin detected at a PEI-CNT fiber electrode before and after cycling for 2 hours in a physiological concentration of 5-HIAA (10  $\mu\text{M}$ ) using the serotonin waveform (.2 to 1.0 to -0.1 to .2 V at 1000 V/sec). The CVs are similar, and the PEI-CNT fiber electrode is not fouled by 5-HIAA. **B.** 1  $\mu\text{M}$  serotonin detected at a glass capillary insulated CFME after cycling for 2 hours in 10  $\mu\text{M}$  5-HIAA using the serotonin waveform. The oxidation peak of serotonin is no longer visible. **C.** Bar graphs depicting the change in peak oxidative current for serotonin before and after exposing the electrode to 10  $\mu\text{M}$  5-HIAA for two hours. The decrease in peak oxidative current is significant for CFMEs ( $n=4$  each,  $p < 0.0001$ , t-test, error bars SEM), while it is not significantly different for PEI-CNT fiber microelectrodes ( $n=4$  each,  $p = .6270$ , t-test, error bars SEM).

The mechanism of the resistance to serotonin fouling to PEI-CNT fiber electrodes is not entirely understood. Not all CNT-based electrodes are anti-fouling for serotonin, and the extent of fouling is dependent on applied waveform.<sup>31</sup> The Ewing group studied the fouling by large concentrations of dopamine at PVA-CNT fiber microelectrodes and found CNTs offer resistance to the first phase of fouling, the growth of the insulating layer from the

polymerization products.<sup>17</sup> Resistance to fouling at CNT ends is often attributed to the higher density of edge plane sites. Indeed, some studies of edge-plane pyrolytic graphite electrodes have found that they have similar anti-fouling properties to CNT based electrodes.<sup>32</sup> The CNT ends in an aligned PEI-CNT fiber might contain more edge plane sites that reduce fouling. Moreover, the mechanism of adsorption of serotonin or 5-HIAA products to the surface of the PEI-CNT fiber could differ from that of adsorption to a CFME. Studies of thin carbon films have found that adding oxide groups while maintaining a high  $sp^2$  conjugation also helps with resistance to serotonin fouling.<sup>33</sup> Thus, electrochemical pretreatments such as extending the switching potential, that add oxide groups without significantly reducing the  $sp^2$  hybridization, may also help with anti-fouling properties of PEI-CNT electrodes. Future studies are needed to tease out this complex mechanism of the anti-fouling properties of CNT fibers.

One primary advantage of PEI-CNT fiber microelectrodes is that they do not become passivated by either 5-HT or 5-HIAA. Thus, PEI-CNT fiber microelectrodes could be used *in vivo* for detection of serotonin without any modification. Detection of serotonin *in vivo* with CFMEs requires the deposition of Nafion which is time consuming and difficult to reproduce. With PEI-CNT fiber microelectrodes, the dopamine waveform can be used for detection without fouling, which is not possible at CFMEs.<sup>30</sup> The advantage of using the dopamine waveform is that dopamine and serotonin can both be detected by using their reduction peaks. The serotonin waveform does not yield the reduction peak of

dopamine and, thus, dopamine cannot be discriminated easily with it from serotonin. Detection of other analytes that cause surface fouling could be explored in the future with PEI-CNT fiber microelectrodes. Therefore, PEI-CNT fibers demonstrate high sensitivity and resistance to fouling which should make them useful for future neurotransmitter studies.

### 3.5 Conclusion

PEI-CNT fiber microelectrodes provide attractive properties for neurotransmitter detection: high sensitivity and resistance to fouling. The PEI-CNT fiber microelectrodes have improved electrochemical properties compared to PVA-CNT fiber microelectrodes, as well as lower limits of detection than traditional CFMEs. Dopamine detection is adsorption controlled at PEI-CNT fiber microelectrodes, and the electrodes have a linear range comparable to CFMEs. In addition, PEI-CNT fiber microelectrodes are stable over long periods of measurement and are resistant to surface fouling by both serotonin and 5-HIAA. Thus, PEI-CNT fiber microelectrodes have increased sensitivity for dopamine and serotonin and resistance to fouling with serotonin that would be beneficial for use as future *in vivo* neurotransmitter sensors.

**Acknowledgments.** This work was funded by NSF (CHE0645587522) and NIH (R01 MH085159).

## Reference List

1. Iijima, S. Helical Microtubules of Graphitic Carbon. *Nature* **1991**, *354* (6348), 56-58.
2. Iijima, S.; Ichihashi, T. Single-Shell Carbon Nanotubes of 1-Nm Diameter (Vol 363, Pg 603, 1993). *Nature* **1993**, *364* (6439), 737.
3. Iijima, S. Carbon nanotubes: past, present, and future. *Physica B-Condensed Matter* **2002**, *323* (1-4), 1-5.
4. Britto, P. J.; Santhanam, K. S. V.; Ajayan, P. M. Carbon nanotube electrode for oxidation of dopamine. *Bioelectrochem. Bioenerg.* **1996**, *41* (1), 121-125.
5. Nugent, J. M.; Santhanam, K. S. V.; Rubio, A.; Ajayan, P. M. Fast electron transfer kinetics on multiwalled carbon nanotube microbundle electrodes. *Nano Letters* **2001**, *1* (2), 87-91.
6. Swamy, B. E. K.; Venton, B. J. Carbon nanotube-modified microelectrodes for simultaneous detection of dopamine and serotonin in vivo. *Analyst* **2007**, *132*, 876-884.
7. Jacobs, C. B.; Vickrey, T. L.; Venton, B. J. Functional groups modulate the sensitivity and electron transfer kinetics of neurochemicals at carbon nanotube modified microelectrodes. *Analyst* **2011**.
8. Viry, L.; Derre, A.; Poulin, P.; Kuhn, A. Discrimination of dopamine and ascorbic acid using carbon nanotube fiber microelectrodes. *Physical Chemistry Chemical Physics* **2010**, *12* (34), 9993-9995.
9. Peairs, M. J.; Ross, A. E.; Venton, B. J. Comparison of Nafion- and overoxidized polypyrrole-carbon nanotube electrodes for neurotransmitter detection. *Analytical Methods* **2011**, *3* (10), 2379-2386.
10. Ross, A. E.; Venton, B. J. Nafion-CNT coated carbon-fiber microelectrodes for enhanced detection of adenosine. *Analyst* **2012**, *137* (13), 3045-3051.
11. Xiao, N.; Venton, B. J. Rapid, Sensitive Detection of Neurotransmitters at Microelectrodes Modified with Self-assembled SWCNT Forests. *Analytical Chemistry* **2012**, *84* (18), 7816-7822.
12. Schmidt, A. C.; Wang, X.; Zhu, Y.; Sombers, L. A. Carbon Nanotube Yarn Electrodes for Enhanced Detection of Neurotransmitter Dynamics in Live Brain Tissue. *ACS Nano* **2013**.
13. Vigolo, B.; Penicaud, A.; Coulon, C.; Sauder, C.; Pailler, R.; Journet, C.; Bernier, P.; Poulin, P. Macroscopic fibers and ribbons of oriented carbon nanotubes. *Science* **2000**, *290* (5495), 1331-1334.

14. Wang, J.; Deo, R. P.; Poulin, P.; Mangey, M. Carbon nanotube fiber microelectrodes. *J. Am. Chem. Soc.* **2003**, *125* (48), 14706-14707.
15. Viry, L.; Derre, A.; Garrigue, P.; Sojic, N.; Poulin, P.; Kuhn, A. Optimized carbon nanotube fiber microelectrodes as potential analytical tools. *Analytical and Bioanalytical Chemistry* **2007**, *389* (2), 499-505.
16. Viry, L.; Derre, A.; Garrigue, P.; Sojic, N.; Poulin, P.; Kuhn, A. Carbon nanotube fiber microelectrodes: Design, characterization, and optimization. *Journal of Nanoscience and Nanotechnology* **2007**, *7* (10), 3373-3377.
17. Harreither, W.; Trouillon, R.; Poulin, P.; Neri, W.; Ewing, A. G.; Safina, G. Carbon nanotube fiber microelectrodes show a higher resistance to dopamine fouling. *Anal. Chem.* **2013**, *85* (15), 7447-7453.
18. Munoz, E.; Suh, D. S.; Collins, S.; Selvidge, M.; Dalton, A. B.; Kim, B. G.; Razal, J. M.; Ussery, G.; Rinzler, A. G.; Martinez, M. T.; Baughman, R. H. Highly conducting carbon nanotube/polyethyleneimine composite fibers. *Advanced Materials* **2005**, *17* (8), 1064-+.
19. Venton, B. J.; Troyer, K. P.; Wightman, R. M. Response times of carbon fiber microelectrodes to dynamic changes in catecholamine concentration. *Anal. Chem.* **2002**, *74* (3), 539-546.
20. Zestos, A. G.; Nguyen, M. D.; Poe, B. L.; Jacobs, C. B.; Venton, B. J. Epoxy insulated carbon fiber and carbon nanotube fiber microelectrodes. *Sensors and Actuators B-Chemical* **2013**, *182*, 652-658.
21. Jackson, B. P.; Dietz, S. M.; Wightman, R. M. Fast-scan cyclic voltammetry of 5-hydroxytryptamine. *Anal. Chem.* **1995**, *67*, 1115-1120.
22. Huffman, M. L.; Venton, B. J. Electrochemical Properties of Different Carbon-Fiber Microelectrodes Using Fast-Scan Cyclic Voltammetry. *Electroanalysis* **2008**, *20* (22), 2422-2428.
23. Bath, B. D.; Michael, D. J.; Trafton, B. J.; Joseph, J. D.; Runnels, P. L.; Wightman, R. M. Subsecond adsorption and desorption of dopamine at carbon-fiber microelectrodes. *Anal. Chem.* **2000**, *72* (24), 5994-6002.
24. Zachek, M. K.; Takmakov, P.; Park, J.; Wightman, R. M.; McCarty, G. S. Simultaneous monitoring of dopamine concentration at spatially different brain locations in vivo. *Biosensors & Bioelectronics* **2010**, *25* (5), 1179-1185.
25. Phillips, P. E. M.; Wightman, R. M. Critical guidelines for validation of the selectivity of in-vivo chemical microsensors. *Trac-Trends in Analytical Chemistry* **2003**, *22* (9), 509-514.
26. Williams, J. E.; Wieczorek, W.; Willner, P.; Kruk, Z. L. Parametric analysis of the effects of cocaine and cocaine pretreatment on dopamine release in the

nucleus accumbens measured by fast cyclic voltammetry. *Brain Res.* **1995**, *678* (1-2), 225-232.

27. Heien, M. L. A. V.; Phillips, P. E. M.; Stuber, G. D.; Seipel, A. T.; Wightman, R. M. Overoxidation of carbon-fiber microelectrodes enhances dopamine adsorption and increases sensitivity. *Analyst* **2003**, *128*, 1413-1419.
28. Takmakov, P.; Zacek, M. K.; Keithley, R. B.; Walsh, P. L.; Donley, C.; McCarty, G. S.; Wightman, R. M. Carbon microelectrodes with a renewable surface. *Anal. Chem.* **2010**, *82* (5), 2020-2028.
29. Uher, R.; McGuffin, P. The moderation by the serotonin transporter gene of environmental adversity in the aetiology of mental illness: review and methodological analysis. *Molecular Psychiatry* **2008**, *13* (2), 131-146.
30. Hashemi, P.; Dankoski, E. C.; Petrovic, J.; Keithley, R. B.; Wightman, R. M. Voltammetric Detection of 5-Hydroxytryptamine Release in the Rat Brain. *Analytical Chemistry* **2009**, *81* (22), 9462-9471.
31. Guell, A. G.; Meadows, K. E.; Unwin, P. R.; Macpherson, J. V. Trace voltammetric detection of serotonin at carbon electrodes: comparison of glassy carbon, boron doped diamond and carbon nanotube network electrodes. *Physical Chemistry Chemical Physics* **2010**, *12* (34), 10108-10114.
32. Banks, C. E.; Compton, R. G. Exploring the electrocatalytic sites of carbon nanotubes for NADH detection: an edge plane pyrolytic graphite electrode study. *Analyst* **2005**, *130* (9), 1232-1239.
33. Sekioka, N.; Kato, D.; Ueda, A.; Kamata, T.; Kurita, R.; Umemura, S.; Hirono, S.; Niwa, O. Controllable electrode activities of nano-carbon films while maintaining surface flatness by electrochemical pretreatment. *Carbon* **2008**, *46* (14), 1918-1926.

# Chapter 4: High Temporal Resolution Measurements by Carbon Nanotube Fiber and Yarn Microelectrodes

---

#### 4.1 Abstract

Carbon nanotube fiber microelectrodes have been developed as electrode materials for the detection of neurotransmitters using fast scan cyclic voltammetry (FSCV). We have used acid-wet spinning to create “neat” carbon nanotube fibers and utilized them as electrode materials. Thirty-four micron diameter acid spun CNT fiber microelectrodes were more sensitive than PEI-CNT fiber microelectrodes, with a 3 nM limit of detection. They also had faster electron transfer kinetics and a greater reversibility for the oxidation of dopamine using FSCV than CFMEs and other carbon nanomaterials. The acid spun CNT fiber microelectrodes also displayed a frequency independent response for the peak oxidation current of dopamine. This property was also seen in other CNT materials such as PEI-CNT fiber microelectrodes and CNT-Yarn microelectrodes. Upon varying the frequency from 10 Hz to 100 Hz, there was no decrease in sensitivity. When scanning at 2,000 V/s, there was no decrease in sensitivity upon changing the frequency from 10 Hz to 500 Hz. This could potentially allow for a 2 ms sampling rate for FSCV, comparable to those used with amperometry as opposed to 100 ms temporal resolution of traditional FSCV, an almost two orders of magnitude difference. Since the frequency independent response is seen with many CNT fibers/yarns, it suggests it is a fundamental property of the CNTs shared by many types of CNT fibers and yarns.

## 4.2 Introduction

Carbon nanotube based electrodes have found much use in the electrochemical detection of biomolecules<sup>1,2</sup>. The high conductivity of carbon nanotubes allows for fast electron-transfer kinetics for the detection of rapid fluctuations of neurotransmitters *in vivo*<sup>3,4</sup>. The cylindrical CNT structure provides a relatively large aspect ratio (surface area: volume) for the adsorption of biomolecules<sup>5,6</sup>. Also, carbon nanotubes have a higher density of edge-plane carbon on the ends, which is thought to be the catalytic site for neurotransmitter oxidation<sup>7</sup>. Because of all of these properties, carbon nanotubes have been frequently incorporated into sensor technology.<sup>3</sup> Wang's group has explored carbon nanotube based electrodes for the detection of peptides<sup>8</sup>, neurotransmitters<sup>9</sup>, DNA<sup>10,11</sup>, cholesterol<sup>12</sup>, proteins<sup>13</sup>, insulin<sup>13</sup>, and other biomolecules<sup>14-17</sup>. Many of these sensors have been carbon nanotube fiber microelectrodes whose electrochemical properties have not been fully examined.

More recently, carbon nanotube based electrode technology has been used with fast scan cyclic voltammetry (FSCV)<sup>18</sup>. Before CNT fiber microelectrodes were developed, the Wightman group pioneered the usage of the T-650 carbon-fiber microelectrode as the standard for the field<sup>19-24</sup>. Carbon nanotubes have been incorporated onto CFMEs via dip coating the carbon fiber into a suspension of carbon nanotubes in an organic solvent such as dimethylformamide (DMF). The method increases sensitivity towards dopamine and other neurotransmitters, but also produces much noise and is not reproducible<sup>6,25-28</sup>. The development of carbon nanotube fiber and yarn

microelectrodes is an alternative method of electrode construction to incorporate purely carbon nanotube-based materials into electrode technology for sensing applications<sup>29,30</sup>.

Carbon nanotube fibers are produced by wet spinning<sup>31</sup>. In contrast, CNT yarns are produced through a method developed by textile industry where they are produced via dry-spinning from the furnace and twisted into yarns<sup>32</sup>. Carbon nanotube fibers and yarns were made into microelectrodes that have been examined preliminarily via voltammetry. PEI-CNT<sup>33</sup> and CNT yarn<sup>32</sup> microelectrodes both have lower limits of detection than CFMEs due to their larger electroactive surface areas. As shown in chapter 3, PEI-CNT fiber microelectrodes have shown a resistance to surface fouling by 5-HT and 5-HIAA and faster electron transfer kinetics than PVA-CNT fiber microelectrodes.<sup>33</sup> In this chapter, we examine an additional type of CNT fiber, the acid-spun CNT fiber, as way to avoid polymer and surfactant impurities produced through polymer wet spinning. CNTs are dissolved in chlorosulfonic acid and syringed into an acetone bath that displaces the acid to spontaneously form a fiber. The acid wet spinning technique precludes the use of sonication used in polymer wet spinning, which cuts CNTs to shorter lengths and reduces conductivity. Also, dissolving the CNTs in acid could possibly oxidize functionalize the CNTs, which would make the negatively charged electrode more sensitive to the cationic dopamine.<sup>34,35</sup> Acid spun CNT fibers have high sensitivities towards dopamine, although they are larger in diameter than the PEI-CNT and CNT yarns.

The sensitivity of CNT yarn based electrodes towards dopamine was found to be independent of the waveform application frequency, which could greatly improve the temporal resolution of current electrode technology.<sup>32</sup> This phenomenon occurs in CNT yarn microelectrodes because the rate of desorption of dopamine and the oxidation product, dopamine-orthoquinone (DOQ), are equal at CNT based electrodes, while the desorption of DOQ is much faster at CFMEs. Here, we find that PEI and acid-spun CNT fiber microelectrodes also have this frequency independent response. We can perform measurements at higher frequencies (500 Hz) and scan rates (2,000 V/s) where the time for the triangle is now 2 ms instead of the traditional 100 ms (at 400 V/s), an almost two orders of magnitude difference. This new property could enable measurements of dopamine release at the millisecond timescale using FSCV. We show that the high temporal resolution of the PEI and acid-spun CNT fiber and CNT yarn microelectrodes is an inherent property of the carbon nanotubes and not dependent on the manner of the fiber/yarn construction.

### **4.3 Methods and Materials**

#### ***4.3.1 Chemicals and Materials***

Dopamine was purchased from Sigma (St. Louis, MO, U.S.). A 10 mM stock solution was prepared in 0.1 M perchloric acid and diluted to 1.0  $\mu$ M daily with phosphate-buffered saline (PBS) (131.5 mM NaCl, 3.25 mM KCl, 1.2 mM CaCl<sub>2</sub>, 1.25 mM NaH<sub>2</sub>PO<sub>4</sub>, 1.2 mM MgCl<sub>2</sub>, and 2.0 mM Na<sub>2</sub>SO<sub>4</sub> with the pH adjusted to 7.4) (all from Fisher Scientific, Fair Lawn, New Jersey, U.S.). All

aqueous solutions were made with deionized water (EMD Millipore, Billerica, MA, U.S.). Armstrong C7 Resin and Armstrong A2 Activator were obtained from Ellsworth Adhesives (Germantown, WI, U.S.). Diethylenetriamine hardener (DETA) was used as received from Fisher Scientific.

#### **4.3.2. Instrumentation**

Fast scan cyclic voltammetry (FSCV) was performed using a ChemClamp potentiostat (Dagan, Minneapolis, MN, U.S.). Data were collected and analyzed with Tarheel CV software (gift of Mark Wightman, UNC, Chapel Hill, NC, U.S.) using custom data acquisition hardware previously described.<sup>36</sup> A triangle waveform was applied to the electrode from a holding potential of -0.4 V to 1.3 V and back at a scan rate of 400 V/s and a frequency of 10 Hz unless otherwise noted. A silver-silver chloride wire was used as the reference electrode. Samples were tested in a flow injection analysis system consisting of a six-port, stainless steel HPLC loop injector mounted on a two-position air actuator (VICI Valco Instruments, Co., Houston, TX, U.S.). Buffer and samples were pumped through the flow cell at 2 mL/min using a syringe pump (Harvard Apparatus, Holliston, MA, U.S.).

#### **4.3.3. Scanning electron microscopy**

Scanning electron microscope (SEM) images were collected on a FEI Quanta 650 microscope with a secondary electron detector using an accelerating voltage of 5 kV and a working distance of 5.6 mm.

#### 4.3.4 Carbon Nanotube Fiber and Yarn Microelectrode Preparation<sup>32</sup>

All carbon nanotube fiber microelectrodes were made with epoxy insulation.<sup>18</sup> Nanotubes are either separated by the use of a surfactant or acid and are then syringed into a solution of polymer (polyethyleneimine, PEI) or acetone, respectively. We call these fibers PEI-CNT fibers<sup>33</sup> and acid-spun CNT fibers, respectively<sup>34</sup>. A mold was made in Teflon with 60-70  $\mu\text{m}$  wide and deep channels.<sup>18</sup> Under a stereoscope, Armstrong Resin C7 and 0.8% Armstrong Activator A2 were syringed into each channel using a 30 gauge needle. A single carbon nanotube fiber or carbon fiber was manually inserted into each channel, and the epoxy was allowed to cure for three hours at 165°C before being removed from the mold. Silver epoxy (H20E, equal portions of Parts A and B, Epoxy Technology, Billerica, MA, U.S.) was applied with a syringe to the other end of the epoxied carbon fiber and connected to a gold pin (0.035" x 0.249", Digikey, Thief River Falls, MN, U.S.) to connect to the potentiostat. The silver epoxy was cured for one hour at 150°C. CNT fibers were cut at the surface to form "disk-like" electrodes. Carbon fibers were cut at 100  $\mu\text{m}$  to give them more surface area.

Poly (vinyl alcohol) (PVA) carbon nanotube (CNT) fibers were prepared as previously described.<sup>31</sup> Gloves and glasses are recommended to be worn when handling raw powders of nanotubes. A suspension of 0.35% HiPCO CNTs (high pressure carbon monoxide, Unidym, Sunnyvale, CA) in 1.2% sodium dodecylbenzenesulfonic acid (SDBS, Sigma) in water was pumped through a 30 G syringe needle (flow rate 0.5 mL/minute) into a 4% aqueous solution of

poly(vinyl alcohol) (PVA) (Aqua Solutions, Deer Park, TX, MW = 124,000-186,000). The PVA solution was revolved using a custom built rotating stage. CNT ribbons were subsequently purified and rinsed in water and then methanol, which washed away the excess polymer. Ribbons collapsed into fibers upon being allowed to dry in air and then in the oven for 1 hour at 180°C.

Polyethyleneimine (PEI) CNT fibers were formed as previously described.<sup>37</sup> HiPCO CNTs (0.4%) were suspended in water with SDBS (1.2%) and were syringed into a streaming solution of 40% PEI (branched, MW = 50,000 – 100,000, MP Biomedicals, LLC, Santa Ana, CA) in methanol. The CNT ribbons were subsequently purified in methanol. CNT fibers were dried in the oven for approximately one hour at 180°C to remove any excess impurities. All CNT fiber microelectrodes were equilibrated in the flow cell by scanning with the applied waveform for 1 hour before testing.<sup>33</sup> The limit of detection (LOD) was calculated using a S/N ratio of 3 from 100 nM measurements for dopamine.

Acid spun CNT fibers were made as previously described.<sup>34</sup> 1-8% HiPCO CNTs were dissolved into chlorosulfonic acid (Fluka Analytical/Sigma, St. Louis, MO, U.S.). They were then syringed into a bath of acetone on a rotating stage with a Harvard Apparatus pump. Fibers were spontaneously formed in the acetone bath and were removed with forceps. They were washed with water and then dried in an oven for one hour at 150°C.

A 1 – 2 cm length of CNT Yarn of 10-20 µm diameter (General Nano, LLC, Cincinnati, OH) was either (1) placed into a polyimide coated fused-silica capillary while submerged in isopropanol, to lower resistance and alleviate

placement (45  $\mu\text{m}$  I.D. x 90  $\mu\text{m}$  O.D., Polymicro Technologies, Phoenix, AZ), or (2) inserted into a 0.68 mm I.D. x 1.2 mm O.D. glass capillary tube that had been tapered into a glass capillary and cut with scissors to have an opening of about sixty micrometer diameter.<sup>32</sup> The solvent evaporated from inside of the capillary before the CNT yarn was sealed into the capillary with Loctite brand five-minute epoxy and cured for one day. The produced electrode was polished at about a ninety degree angle on a Sutter Instruments polishing wheel with the coarse and fine polishing disks to make a disk CNTYME. Carbon-fiber microelectrodes (CFMEs) were also made, manufactured, and polished in a similar manner using 7  $\mu\text{m}$  diameter T-650 carbon fibers (Cytec Technologies, Woodland Park, NJ).<sup>32</sup>

## **4.4 Results**

### **4.4.1 Synthesis of Carbon Nanotube Fibers and Yarns**

In this study, we compare three different types of carbon nanotube microelectrodes (PEI-CNT fiber, acid-spun CNT fiber, and CNT yarn) to determine the extent to which their electrochemical properties are a function of the fiber/yarn construction or are an inherent property of the carbon nanotubes. In chapter 3, we discussed polyethyleneimine (PEI) CNT fibers that are formed by wet spinning. HiPCO CNTs are suspended in an aqueous solution of water via tissue sonication and the addition of a surfactant, SDBS (sodium dodecyl benzenesulfonic acid) to prevent van der Waals aggregation. When pushed into a streaming solution of polymer, the CNTs collapse into ribbons as the polymer displaces the surfactant. The CNT ribbons are then washed in water to remove

the excess polymer to form thin CNT fibers (~20 microns in diameter). Despite washing, rinsing, and heating to remove impurities, some remain. The presence of polymer on the surface of the CNT fiber could be blocking sites for further adsorption of biomolecules to the CNT surface. PEI was chosen to replace the traditional, less-conductive PVA because the amine group of the PEI physisorbs to the walls of the CNTs to induce an intermolecular charge transfer, which increases conductivity 100-fold more than PVA-wet-spun CNT fibers.<sup>37</sup> This increase in conductivity makes PEI-CNT fibers very attractive as electrode-based materials for neurotransmitter detection with fast scan cyclic voltammetry (FSCV).

More recently, wet-spinning with acids instead of polymers has been investigated. Using sulfuric acid, neat carbon nanotube fibers have been constructed.<sup>35</sup> The mechanism of fiber formation involves the oxides of the sulfuric acid separating each CNT bundle through an electrostatic repulsion. Once pushed into water or acetone, which displaces the acid, the CNTs are then oriented into vertically aligned carbon nanotube fibers. Chlorosulfonic acid has recently been shown to be a solvent for carbon nanotubes, which can dissolve the CNTs.<sup>34</sup> The oxide group of the chlorosulfonic acid can separate CNT bundles and align them into fibers<sup>34</sup>. Using chlorosulfonic acid is advantageous since it does not require the use of polymer or surfactant impurities for fiber formation, which can hinder biomolecule adsorption and electron transfer. It also does not require sonication, which cuts CNTs to shorter lengths, thus reducing conductivity.<sup>34</sup>

CNT yarns are made by growing nanotubes with chemical vapor deposition on a surface, and yanking a bundle of CNTs from the surface and twirling them into a yarn.<sup>32</sup> The dry spinning technique directly from the oven was produced from the clothing industry and can produce foot length fibers for industrial purposes.<sup>32</sup> Again, these CNT yarns are relatively impurity free, which could account for their enhanced properties when used as electrode materials. The twisting of the fibers into yarns creates a larger surface area for neurotransmitter detection.

#### **4.4.2. Surface Characterization**

As discussed in chapter 3, scanning electron microscope images show PEI-CNT fibers that have diameters of 15 to 25  $\mu\text{m}$  (Fig. 4.1A).<sup>33</sup> The diameter is dependent on the flow rate of the syringe pump and the rotation speed of the stage and can be controlled by varying these two parameters. Fig. 4.1A shows the side of a fiber. The surface of the fiber is primarily comprised of SWCNTs with distinct regions of PEI that were not fully removed during the rinse. Fewer regions of polymer impurities are observed on the outside of the CNT fiber walls for PEI-CNT fibers than for PVA-CNT fibers.<sup>31</sup> Fig. 4.1B shows an end of a CNT fiber. The CNTs appear to be in thick bundles and thin CNT bundles are seen protruding from the surface. Fig. 4.1 C is an SEM image of an acid-spun CNT fiber made with chlorosulfonic acid. The fiber has a larger diameter than PEI-CNT fibers. Vertically aligned CNT bundles form the CNT fiber. The fiber also has more pits and is not as round as the PEI-CNT fiber.

Carbon nanotube yarns (CNTYs) consist of many CNT bundles twisted together, each typically around 8  $\mu\text{m}$  in diameter.<sup>32</sup> Since many bundles are twirled together, yarns do not have circular cross-sections, and contain regional areas that vary in carbon nanotube profile. The cross-section of the CNTY typically varies between 8  $\mu\text{m}$  and 25  $\mu\text{m}$ , but electrode creation in tapered tubes can produce carbon nanotube yarn microelectrodes (CNTYMEs) with electrode ends smaller than the original measured end of the CNTY since the yarn can condense.<sup>32</sup> The image in Figure 4.1D shows an example of a tapered glass tube disk electrode, with a tip diameter of 8  $\mu\text{m}$ . High magnification SEM images of the carbon nanotube yarn microelectrode surface, Figure 4.1E, shows a multitude of small circles, each about 8-25 nm in diameter, which suggests the surface consists primarily of CNT termini.<sup>32</sup>

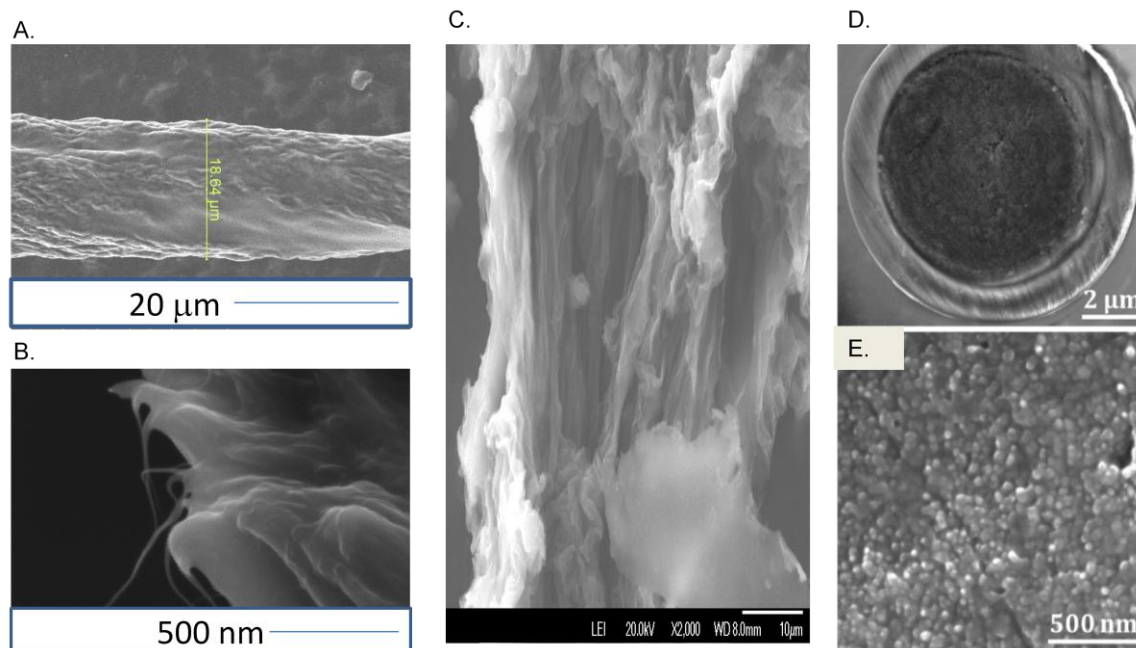


**Figure 4.1: SEM Images of Carbon Nanotube Fibers and Yarn**

(A). SEM Image of a PEI CNT fiber with darker regions containing more conductive CNTs. (B) SEM image of a PEI CNT fiber end. Thin whiskers of individual CNTs protrude from the bundles in the cross-section. (C). SEM of Acid Spun CNT fiber. (D) A beveled end a CNT yarn microelectrode. (E) High magnification CNT yarn with 30-50 nm diameter CNTs bundled tightly together to form a nanostructured surface. Panels D and E are taken from reference 32.

#### 4.4.3. Electrochemical Characterization

Acid-spun CNT fiber microelectrodes are a novel electrode material for neurotransmitter sensing using fast scan cyclic voltammetry (FSCV). Figure 4.2A shows an example cyclic voltammogram for 1  $\mu\text{M}$  dopamine using an acid-spun CNT fiber microelectrode, while Figure 4.2B shows the example background charging current, which is dependent on the surface area of the electrode material. The acid-spun fibers produced through wet spinning are approximately 30-50 microns in diameter. The acid-spun fibers were tested with a waveform

going to 1.0 V because the surface area was larger and they often overloaded, with background currents over 10  $\mu\text{A}$ , with the 1.3 V switching potential. The oxidation and reduction peaks for dopamine in Fig. 4.2A are large and nearly identical in size, indicating the reaction is more reversible. The background current is about 6000 nA in Fig. 4.2B, which indicates a large surface area. The acid-spun fiber electrodes are very sensitive, with about 100 nA of current for 1  $\mu\text{M}$  dopamine, as they have larger surface areas made up of vertically aligned CNTs. Future work could concentrate on reducing the diameter of the acid spun fibers. For example, at the Smalley Institute, they have a custom built compression system that continually compresses and stretches the CNT fibers to smaller diameters and more vertically aligned orientations<sup>35</sup>.

The acid-spun CNT fiber microelectrodes display many interesting characteristics (Table 1). The high sensitivity and low limit of detection, 3 nM, are a function of the large electroactive surface area of the acid spun CNT fiber. The background charging current is 5-fold greater than PEI-CNT fiber microelectrodes that are also disk-like. Even though the CFMEs are cylindrical in shape, their background charging currents are still markedly smaller than acid-spun CNT fiber microelectrodes. This is most likely due to the higher conductivity and larger diameter of the CNT fiber. Also, the electron transfer kinetics are markedly faster than CFMEs and PEI-CNT fiber microelectrodes by about 100 mV (Table 1). This is thought to occur due to the higher conductivity of the CNT materials over the traditional CFMEs with no impurity present to hinder electron transfer.

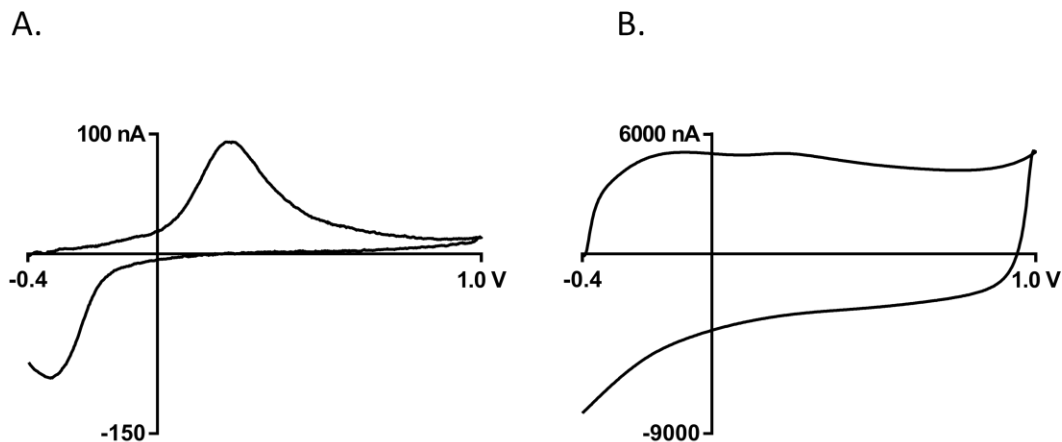


**Figure 4.2:** Acid Spun-CNT Fiber Microelectrode Data **A.** Cyclic Voltammogram for 1  $\mu\text{M}$  dopamine. **B.** Background charging current. The acid spun CNT fiber is 40  $\mu\text{m}$  in diameter and are cut at the tip to form a disk-like electrode.

CNT fibers and CNT yarns have been made into electrode materials for testing with fast-scan cyclic voltammetry for a comparison study. CNT fibers were epoxy insulated and attached to a gold pin, while CNT yarns were placed in a polyimide coated fused silica capillary that was slid into a glass capillary and then polished.<sup>32</sup> Zestos et. al have already shown that the sensitivity, temporal resolution, and electron transfer kinetics of a carbon-fiber microelectrode is independent of the electrode insulation.<sup>18</sup> The electrochemical properties of different carbon nanotube fibers/yarns were compared (Table 1). The limits of detection of each carbon nanotube/yarn are a function of the surface area. Geometric areas were approximated using the diameter of the fiber/yarn and simple geometrical formulas for the areas of a circle or cylinder. This assumes that the CFMEs were cylindrical electrodes of 100  $\mu\text{m}$  length while the CNT fibers and yarns were disk electrodes. Because PEI-CNT and acid-spun fibers were cut instead of polished, the surface roughness may be greater than approximated

by the calculations. The large size of the backgrounds for the acid-spun fibers suggests that they may be substantially larger than the geometric area indicates. The CNT yarn and fiber microelectrodes, with the exception of the less conductive PVA-CNT fiber that has non-conductive polymer blocking sites for adsorption, have lower limits of detection than CFMEs, but similar or smaller geometric areas. This could be explained by an electrocatalytic effect of the edge-plane carbon that the CNTs have for dopamine oxidation. The surface areas of acid-spun CNT fiber microelectrodes are approximately 4-times greater than PEI-CNT fibers, which is similar to the increase in background charging currents and peak oxidative currents that are 4-5 greater than PEI-CNT fiber microelectrodes (see Figure 1 and Chapter 3).

PEI CNT fiber microelectrodes have  $\Delta E_p$  values that are comparable to CFMEs. PVA-CNT fiber microelectrodes have  $\Delta E_p$  values that are approximately 300 mV greater. Non-conductive PVA likely coats the surface of the CNT fiber, which slows electron transfer. The PEI fiber is more conductive because the amine group of the PEI undergoes an intermolecular charge transfer with the sidewall of the CNTs, which increases conductivity over 100-fold more than the PVA fiber.<sup>37</sup> The acid-spun fibers and CNT yarns have  $\Delta E_p$  values that are approximately 100 mV less than CFMEs and polymer-CNT fiber electrodes because they have no polymer or surfactant impurities on the surface (see Table 1). The conductivity of the acid spun CNT fiber is solely a function of the CNTs without any other surface impurities present to diminish electron transfer.

All of the of CNT yarns/fiber microelectrodes have a greater reversibility of dopamine oxidation with respect to CFMEs as seen in the ratio of peak cathodic current to peak anodic current in Table 1. A ratio of 1 would indicate all the dopamine that was oxidized was reduced to dopamine on the return scan. The oxidation of dopamine appears to be almost completely reversible at acid-spun fibers. This property has also been observed with CNT yarn microelectrodes, but not CFMEs.<sup>19,30</sup> For CFMEs, the oxidation of dopamine is quasi-reversible, meaning that not all of the DOQ that is oxidized is reduced back to dopamine. For CNT-based electrode, more of the DOQ is reduced back to dopamine. A hypothesis for this phenomenon is that less DOQ desorbs from the electrode at CNT fibers than at CFMEs.

1 $\mu\text{M}$ DA	n	Approximate Area ( $\mu\text{m}^2$ )	LOD (nM)	$\Delta E_p$ (mV)	$i_{p,c}/i_{p,a}$
CFME	4	362 $\pi$	24 $\pm$ 2 nM	680 $\pm$ 5	0.63 $\pm$ 0.01
ACID-CNTFME	6	400 $\pi$	3 $\pm$ 0.5 nM	570 $\pm$ 7	0.95 $\pm$ 0.01
PEI-CNTFME	6	156 $\pi$	5 $\pm$ 1 nM	670 $\pm$ 6	0.78 $\pm$ 0.01
PVA-CNTFME	6	156 $\pi$	53 $\pm$ 5 nM	970 $\pm$ 3	0.72 $\pm$ 0.01
CNTYME	5	156 $\pi$	10 $\pm$ 0.8 nM	580 $\pm$ 3	0.77 $\pm$ 0.01

**Table 4.1:** Electrochemical Data. Some data is reproduced from reference 32 and chapter 3. A chart of the approximate area, limit of detection for dopamine, overpotentials, and ratios of peak reductive to peak oxidative currents comparing CFMEs to ACID CNTFMEs, PEI CNTFMEs, PVA-CNTFMEs, and CNTYMEs.

#### 4.4.4. Frequency Independent Response

We recently discovered an interesting property of CNT yarn microelectrodes: their sensitivity for dopamine is independent of the wave application frequency<sup>32</sup>. Traditionally with CFMEs, the peak oxidative current of dopamine decreases as the frequency is increased because there is less time for dopamine to adsorb at higher frequencies. Thus, there is less time at the negative holding potential which electrostatically attracts the positively charged dopamine. The rate of desorption of DOQ is 10 times faster than the rate of desorption of dopamine from the surface of the CFME<sup>32</sup>. The rate of desorption of dopamine and DOQ are approximately equal at the surface of CNT yarn microelectrodes based on previous modeling studies of dopamine adsorption kinetics on CNT yarns.

Here, we tested the extent to which PEI-CNT fibers and acid spun fibers would exhibit the same frequency response. As shown in Figure 4.3 A, upon increasing the frequency from 10 Hz to 90 Hz, peak oxidative current for dopamine decreases 75% for CFMEs. There is no decrease in peak oxidative current for dopamine for CNTYMEs upon increasing the frequency from 10 to 90 Hz (Fig. 2.3B). Similar results are observed for PEI-CNT and acid-spun CNT fiber microelectrodes (Figures 4.3C-D). There is no drop in peak oxidative current for dopamine upon increasing the wave application frequency from 10 Hz to 90 Hz. Again, this is hypothesized to occur due to the fact that dopamine and DOQ desorb at equal rates from the nanostructured CNT fiber/yarn.

CNTYMEs, PEI-CNTFMEs, and Acid CNTFMEs all display a sensitivity that is independent of the frequency. Since all three materials are composed almost exclusively of CNTs, then it is assumed that the catalytic properties of the CNTs cause this phenomenon. However, CFMEs that were chemically modified with vertically aligned CNT forests do not exhibit a sensitivity that is independent of the frequency.<sup>27</sup> We hypothesize that the less conductive carbon fiber core convolutes the signal and slows down electron transfer, which is why we do not see this phenomenon for the CNT modified CFME. The self-assembled CNTs also do not appear to be as well aligned as in the CNT yarns and fibers, so the CNT alignment and structure may also play a role. The temporal response is likely due to aligned, purely CNT-based electrode materials such as the CNT yarns and CNT fibers.

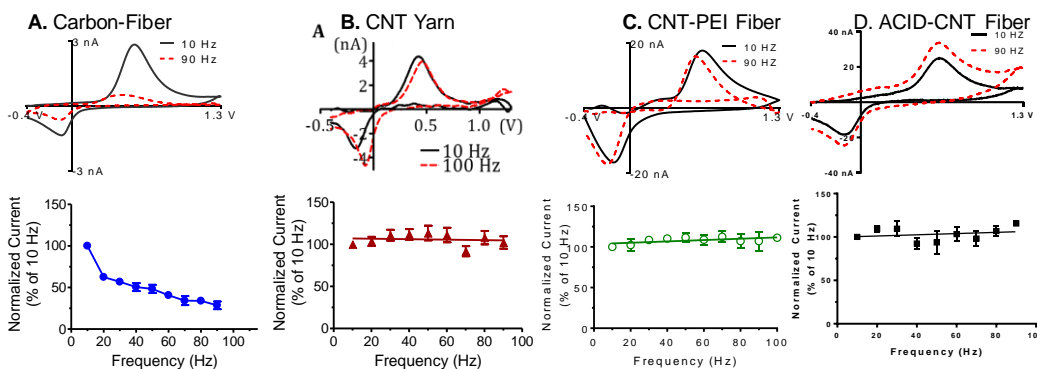


**Figure 4.3:** Frequency Independent Response. Current for 1  $\mu$ M dopamine for different microelectrodes as the frequency of the applied FSCV waveform is increased. Some of the data is reproduced from reference 32. **A.** The current at a disk-carbon-fiber microelectrode drops dramatically by 90 Hz. **B.** For a disk CNT yarn microelectrode, the current is steady over all the frequencies. **C.** For a CNT-PEI fiber microelectrode, the current does not decrease with increasing frequency. **D.** There is also no decrease in sensitivity for acid spun CNT fiber microelectrodes upon increasing the frequency from 10 Hz to 90 Hz. The scan rate is 400 V/s for all.  $n = 4-6$ .

A useful application of having a frequency independent response for the peak oxidative current of dopamine is the ability to use faster scan rates. With the traditional waveform (400 V/s), the triangle takes about 10 ms, therefore, the maximum repetition rate is approximately 100 Hz. At faster scan rates, the time for the triangle can be decreased. At 2000 V/s, the time for the triangle is about 2 ms; therefore, a 500 Hz wave application frequency can be utilized. Figure 4.4 A shows a CFME at 2,000 V/s at 10 and 500 Hz, respectively. The peak oxidative current for dopamine drops dramatically at 500 Hz. On the other hand, there is no decrease in peak oxidative current for CNTYMEs (Fig 4.4 B) and PEI-CNT fiber microelectrodes (Fig. 4.4 C), respectively upon increasing the frequency from 10 to 500 Hz.

This markedly increases the sampling rate at our electrodes from 100 ms to 2 ms, about a two-order of magnitude difference. This makes the sampling rate comparable to that used with amperometry<sup>38</sup>, however, holding at single potential provides no chemical information about the molecules being detected. The work could possibly provide a breakthrough in neurotransmitter detection by providing the first FSCV measurement of dopamine release on the millisecond timescale. Therefore, it may even allow for measurements of dopamine during individual pulses of burst firing. Obviously, future *in vivo* measurements are necessary with CNT fiber/yarn microelectrodes to realize this claim.

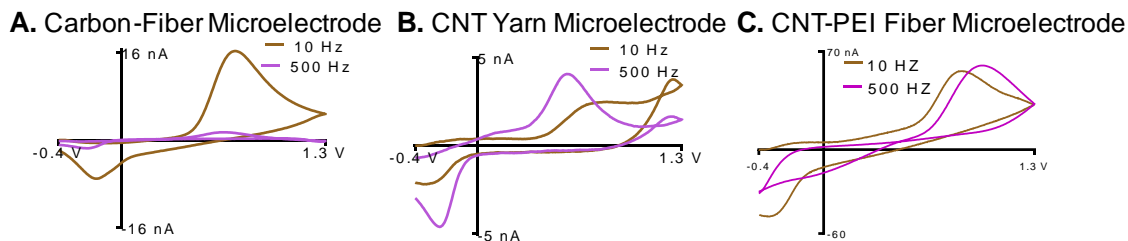


**Figure 4.4:** High Temporal Resolution Measurements. FSCV at 2000 V/s. Example CVs of 1  $\mu$ M dopamine at 10 Hz and 500 Hz repetition rates at **A.** CFMEs, **B.** CNT yarn microelectrodes and **C.** CNT-PEI fiber microelectrodes. (Reproduced from Reference 32)

#### 4.5 Conclusion and Discussion

We have shown that CNT fiber and CNT yarn microelectrodes have enhanced properties for neurotransmitter detection. The PEI-CNT and acid-CNT fibers were produced by wet spinning with polymers/surfactants and acids/acetone, respectively, while CNT yarns were dry-spun directly from the furnace and twisted into yarns using techniques developed by the textile industry. SEM images show high vertical alignment of CNTs on all three electrode materials. The enhanced electrochemical properties, with the exception of PVA-CNTFMEs, are evident as faster electron transfer kinetics, lower limits of detection, and increased cathodic/anodic peak ratios. The kinetics of dopamine oxidation are adsorption controlled for all CNT fibers and yarns, similar to CFMEs. The sensitivity towards dopamine is independent of the wave application frequency, which is a function of DA and DOQ desorbing from the surface of the CNT yarns and fibers at equal rates, while the DOQ desorbs from the electrode about 10-times faster than dopamine at the surface of CFMEs. CFMEs

chemically modified with a CNT-forest did not exhibit a frequency independent response. Therefore, it is thought that the carbon-fiber core of the heterogeneous electrode convoluted the enhanced electron transfer and the electrochemical properties of the CNTs.

In our initial studies, the frequency independent response only occurs for electrode materials whose sole carbon source comes from vertically aligned CNTs. Therefore, we argue that the enhanced electrochemical properties of the CNT fiber and yarn microelectrodes are a function of the intrinsic properties of the CNTs and not the manner of the construction of fibers or yarns, respectively. The frequency independent response allows for testing at 500 Hz and 2,000 V/s, which increases the temporal resolution to 2 ms from the previous 100 ms. Using CNT fiber or yarn microelectrodes could potentially enable the first measurement of dopamine release on the millisecond timescale using fast scan cyclic voltammetry. More rapid measurements would allow a better understanding of the dopamine signaling in the brain on a millisecond time scale.

## Reference List

1. Deo, R. P.; Lawrence, N. S.; Wang, J. Electrochemical detection of amino acids at carbon nanotube and nickel-carbon nanotube modified electrodes. *Analyst* **2004**, *129* (11), 1076-1081.
2. Hocevar, S. B.; Wang, J.; Deo, R. P.; Musameh, M.; Ogorevc, B. Carbon nanotube modified microelectrode for enhanced voltammetric detection of dopamine in the presence of ascorbate. *Electroanalysis* **2005**, *17* (5-6), 417-422.
3. Britto, P. J.; Santhanam, K. S. V.; Ajayan, P. M. Carbon nanotube electrode for oxidation of dopamine. *Bioelectrochem. Bioenerg.* **1996**, *41* (1), 121-125.
4. Britto, P. J.; Santhanam, K. S. V.; Rubio, A.; Alonso, J. A.; Ajayan, P. M. Improved charge transfer at carbon nanotube electrodes. *Advanced Materials* **1999**, *11* (2), 154-157.
5. Jacobs, C. B.; Vickrey, T. L.; Venton, B. J. Wiley Encyclopedia of Chemical Biology. Neurotransmission, Measuring Chemical Events in. **2007**. John Wiley & Sons, Inc.
6. Jacobs, C. B.; Vickrey, T. L.; Venton, B. J. Functional groups modulate the sensitivity and electron transfer kinetics of neurochemicals at carbon nanotube modified microelectrodes. *Analyst* **2011**.
7. Jacobs, C. B.; Peairs, M. J.; Venton, B. J. Review: Carbon nanotube based electrochemical sensors for biomolecules. *Anal. Chim. Acta* **2010**, *662* (2), 105-127.
8. Zhou, X. J.; Moran-Mirabal, J. M.; Craighead, H. G.; Mceuen, P. L. Supported lipid bilayer/carbon nanotube hybrids. *Nature Nanotechnology* **2007**, *2* (3), 185-190.
9. Wang, J.; Deo, R. P.; Poulin, P.; Mangey, M. Carbon nanotube fiber microelectrodes. *J. Am. Chem. Soc.* **2003**, *125* (48), 14706-14707.
10. Kim, J. H.; Kataoka, M.; Jung, Y. C.; Ko, Y. I.; Fujisawa, K.; Hayashi, T.; Kim, Y. A.; Endo, M. Mechanically Tough, Electrically Conductive Polyethylene Oxide Nanofiber Web Incorporating DNA-Wrapped Double-Walled Carbon Nanotubes. *Acs Applied Materials & Interfaces* **2013**, *5* (10), 4150-4154.
11. Ko, J. W.; Woo, J. M.; Ahn, J.; Cheon, J. H.; Lim, J. H.; Kim, S. H.; Chun, H.; Kim, E.; Park, Y. J. Multi-Order Dynamic Range DNA Sensor Using a Gold Decorated SWCNT Random Network. *Acs Nano* **2011**, *5* (6), 4365-4372.
12. Gopalan, A. I.; Lee, K. P.; Ragupathy, D. Development of a stable cholesterol biosensor based on multi-walled carbon nanotubes-gold nanoparticles

composite covered with a layer of chitosan-room-temperature ionic liquid network. *Biosensors & Bioelectronics* 2009, 24 (7), 2211-2217.

13. Wang, J.; Musameh, M. Electrochemical detection of trace insulin at carbon-nanotube-modified electrodes. *Anal. Chim. Acta* **2004**, 511 (1), 33-36.
14. Sebez, B.; Su, L.; Ogorevc, B.; Tong, Y.; Zhang, X. J. Aligned carbon nanotube modified carbon fibre coated with gold nanoparticles embedded in a polymer film: Voltammetric microprobe for enzymeless glucose sensing. *Electrochemistry Communications* **2012**, 25, 94-97.
15. Zhu, Z. G.; Garcia-Gancedo, L.; Flewitt, A. J.; Xie, H. Q.; Moussy, F.; Milne, W. I. A Critical Review of Glucose Biosensors Based on Carbon Nanomaterials: Carbon Nanotubes and Graphene. *Sensors* 2012, 12 (5), 5996-6022.
16. Zhu, Z. G.; Garcia-Gancedo, L.; Flewitt, A. J.; Moussy, F.; Li, Y. L.; Milne, W. I. Design of carbon nanotube fiber microelectrode for glucose biosensing. *Journal of Chemical Technology and Biotechnology* **2012**, 87 (2), 256-262.
17. Wen, H.; Nallathambi, V.; Chakraborty, D.; Barton, S. C. Carbon fiber microelectrodes modified with carbon nanotubes as a new support for immobilization of glucose oxidase. *Microchimica Acta* **2011**, 175 (3-4), 283-289.
18. Zestos, A. G.; Nguyen, M. D.; Poe, B. L.; Jacobs, C. B.; Venton, B. J. Epoxy insulated carbon fiber and carbon nanotube fiber microelectrodes. *Sensors and Actuators B-Chemical* **2013**, 182, 652-658.
19. Bath, B. D.; Michael, D. J.; Trafton, B. J.; Joseph, J. D.; Runnels, P. L.; Wightman, R. M. Subsecond adsorption and desorption of dopamine at carbon-fiber microelectrodes. *Anal. Chem.* **2000**, 72 (24), 5994-6002.
20. Bunin, M. A.; Prioleau, C.; Mailman, R. B.; Wightman, R. M. Release and uptake rates of 5-hydroxytryptamine in the dorsal raphe and substantia nigra reticulata of the rat brain. *J. Neurochem.* **1998**, 70 (3), 1077-1087.
21. Forry, S. P.; Murray, J. R.; Heien, M. L.; Locascio, L. E.; Wightman, R. M. Probing electric fields inside microfluidic channels during electroosmotic flow with fast-scan cyclic voltammetry. *Anal. Chem.* **2004**, 76 (17), 4945-4950.
22. Garris, P. A.; Wightman, R. M. Distinct pharmacological regulation of evoked dopamine efflux in the amygdala and striatum of the rat in vivo. *Synapse* **1995**, 20 (3), 269-279.
23. Heien, M. L.; Johnson, M. A.; Wightman, R. M. Resolving neurotransmitters detected by fast-scan cyclic voltammetry. *Anal. Chem.* **2004**, 76 (19), 5697-5704.
24. Hermans, A.; Seipel, A. T.; Miller, C. E.; Wightman, R. M. Carbon-fiber microelectrodes modified with 4-sulfobenzene have increased sensitivity and selectivity for catecholamines. *Langmuir* **2006**, 22 (5), 1964-1969.

25. Swamy, B. E.; Venton, B. J. Carbon nanotube-modified microelectrodes for simultaneous detection of dopamine and serotonin in vivo. *Analyst* **2007**, *132* (9), 876-884.
26. Peairs, M. J.; Ross, A. E.; Venton, B. J. Comparison of Nafion- and overoxidized polypyrrole-carbon nanotube electrodes for neurotransmitter detection. *Analytical Methods* **2011**, *3* (10), 2379-2386.
27. Xiao, N.; Venton, B. J. Rapid, Sensitive Detection of Neurotransmitters at Microelectrodes Modified with Self-assembled SWCNT Forests. *Analytical Chemistry* **2012**, *84* (18), 7816-7822.
28. Ross, A. E.; Venton, B. J. Nafion-CNT coated carbon-fiber microelectrodes for enhanced detection of adenosine. *Analyst* **2012**, *137* (13), 3045-3051.
29. Inoue, Y.; Kakihata, K.; Hirono, Y.; Horie, T.; Ishida, A.; Mimura, H. One-step grown aligned bulk carbon nanotubes by chloride mediated chemical vapor deposition. *Applied Physics Letters* **2008**, *92* (21).
30. Schmidt, A. C.; Wang, X.; Zhu, Y.; Sombers, L. A. Carbon Nanotube Yarn Electrodes for Enhanced Detection of Neurotransmitter Dynamics in Live Brain Tissue. *ACS Nano* **2013**.
31. Vigolo, B.; Penicaud, A.; Coulon, C.; Sauder, C.; Pailler, R.; Journet, C.; Bernier, P.; Poulin, P. Macroscopic fibers and ribbons of oriented carbon nanotubes. *Science* **2000**, *290* (5495), 1331-1334.
32. Jacobs, C. B. Carbon Nanotube-based microelectrodes for enhanced detection of neurotransmitters. Dissertation . **2012**.
33. Zestos, A. G.; Jacobs, C. B.; Trikantopoulos, E.; Venton, B. J. Polyethyleneimine Carbon Nanotube Fiber Microelectrodes for Enhanced Detection of Neurotransmitters. Chapter 3. **2014**.
34. Behabtu, N.; Young, C. C.; Tsentelovich, D. E.; Kleinerman, O.; Wang, X.; Ma, A. W.; Bengio, E. A.; ter Waarbeek, R. F.; de Jong, J. J.; Hoogerwerf, R. E.; Fairchild, S. B.; Ferguson, J. B.; Maruyama, B.; Kono, J.; Talmon, Y.; Cohen, Y.; Otto, M. J.; Pasquali, M. Strong, light, multifunctional fibers of carbon nanotubes with ultrahigh conductivity. *Science* **2013**, *339* (6116), 182-186.
35. Ericson, L. M.; Fan, H.; Peng, H.; Davis, V. A.; Zhou, W.; Sulpizio, J.; Wang, Y.; Booker, R.; Vavro, J.; Guthy, C.; Parra-Vasquez, A. N.; Kim, M. J.; Ramesh, S.; Saini, R. K.; Kittrell, C.; Lavin, G.; Schmidt, H.; Adams, W. W.; Billups, W. E.; Pasquali, M.; Hwang, W. F.; Hauge, R. H.; Fischer, J. E.; Smalley, R. E. Macroscopic, neat, single-walled carbon nanotube fibers. *Science* **2004**, *305* (5689), 1447-1450.

36. Venton, B. J.; Troyer, K. P.; Wightman, R. M. Response times of carbon fiber microelectrodes to dynamic changes in catecholamine concentration. *Anal. Chem.* **2002**, *74* (3), 539-546.
37. Munoz, E.; Suh, D. S.; Collins, S.; Selvidge, M.; Dalton, A. B.; Kim, B. G.; Razal, J. M.; Ussery, G.; Rinzler, A. G.; Martinez, M. T.; Baughman, R. H. Highly conducting carbon nanotube/polyethyleneimine composite fibers. *Advanced Materials* **2005**, *17* (8), 1064-+.
38. Chakraborty, S.; Raj, C. R. Amperometric biosensing of glutamate using carbon nanotube based electrode. *Electrochemistry Communications* **2007**, *9* (6), 1323-1330.

## Chapter 5: Carbon Nanopetals Grown on Metal Wires for Dopamine Detection

---

## 5.1 Abstract

Chemical vapor deposition (CVD) has been used to grow vertically aligned carbon on a variety of substrates. Plasma enhanced chemical vapor deposition (PECVD) helps orient the growth of aligned carbon by applying an electric field. In this study, we used PECVD to grow carbon nanopetals, a type of edge plane graphene, on a variety of metal wire substrates, including tantalum, niobium, palladium, and nickel. The technique is advantageous because it does not require the deposition of a catalyst, and scanning electron micrographs show uniform surface coverage over the entire metal wire. A growth time of 7.5 min was optimal to provide enhanced sensitivity without too much noise. Bare metal wires could not detect 1  $\mu\text{M}$  dopamine with fast-scan cyclic voltammetry, but the carbon-grown wires could. Upon carbon coating, the background charging current increased 10-25 fold, and the shape was similar to other carbonaceous materials. Dopamine was found to be adsorption controlled to carbon nanopetal-wires and had a stable response up to ten hours *in vitro*. The highest sensitivity was for Tantalum (Ta)-carbon nanopetal microelectrodes, with a LOD of 12 +/- 3 nM for dopamine. Ta-carbon nanopetal microelectrodes were more reversible than carbon fibers and had a smaller  $\Delta E_p$ , indicating better reversibility. The growth of carbon nanopetals onto metal wires is a novel method for producing fully coated, cylindrical microelectrodes sensitive to dopamine.

## 5.2 Introduction

Distinct forms of carbon have been grown onto a variety of substrates with chemical vapor deposition (CVD),<sup>1-10</sup> including carbon nanotubes,<sup>1,9,11</sup> edge plane graphene,<sup>12-17</sup> and carbon nanofibers.<sup>18-21</sup> In CVD, a vaporized hydrocarbon flows through a tube reactor at high temperature (700 – 1100 °C), which decomposes the carbon. The metal catalyst coordinates and directs carbon growth from the acetylene source to form vertically aligned carbon nanotubes. Oriented aligned carbon growth offers many possibilities for the creation of electrochemical sensors;<sup>22</sup> however, many of these novel carbonaceous materials have not been fully characterized for electrochemistry.

Carbon-fiber microelectrodes (CFMEs) have been used for neurotransmitter detection with fast scan cyclic voltammetry (FSCV) because of their biocompatibility,<sup>23</sup> small size appropriate for tissue implantation,<sup>24</sup> and because they do not oxidize water as opposed to most metals.<sup>25</sup> Alternative carbon nanomaterials have been used because of their higher aspect ratios for analyte adsorption,<sup>26</sup> electrocatalytic anti-fouling properties,<sup>27</sup> and higher conductivity which can lead to fast-electron transfer kinetics.<sup>28</sup> The growth of aligned carbon provides many advantages in the development of a novel electrochemical sensor such as a high aspect ratio, which allows for many sites for the adsorption of neurotransmitters such as dopamine to the surface. Vertically aligned carbon nanotubes deposited on substrates have been known to grow in a comb-like structure potentially allowing a large surface area for adsorption if used as an electrode material. The carbon sheets align with the field

direction perpendicular to the substrate surface, which is the most energetically favorable orientation.<sup>29</sup> Increased microwave power causes more ionization of the acetylene gas that promotes the nucleation of graphitic clusters, which leads to the formation of carbon of smaller size and higher density.<sup>29</sup>

Plasma enhanced chemical vapor deposition (PECVD) has been used to orient and direct carbon growth through an electric field that supplies high energy electrons to further dissociate the carbon source at lower temperatures. This allows for vertically aligned growth as opposed to the spaghetti like growth at higher temperatures.<sup>30</sup> The Meyyappan group used PECVD to grow vertically aligned carbon nanofibers with the application of a nickel catalyst.<sup>20</sup> Carbon nanofiber based electrodes have been used for a wide variety of electrode materials<sup>18-20,30,31</sup> including electrodes used for extracellular recording of spontaneous and evoked neuroelectrical activity in organotypic hippocampal slice cultures<sup>32</sup> and in brain tissue *in vivo*.<sup>33</sup> CNFs were also used with FSCV with a wireless system for electrochemical detection of neurotransmitters *in vitro* and *in vivo*.<sup>18,19,21,34</sup> More recently, flaky, rose-like carbon nanopetals (CNPs) have been grown with PECVD without the use of a catalyst.<sup>29</sup> Similar nanopetal like carbon has been grown via hot filament CVD<sup>35</sup> and with arc discharge.<sup>12</sup> However, this type of carbon has not been characterized electrochemically.

The growth of carbon nanopetals onto metal substrates has many advantages for use as an electrochemical sensor. First, they do not require the deposition of the catalyst for growth, which is difficult to deposit on cylindrical electrodes reproducibly. Also, the carbon grows uniformly over the entire metal.

Finally, the metal substrate is very conductive, which should enable fast electron transfer. In this study, CNP-coated metal wire microelectrodes were characterized for dopamine detection using fast scan cyclic voltammetry (FSCV). The CNP coated electrodes showed adsorption-controlled behavior with respect to dopamine and repeated flow injection analysis experiments yielded stable currents up to through 10 hours of testing. The amount and morphology of carbon depended on the substrate and the growth time. Tantalum-CNP microelectrodes had faster electron transfer kinetics and lower limits of detection than CFMEs and would be a good choice for future studies measuring dopamine dynamics *in vivo*.

### **5.3 Methods and Materials**

#### **5.3.1 Chemicals and Materials**

Dopamine was purchased from Sigma (St. Louis, MO). A 10 mM stock solution was prepared in 0.1 M perchloric acid and diluted to 1.0  $\mu$ M daily with phosphate-buffered saline (PBS) (131.5 mM NaCl, 3.25 mM KCl, 1.2 mM CaCl<sub>2</sub>, 1.25 mM NaH<sub>2</sub>PO<sub>4</sub>, 1.2 mM MgCl<sub>2</sub>, and 2.0 mM Na<sub>2</sub>SO<sub>4</sub> with the pH adjusted to 7.4). All aqueous solutions were made with deionized water (EMD Millipore, Billerica, MA). Armstrong C7 Resin and Armstrong A2 Activator were obtained from Ellsworth Adhesives (Germantown, WI). Diethylenetriamine hardener (DETA) was used as received from Fisher Scientific (Waltham, MA).

### **5.3.2 Instrumentation**

Fast scan cyclic voltammetry (FSCV) was performed using a ChemClamp potentiostat (Dagan, Minneapolis, MN). Data were collected and analyzed with Tarheel CV software (gift of Mark Wightman, UNC) using custom data acquisition hardware previously described.<sup>36</sup> A triangle waveform was applied to the electrode from a holding potential of -0.4 V to 1.3 V and back at a scan rate of 400 V/sec and a frequency of 10 Hz, unless otherwise noted. A silver-silver chloride wire was used as the reference electrode. Samples were tested in a flow injection analysis system consisting of a six-port, stainless steel HPLC loop injector mounted on a two-position air actuator (VICI Valco Instruments, Co., Houston, TX). Buffer and samples were pumped through the flow cell at two mL/min unless otherwise noted using a syringe pump (Harvard Apparatus, Holliston, MA).

### **5.3.3 Plasma Enhanced Chemical Vapor Deposition**

Metal wires (ESPI Metal, Ashland, OR) approximately 25  $\mu\text{m}$  in diameter were cut into pieces 3 to 5 cm in length. Metal wires were loaded using a stainless steel stage into a custom built DC plasma-enhanced chemical vapor deposition chamber (Center for Nanophase and Materials Sciences, Oak Ridge National Laboratory, Oak Ridge, TN) in a clean room. During growth, the metal wires served as the cathode for the DC plasma. In the chamber (6 -15 torr chamber pressure), the wires were exposed to 100 sccm (standard cubic centimeters per minute flow rate) ammonia and 80 sccm acetylene for 3.5, 5, 7.5, 15, or 30 minutes. After the plasma is started, the carbon nanopetal growth

begins. The dc plasma discharge was operated at 250 mA and roughly 480–550 V at 650°C.

#### **5.3.4. Scanning Electron Microscopy (SEM)**

SEM and Energy Dispersive X-Ray Spectroscopy (EDS) images were taken with a ZEISS Merlin VP SEM microscope (Oberkochen, Germany) microscope with a secondary electron detector using an accelerating voltage of 5 kV and a working distance of 5.6 mm.

#### **5.3.5. Electrode Construction**

Epoxy-insulated microelectrodes were formed as previously described<sup>37</sup>. A 2 cm thick teflon block (McMaster Carr, Atlanta GA) was cut into rectangles using a band saw. Channels in the teflon mold (~70-80  $\mu\text{m}$  thick, ~70-80  $\mu\text{m}$  deep, and 2-6 cm long) were laser etched using a CO<sub>2</sub> engraving machine (Versa Laser® 350 with High Power Density Focusing Optic lens unit, Universal Laser Systems, Scottsdale, AZ, USA). Under a stereoscope, epoxy (Armstrong Resin C7 and 0.8% Activator A2) was placed in each channel using a syringe with a 30 gauge needle. Metal wires were laid manually into each channel, and the wires were pulled from the back to allow approximately 100  $\mu\text{m}$  of the tip to protrude. The epoxy was cured for three hours at 165°C and then electrodes pried out of the channels. The non-electrode end of the metal wire was connected to a gold pin (0.035" x 0.249", Digikey, Thief River Falls, MN) by silver epoxy (H20E, equal portions of Parts A and B, Epoxy Technology, Billerica, MA) to facilitate connection to the potentiostat. The silver epoxy was cured for one hour at 150°C.

## 5.4 Results

### 5.4.1. Surface Characterization

PECVD was used to synthesize carbon nanopetals,<sup>29</sup> and SEM was used to compare the carbon nanostructures on different types of metals (Fig. 5.1). The first SEM is of bare tantalum wire (Fig. 5.1A), and the second (Fig. 5.1B) is of a wire with carbon nanopetals grown on it. Distinct ridges and grooves are seen on the bare metal wire, which is approximately 25  $\mu\text{m}$  in diameter (Fig. 5.1A), and these surface features are not evident after PECVD growth (Fig. 5.1B). At high resolution, Figure 5.1C shows the surface has distinct petal-like features less than 10 nm in length. The petal-like substrates appear to have high aspect ratios with sharp edges perpendicular to the substrate.

CNP growth was compared on tantalum (Ta), palladium (Pd), niobium (Nb), and nickel (Ni) wires. Figure 5.1D shows the surface of a Pd metal wire grown with CNPs that has a very similar structure to Ta wires grown with CNPs. Nb wires grown with CNPs (Figure 5.1E) and Ni wires grown with CNPs (Figure 5.1F) have slightly different structures. The carbon grown on the Nb wire appears to have less rigid and more curved edges of carbon with heterogeneous clumps and smaller surface features. The size of the carbon features is much larger on the Ni wire than the other wires. The SEM images demonstrate that the type of carbon growth is highly dependent on the metal substrate.

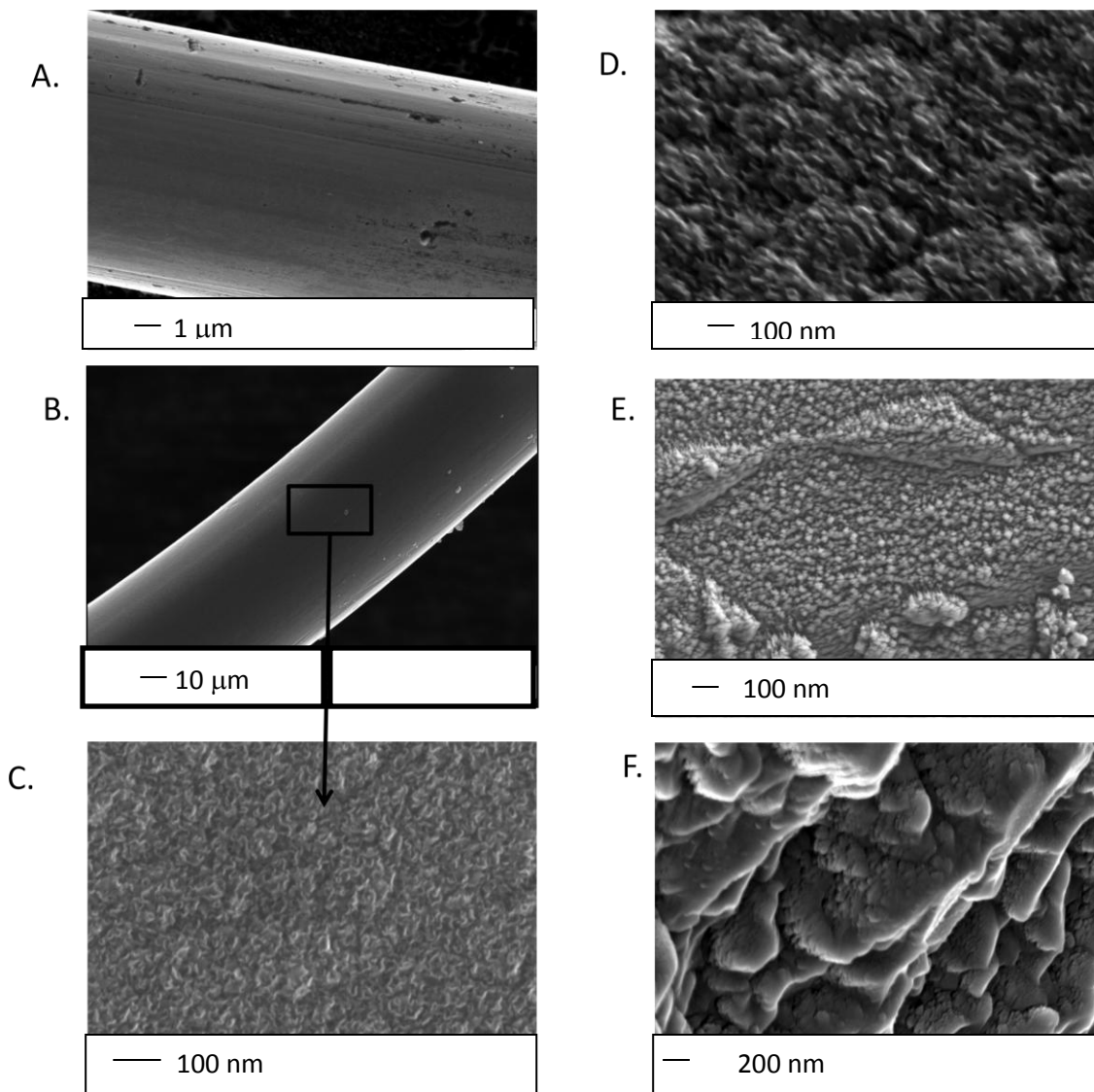


**Figure 5.1:** Carbon nanopetal surfaces. A. SEM of a bare tantalum wire showing distinct grooves and ridges of rough metal surface. B. CNP Coated Ta wire. All carbon nanopetal panels are produced at a 7.5 minute growth time. C. High magnification of carbon nanopetals grown on Ta wire. Ridges of petal like carbon have uniform surface coverage over the entire metal wire. D. High magnification of CNPs on Pd wire shows similar ridges. E. CNPs grown on Nb wire have a different surface with heterogeneous of both large and small growth in clusters. F. CNPs grown on Ni wire have much larger surface features than the other metals.

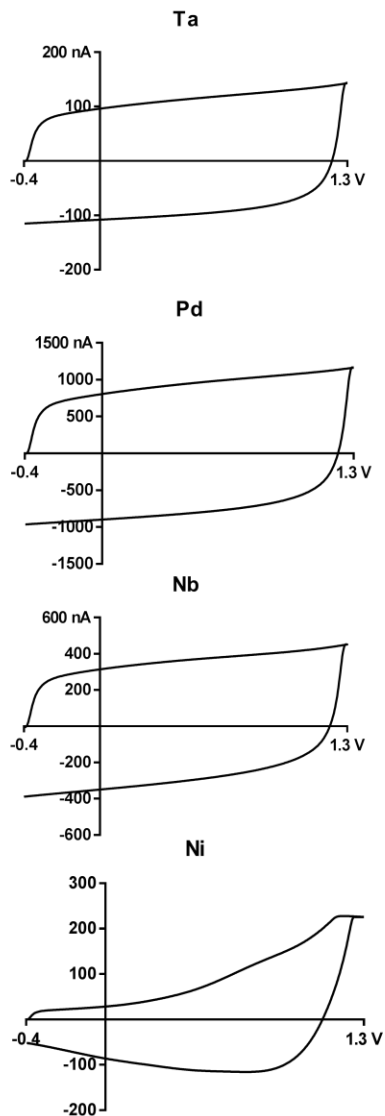
#### 5.4.2. Background Charging Currents

Background charging current are a function of capacitance, scan rate, surface functional groups, and electrode area. Charging currents were compared for the four metal wires: tantalum, palladium, niobium, and nickel (top to bottom, respectively). Fig. 5.2A shows example background currents for bare metal wires, and Fig. 5.2B shows wires grown with carbon nanopetals. The background charging currents of bare tantalum, palladium, and niobium wire are square which indicates that they are mainly capacitive with little surface functionalization (Figure 5.2A).<sup>25</sup> Palladium has higher background currents than any of the other metals. The background charging current of Nickel (Ni) is small, but the shape is less capacitive, although it does not resemble carbon-based electrode background charging currents. The higher current around the switching potential for Ni may indicate water oxidation.<sup>36</sup>

After PECVD coating for 7.5 min, the background charging currents change shape and increase in magnitude, by 5-20 fold (Figure 5.2B). These large increases in charging current indicate there is a marked increase in surface area due to the increased surface roughness of the carbon.<sup>27</sup> The backgrounds are dependent on the amount of carbon, which can be used to monitor the extent of carbon nanopetal growth on a particular metal. The carbon coated electrodes also have a more curved shape; for example, tantalum has more of a curve around 0.6 V that is indicative of surface oxide groups on a carbon surface.<sup>38</sup> The background charging current for CNP coated metals is similar in shape to that of carbon-fiber electrodes.<sup>27</sup> Niobium has more current at the switching potential,

which may indicate a change in the overpotential for water oxidation or specific oxide functional groups that can be oxidized at those potentials.

### A. Bare Metal Wires



### B. CNP Coated Wires

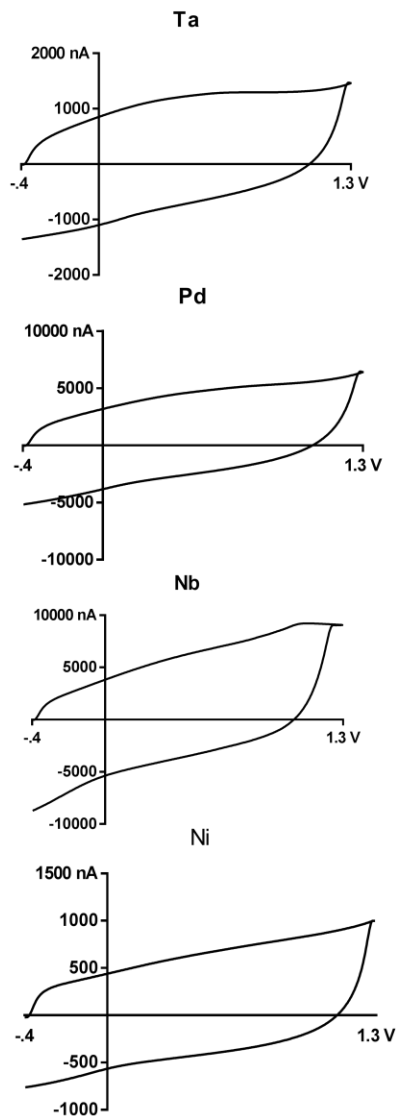


**Figure 5.2:** Background Charging Currents. A. Background charging currents of bare metal wire electrodes. The rectangular shape of most of the metal wires is indicative of an ideal capacitor. B. Background currents of CNP coated metal wire electrodes for a 7.5 minute coating time. Upon coating, the background currents change in shape and increase in magnitude.

### 5.4.3 Detection of Dopamine

The response to 1  $\mu\text{M}$  dopamine was compared for bare metal wire electrodes (Figure 5.3A) and carbon nanopetal coated metal wire electrodes (Figure 5.3B) using FSCV. The background-subtracted cyclic voltammograms for bare tantalum and palladium wire electrodes have small, square responses that have no faradaic peaks and resemble background charging currents (Figure 5.3 A). These currents are likely just small errors due to imperfect background subtraction. Bare nickel and niobium wire electrodes have small peaks close to the switching potentials, but these are at higher potentials than typically observed for dopamine oxidation at carbon electrodes<sup>38</sup>. The shapes of the peaks are not particularly symmetrical, and these small peaks are also likely to be due to background drift and background subtraction errors.

The cyclic voltammograms for 1  $\mu\text{M}$  dopamine at CNP coated metal wire electrodes are characteristic of dopamine detection<sup>39</sup> (Figure 5.3B). Carbon nanopetals were grown for 7.5 min with PECVD for all wires, and the exposed tip for the microelectrode was 100  $\mu\text{m}$ . Tantalum and palladium have markedly higher currents for dopamine than niobium or nickel. The Faradaic signals for dopamine follow the predictions from the background currents, as Pd and Ta had bigger and more carbon-like background currents than Nb. The oddly shaped background charging current of the Ni is not capacitive, but neither does it represent a carbonaceous background. The extra switching potential peak of Nb is not typical of carbon fibers, neither is the surprisingly large background charging current. The kinetics of dopamine detection differed among the wires,

as the  $\Delta E_p$  (peak separation) for CNP-tantalum was less than other CNP grown wires.

Enhanced signals for dopamine at the carbon nanopetal modified wires are likely due to the edge plane carbon and carbon-oxygen functional groups on the surface.<sup>36</sup> Functionalization could take place during the plasma-enhanced chemical vapor deposition (PECVD) where carbon nanopetals are grown onto the surface of the metal wire at high temperatures.<sup>30</sup> Also, carbon-oxygen functionalization could take place when the waveform is applied to the electrode during the experiment.<sup>36</sup> Carbon fiber microelectrodes are oxidized at switching potentials greater than 1.3 V, and carbon-carbon bonds are broken, allowing more sites for adsorption. We expect the same to be true for the carbon nanopetals.<sup>36</sup> At the 1.3 V waveform, the carbon nanopetal surface would be constantly etched and renewed which would increase the sites for dopamine adsorption creating a more sensitive electrode material.<sup>38</sup> Surface functionality has not been shown with CNP-metal electrodes.

We chose tantalum as our model electrode to study because it has the most uniform growth of carbon nanopetals. Figures 1B-C show that tantalum has the most uniform growth of thin CNPs, covering the entire surface of the metal. The growth of CNPs on tantalum wires also is most similar to the Kumar group's work of CNP growth, which includes uniformly covered petal-like carbon flakes approximately 5-10 nm in length.<sup>29</sup> Palladium, niobium, and nickel also have complete surface coverage, however, the SEMs of the growth differ from that of Kumar's work with thicker ridges and more heterogeneous carbon such as the

larger surface features of nickel. The large background charging current of Pd could possibly cause overloading, and thus, interfere with the signal as well. This possibly could result in altered electrochemical properties of the other carbon-grown metal electrodes.

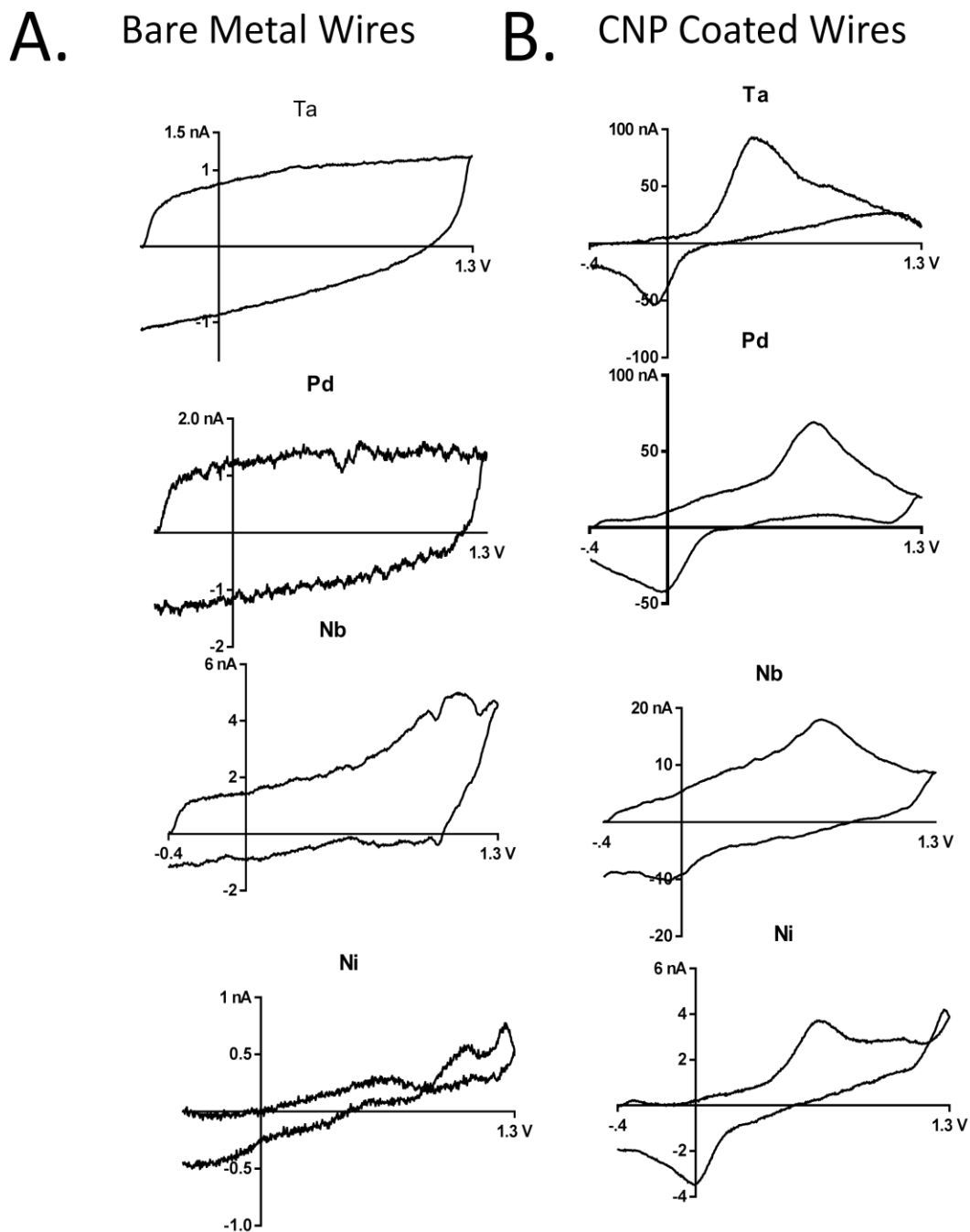


**Figure 5.3: Detection of Dopamine.** A. Detection of 1  $\mu\text{M}$  dopamine with bare metal electrodes. The shapes of the cyclic voltammograms are distorted and sensitivities are low. B. Detection of 1  $\mu\text{M}$  dopamine with carbon nanopetal grown metal wire electrodes. The shape and positions of the voltammograms indicate the detection of dopamine with relatively high sensitivities based on the surface area of the electrodes.

Table 1 compares average electrochemical data for dopamine detection at carbon fiber microelectrodes (CFMEs) and carbon nanopetal (CNP) modified wire microelectrodes. CNP-metal wire electrodes have enhanced electrochemical properties for dopamine compared to CFMEs such as lower limits of detection, faster electron transfer kinetics, and smaller oxidation to reduction ratios. The  $\Delta E_p$  values in Table 1 show that all the metal-wire CNP electrode materials have faster electron transfer kinetics than CFMEs (t-test,  $p < 0.05$ ) with the exception of palladium (t-test,  $p = .65$ ). The peaks are about 100 mV closer together for Ta-CNP electrodes than for carbon fibers. Metal wires were chosen because they have higher conductivities than carbon fibers which may facilitate higher electron transfer kinetics. For example, the conductivity of Ta is 8.06 MS/m<sup>40</sup> compared to 0.067 MS/m for carbon fiber.<sup>23</sup> However, Pd has a similar conductivity to the other metals but did not exhibit increased electron transfer when CNP modified. The carbon metal interface or carbon nanopetal structure may be different on that surface. Electrocatalytic effects could be highly advantageous for using these sensors *in vivo* to detect fast neurotransmitter changes in the brain.

Ta-CNP and Nb-CNP grown metal wire electrodes have lower limits of detection than CFMEs with the same protruding length of 100  $\mu\text{m}$  (Ta and CFME, t-test,  $p = .04$ ; Nb and CFME, t-test,  $p = .006$ ). However, the wires coated with CNPs are all 20-25  $\mu\text{m}$  diameter, which is greater than the 7  $\mu\text{m}$  diameter for uncoated T-650 carbon fibers. Thus, the sensitivity per unit area would be higher

for CFMES. The surface roughness of the CNPs allows more sites for dopamine to adsorb, facilitating low limits of detection. CNP-coated Pd wires had relatively larger magnitudes of background charging currents than the other electrodes, though this was not reflected in significantly lower limits of detection.

Heterogeneous growth at the surface of the electrode might cause more noise. Since LOD depends on the S/N ratio, noise, more noise will result in limits of detection that are not necessarily lower.

Another interesting property of CNP coated metal wire electrodes is that the detection of dopamine is more reversible than at CFMEs, as demonstrated by the lower peak anodic/peak cathodic ( $I_{pa}/I_{pc}$ ) ratios (unpaired t-test,  $p = .007$  for all CNP-wires compared to CFMEs). Dopamine oxidation is known to be quasi-reversible at CFMEs; not all of the dopamine-orthoquinone (DOQ) produced from dopamine oxidation is reduced back to dopamine because DOQ desorbs from the surface of the electrode much faster than dopamine does.<sup>41</sup> However, all four CNP-metal electrodes are more reversible than carbon fibers, and this property has also been observed at CNT-yarn based electrodes.<sup>28</sup>

Material	LOD (nM) (n = 3)	$\Delta E_p$ (V) (n =3)	$I_{pa}/I_{pc}$ (n = 3)
Carbon Fiber <sup>37</sup>	24 $\pm$ 2	0.63 $\pm$ 0.01	1.70 $\pm$ 0.17
Ta-CNP	12 $\pm$ 1*	0.52 $\pm$ 0.01*	1.10 $\pm$ 0.11*
Pd-CNP	22 $\pm$ 2	0.65 $\pm$ .034	1.30 $\pm$ 0.50*
Nb-CNP	14 $\pm$ 2*	0.47 $\pm$ .057*	1.10 $\pm$ 0.20*
Ni-CNP	45 $\pm$ 3	0.57 $\pm$ .027*	1.10 $\pm$ 0.20*

**Table 5.1:** Electrochemical Data. A chart of the limit of detection for dopamine, overpotentials, and ratios of peak oxidative to peak reductive currents comparing CFMEs to Ta, Pd, Ni, and Nb CNP coated metal wires (7.5 minutes growth). \*CNP-wire electrode is significantly different than CFMEs ( $p < 0.05$ )

#### 5.4.4 Adsorption Studies

We chose CNPs grown onto Ta electrodes as our model electrode material because of its high sensitivity, fast electron transfer kinetics, and good reversibility. The scan rate was varied from 100 to 1000 V/s, and Figure 5.4A shows the current for 1  $\mu$ M dopamine increases linearly with respect to scan rate. This indicates that dopamine oxidation at Ta-CNP microelectrodes is an adsorption controlled process, similar to dopamine oxidation at CFMEs and is likely to be dependent upon oxide groups at the surface of the microelectrode.<sup>41</sup>

The concentration range for dopamine was tested for Ta-CNP wire electrodes using samples of 100 nM to 100  $\mu$ M dopamine (Figure 5.4B). The current for Ta-CNP microelectrodes was linear up to 10  $\mu$ M dopamine, similar to carbon-fiber microelectrodes (Fig. 5.4B).<sup>41</sup> At concentrations higher than 10  $\mu$ M, the adsorption sites on the surface of the CNP coated metal wire microelectrode become saturated, and the behavior is more diffusion controlled, which explains the deviation from linearity (Figure 5.3B).<sup>41</sup>

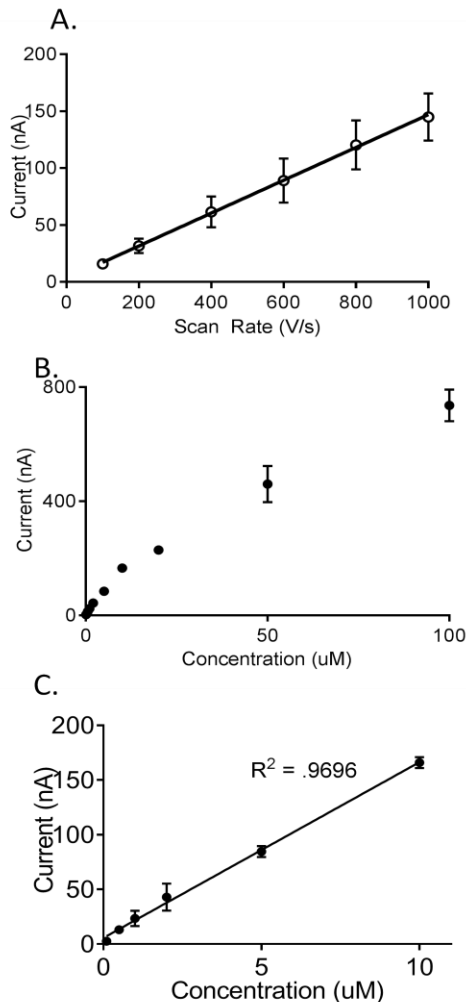


**Figure 5.4.: Adsorption Studies** **A.** Effect of Scan Rate. A linear relationship was observed between scan rate and peak oxidative current for 1  $\mu\text{M}$  dopamine denoting adsorption control ( $n = 3$ )  $R^2 = .90$ . **B.** Concentration Study. Dopamine concentrations were varied from 100 nM to 100  $\mu\text{M}$ . After 10  $\mu\text{M}$ , dopamine is saturated at the surface of the electrode and is diffusion controlled. Error bars are SEM ( $n = 3$ ). **C.** Dopamine concentrations are linear up to 10  $\mu\text{M}$ .

#### 5.4.5 Stability Study

Microelectrodes are typically used *in vivo* for hours at a time to measure neurotransmission in behavioral or pharmacological experiments.<sup>42-45</sup> Therefore, electrodes must have a stable electrochemical response for several hours. The stability of Ta-CNP wire microelectrodes was investigated by continuously applying the potential waveform to the microelectrode for an extended period of

time and injecting a bolus of dopamine every 2 hours. Over a 10 hour period, there was no significant change in peak oxidative current at Ta-CNP wire microelectrodes with a potential waveform of -0.4 to 1.0 V (to not overoxidize<sup>36</sup> the surface) at a scan rate of 400 V/s (Figure 5.5). Both the sensitivity and the stability of Ta-CNP microelectrodes indicate that these microelectrodes are suitable for future *in vivo* studies.

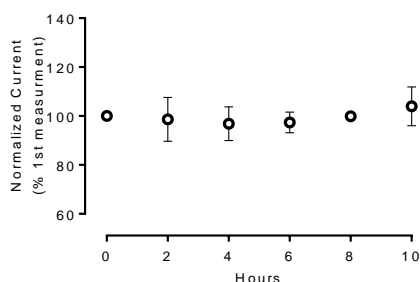


**Figure 5.5:** Stability Study. A stability experiment was performed by testing the response of a Ta-Carbon Nanopetal electrode to 1  $\mu$ M dopamine every 2 hours for 10 hours. There was no change in sensitivity over 10 hours. The electrodes were scanned from -0.4 V to 1.0 V at 400 V/sec at 10 Hz. Error bars are SEM (n = 3).

#### 5.4.6. Effect of Growth Time

The growth time for CNPs will affect the coverage and surface structure of the carbon nanomaterial. Originally, tantalum-CNP metal wire electrodes were grown with 30 minute and 15 minute growth times, but these times produced sensors that had very high noise and were unusable. Ta-CNP wire electrodes grown at 30 minutes had S/N ratios of  $3.9 \pm 1.0$ , while Ta-CNP wires grown at 7.5 minutes have S/N ratios of  $123 \pm 15$  (n = 4, t-test, p = .0002). Excessively long growth times could lead to heterogeneous growth.<sup>46</sup> The amount of carbon

nanopetals on the surface was likely too large resulting in increased background capacitive current which leads to increased noise.<sup>47</sup>

Therefore, we varied the growth time of CNPs onto the surface of the Ta wires, using 7.5, 5, and 3.5 minutes of PECVD growth time. The hypothesis is that longer growth times will produce metal wires that have more carbon on them and that there will be a balance between adding adsorption sites and too much growth which leads to noise. Figure 5.6 shows that the current for dopamine oxidation is greater for 7.5 minute growth than for the other growth times ( $n = 3$ , one-way ANOVA,  $p > .0001$ ). Ta-CNP electrodes grown for 7.5 min were approximately 2-times more sensitive than wires grown for 5 minutes and 14-times more sensitive than wires grown for 3.5 minutes ( $n = 3$ , Bonferonni post-tests,  $p > 0.05$ ). From SEM images, the extent of CNP growth, especially the layering of carbon, cannot be characterized easily. However, we can estimate the electrode surface area by comparing the background charging currents of CNP-metal wire electrode made at different growth times. The background charging current (a function of surface area) of the 7.5 minute growth time is approximately 3-times greater than the 5 minute growth time and 14-times greater the 3.5 minute growth. Thus, the increases in sensitivity follow the increases in background current, suggesting the greater sensitivity of the 7.5 minute growth time is due to a larger surface area. The 7.5 minute growth of CNPs on tantalum created a sensitive electrode material without increasing the noise significantly.

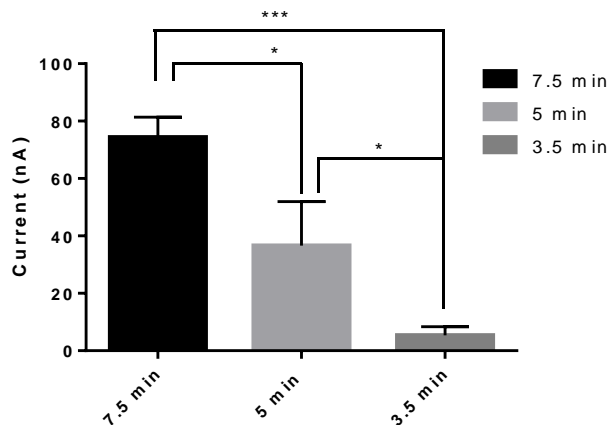


**Figure 5.6:** Effect of Growth Time. The effect of growth time is measured on the sensitivity or the peak oxidative current for 1  $\mu\text{M}$  dopamine detection for Ta-CNP electrodes. As expected, further carbon growth allows for a higher sensitivity by allowing more sites for adsorption of dopamine to the surface of the electrode. The means are all statistically from one another different via one-way ANOVA ( $p = .0004$ ) and Bonferroni's multiple comparison test.

## 5.5 Discussion

The growth of carbon nanopetals on metal wires is advantageous because it provides uniform surface coverage over the entire metal and does not require the deposition of a catalyst. The deposition of the metal catalyst onto a cylindrical metal wire has been known to be difficult and not reproducible. Catalyst free growth of CNPs via PECVD provides an easy and reproducible method of creating carbon nanomaterial surface coverage for electrochemical sensors. Coating the metal wires in CNPs via PECVD greatly increases the magnitude and changes the shape of the background charging current. Wires coated in CNPs were able to detect 1  $\mu\text{M}$  dopamine using FSCV, while uncoated bare wires were not. Table 1 shows CNP coated metal wire microelectrodes have

properties similar to other carbon nanomaterial based microelectrodes, such as CNT-based electrodes<sup>28</sup>. The relatively larger surface areas of the electrodes allow for lower limits of detection than CFMEs as with wet spun CNT-fiber and yarn microelectrodes discussed in chapters 3 and 4. Also, the metal-based electrodes, with the exception of palladium, have significantly faster electron transfer kinetics (peak separation) with respect to CFMEs indicating faster electron transfer. It could possibly be caused by the high conductivity of the metal substrate. CNT-based microelectrodes also have faster electron transfer kinetics with respect to the graphitic CFMEs. They also exhibit larger cathodic:anodic peak ratios indicating a higher reversibility of dopamine at the surface, which has been seen in CNT yarn based microelectrodes.<sup>28</sup> What makes CNP-coated metal wires especially appealing is that several dozen metal wires can be coated using PECVD within a matter of minutes; thus the procedure is amenable to batch fabrication. On the other hand as mentioned in chapters 2-4, manually wetspinning CNT fibers one by one is a tedious process that is not amenable to batch fabrication. The fibers must also be purified one by one that makes this process even longer and more tedious. CNP-coated metal wire microelectrodes provide a novel alternative to the batch fabrication of nanomaterial based electrode materials for enhanced neurotransmitter detection.

There are two major reasons why dopamine is detected at CNP grown metal wire electrodes but not bare wire electrodes. Adsorption to the electrode surface is key for the sensitive detection of dopamine, particularly at carbon-fiber microelectrodes<sup>41</sup>. Bare metal wires do not have the carbon-oxygen functional

groups such as carbonyls and hydroxides that are typically implicated in dopamine adsorption.<sup>25</sup> Thus, using bare metal wires as a substrate is advantageous because there is no current for dopamine except from the carbon nanomaterial. The behavior for CNP coated electrodes is similar to CFMEs, indicating that the properties of carbon that are advantageous for dopamine adsorption and detection are present for this new type of carbon. Higher switching potentials are also advantageous and likely lead to a renewed breaking carbon-carbon bonds and oxide functionalize carbon.<sup>23</sup> Since dopamine is cationic at a physiological pH (7.4), it is electrostatically attracted to the negatively charged oxide functionalized carbon-surface (Figure 5.4). However, metal wires are not thought to be oxide-functionalized greatly due to the relative strength of metal-metal bonds.<sup>25</sup> Metal formed electrodes also lack the surface roughness of carbonaceous formed materials, which may make them harder to surface functionalize, and, thus, have less sites for dopamine adsorption. Therefore, the sensitivity of the metal electrode towards dopamine is expected to be less than carbon based electrodes.

We hypothesize that water oxidation could cause problems in the detection of dopamine for bare metal electrodes, especially for Nb and Ni-based electrodes as denoted by the shape of the background charging current (Figure 1). Carbon-based electrodes have a higher overpotential for the oxidation of water in comparison to metal based electrodes.<sup>25</sup> That means that the electrode can be scanned past 1.3 V without oxidizing water. However, this is not true with metal electrodes.<sup>25</sup> Upon scanning at potentials higher than 1.0 V, water is

oxidized by metal wire electrodes as evidenced by the overloading of background charging currents at the switching potential for Ni and Nb. This signal from water oxidation is thought to be background subtracted from our signal, however, it could increase noise and result in signal distortion through background subtraction errors which makes dopamine harder to detect.

We have ultimately chosen CNP coated tantalum metal wires as our model electrode material. The CNP growth of tantalum is the most uniform (Fig. 1) and has entire surface coverage over the entire metal wire. The growth of CNPs on tantalum wires most closely resembles the growth of CNPs on a variety of substrates as shown by the growth of petal-like carbon from Kumar's group.<sup>29</sup> On the other hand, palladium, niobium, and nickel CNP coated metal wires all have some type of bulky heterogeneous growth on the surface, which could lead to altered electrochemical properties. For example, the large blocks of carbon on the surface of the Ni wire could possibly cause its limit of detection to not be as low and water oxidation as denoted by the distinct shape of its background current (Table 1). The palladium CNP electrode also has slower electron transfer kinetics than the other wires, which could be possibly attributed to heterogeneous growth at the surface (Table 1). The Niobium wire seems to be oxidizing water, as denoted by the overloading of the background charging current (Figure 2), which could presume that there is not a complete surface coverage of carbon over the entire metal wire. Thus, CNP coated Ta metal wire electrodes are the most ideal because they have complete surface coverage of homogeneous

carbon, lower limits of detection, faster electron transfer kinetics, and a higher overpotential for water oxidation.

This research further builds upon on previous work regarding the coating of electrode materials.<sup>48-51</sup> Prior work from our laboratory involved the dip-coating of CNTs onto the surface of CFMEs, which could produce high increases in current but were highly variable. Since the nanotubes are not dissolved in DMF, clumps of varying sizes of CNTs coat the surface, which cause the noise and lack of reproducibility. In addition, the carbon fiber in CNT-modified CFMEs can convolute the kinetics, possibly due to surface changes or conductivity.<sup>48-51</sup> In this work, the high conductivity of the metal substrate allows for fast electron transfer. Coating metal wires with carbon using PECVD allows for an efficient and reproducible method of electrode modification. Future experiments could investigate the anti-fouling properties of these novel sensors and their applicability *in vivo*.

## 5.6 Conclusions

We show that the PECVD growth of carbon nanopetals onto the surface of metal wires facilitates the fabrication of electrode materials used for the voltammetric detection of dopamine. The method is advantageous for two reasons: it provides complete surface coverage of carbon growth over the entire metal material, and it does not require the deposition of a catalyst, which is difficult to be spread uniformly over metal substrates. Background charging currents change in shape and magnitude upon CNP coating, indicating the

surface is carbonaceous. The bare metal wires are unable to detect dopamine, but can detect dopamine after CNP coating. The CNP-metal microelectrodes also have lower limits of detection and faster electron transfer kinetics for dopamine than CFMEs. Dopamine is adsorption controlled at CNP-coated metals. The response towards dopamine is stable up to ten hours in the flow cell showing the electrode's applicability as a possible *in vivo* sensor. This work is significant because we have demonstrated the batch fabrication development and application of novel biosensors with enhanced properties for neurotransmitter detection.

**Acknowledgments.** This work was funded by NSF (CHE0645587522) and NIH (R01 MH085159). User access was provided by Oak Ridge National Lab to the Center for Nanophase and Materials Sciences through awards CNMS2012-070 and CNMS2014-083.

## Reference List

1. Bales, G. S.; Redfield, A. C.; Zangwill, A. Growth dynamics of chemical vapor deposition. *Phys. Rev. Lett.* 1989, *62* (7), 776-779.
2. Bo, Z.; Yang, Y.; Chen, J.; Yu, K.; Yan, J.; Cen, K. Plasma-enhanced chemical vapor deposition synthesis of vertically oriented graphene nanosheets. *Nanoscale* 2013, *5* (12), 5180-5204.
3. Butler, J. E.; Mankelevich, Y. A.; Cheesman, A.; Ma, J.; Ashfold, M. N. Understanding the chemical vapor deposition of diamond: recent progress. *J. Phys. Condens. Matter* 2009, *21* (36), 364201.
4. Cantoro, M.; Hofmann, S.; Pisana, S.; Scardaci, V.; Parvez, A.; Ducati, C.; Ferrari, A. C.; Blackburn, A. M.; Wang, K. Y.; Robertson, J. Catalytic chemical vapor deposition of single-wall carbon nanotubes at low temperatures. *Nano Lett.* 2006, *6* (6), 1107-1112.
5. Chan, J.; Venugopal, A.; Pirkle, A.; McDonnell, S.; Hinojos, D.; Magnuson, C. W.; Ruoff, R. S.; Colombo, L.; Wallace, R. M.; Vogel, E. M. Reducing extrinsic performance-limiting factors in graphene grown by chemical vapor deposition. *ACS Nano* 2012, *6* (4), 3224-3229.
6. Chen, S. Y.; Chang, L. W.; Peng, C. W.; Miao, H. Y.; Lue, J. T. Growth of carbon nanotubes at low powers by impedance-matched microwave plasma enhanced chemical vapor deposition method. *J. Nanosci. Nanotechnol.* 2005, *5* (11), 1887-1892.
7. Cheung, C. L.; Hafner, J. H.; Lieber, C. M. Carbon nanotube atomic force microscopy tips: direct growth by chemical vapor deposition and application to high-resolution imaging. *Proc. Natl. Acad. Sci. U. S A* 2000, *97* (8), 3809-3813.
8. Choi, B. H.; Kim, W. J.; Kim, Y. B.; Lee, J. H.; Park, J. W.; Kim, W. S.; Shin, D. C. Investigation on growth behavior of CNTs synthesized by atmospheric pressure plasma enhanced chemical vapor deposition system on Fe catalyzed substrate. *J. Nanosci. Nanotechnol.* 2008, *8* (10), 4999-5003.
9. Choi, E. C.; Park, Y. S.; Hong, B. Synthesis of carbon nanotubes on diamond-like carbon by the hot filament plasma-enhanced chemical vapor deposition method. *Micron* 2009, *40* (5-6), 612-616.
10. Choi, H.; Gong, J.; Lim, Y.; Im, K. H.; Jeon, M. Effects of the electrical conductivity and orientation of silicon substrate on the synthesis of multi-walled carbon nanotubes by thermal chemical vapor deposition. *Nanoscale Res. Lett.* 2013, *8* (1), 110.

11. Inoue, Y.; Kakihata, K.; Hirono, Y.; Horie, T.; Ishida, A.; Mimura, H. One-step grown aligned bulk carbon nanotubes by chloride mediated chemical vapor deposition. *Applied Physics Letters* 2008, *92* (21).
12. Ando, Y.; Zhao, X.; Ohkohchi, M. Production of petal-like graphite sheets by hydrogen arc discharge. *Carbon* 1997, *35* (1), 153-158.
13. Vlassioug, I.; Regmi, M.; Fulvio, P.; Dai, S.; Datskos, P.; Eres, G.; Smirnov, S. Role of hydrogen in chemical vapor deposition growth of large single-crystal graphene. *ACS Nano* 2011, *5* (7), 6069-6076.
14. Wang, L.; Zhang, X.; Chan, H. L.; Yan, F.; Ding, F. Formation and healing of vacancies in graphene chemical vapor deposition (CVD) growth. *J. Am. Chem. Soc.* 2013, *135* (11), 4476-4482.
15. Yuan, Q.; Gao, J.; Shu, H.; Zhao, J.; Chen, X.; Ding, F. Magic carbon clusters in the chemical vapor deposition growth of graphene. *J. Am. Chem. Soc.* 2012, *134* (6), 2970-2975.
16. Zhang, X.; Wang, L.; Xin, J.; Yakobson, B. I.; Ding, F. Role of Hydrogen in Graphene Chemical Vapor Deposition Growth on a Copper Surface. *J. Am. Chem. Soc.* 2014.
17. Behabtu, N.; Lomeda, J. R.; Green, M. J.; Higginbotham, A. L.; Sinitiskii, A.; Kosynkin, D. V.; Tsentlovich, D.; Parra-Vasquez, A. N.; Schmidt, J.; Kesselman, E.; Cohen, Y.; Talmon, Y.; Tour, J. M.; Pasquali, M. Spontaneous high-concentration dispersions and liquid crystals of graphene. *Nat. Nanotechnol.* 2010, *5* (6), 406-411.
18. Koehne, J. E.; Marsh, M.; Boakye, A.; Douglas, B.; Kim, I. Y.; Chang, S. Y.; Jang, D. P.; Bennet, K. E.; Kimble, C.; Andrews, R.; Meyyappan, M.; Lee, K. H. Carbon nanofiber electrode array for electrochemical detection of dopamine using fast scan cyclic voltammetry. *Analyst* 2011, *136* (9), 1802-1805.
19. Koehne, J. E.; Chen, H.; Cassell, A.; Liu, G. Y.; Li, J.; Meyyappan, M. Arrays of carbon nanofibers as a platform for biosensing at the molecular level and for tissue engineering and implantation. *Biomed. Mater. Eng* 2009, *19* (1), 35-43.
20. Matthews, K.; Cruden, B. A.; Chen, B.; Meyyappan, M.; Delzeit, L. Plasma-enhanced chemical vapor deposition of multiwalled carbon nanofibers. *J. Nanosci. Nanotechnol.* 2002, *2* (5), 475-480.
21. Rand, E.; Periyakaruppan, A.; Tanaka, Z.; Zhang, D. A.; Marsh, M. P.; Andrews, R. J.; Lee, K. H.; Chen, B.; Meyyappan, M.; Koehne, J. E. A carbon nanofiber based biosensor for simultaneous detection of dopamine and serotonin in the presence of ascorbic acid. *Biosens. Bioelectron.* 2013, *42*, 434-438.
22. Zhu, Z. G.; Garcia-Gancedo, L.; Flewitt, A. J.; Moussy, F.; Li, Y. L.; Milne, W. I. Design of carbon nanotube fiber microelectrode for glucose biosensing. *Journal of Chemical Technology and Biotechnology* 2012, *87* (2), 256-262.

23. Huffman, M. L.; Venton, B. J. Electrochemical Properties of Different Carbon-Fiber Microelectrodes Using Fast-Scan Cyclic Voltammetry. *Electroanalysis* 2008, 20 (22), 2422-2428.
24. Heien, M. L.; Johnson, M. A.; Wightman, R. M. Resolving neurotransmitters detected by fast-scan cyclic voltammetry. *Anal. Chem.* 2004, 76 (19), 5697-5704.
25. Hermans, A.; Wightman, R. M. Conical tungsten tips as substrates for the preparation of ultramicroelectrodes. *Langmuir* 2006, 22 (25), 10348-10353.
26. Banks, C. E.; Compton, R. G. New electrodes for old: from carbon nanotubes to edge plane pyrolytic graphite. *Analyst* 2006, 131 (1), 15-21.
27. Swamy, B. E. K.; Venton, B. J. Carbon nanotube-modified microelectrodes for simultaneous detection of dopamine and serotonin in vivo. *Analyst* 2007, 132, 876-884.
28. Schmidt, A. C.; Wang, X.; Zhu, Y.; Sombers, L. A. Carbon nanotube yarn electrodes for enhanced detection of neurotransmitter dynamics in live brain tissue. *ACS Nano* 2013, 7 (9), 7864-7873.
29. Srivastava, S. K.; Shukla, A. K.; Vankar, V.; Kumar, V. Growth, structure and field emission characteristics of petal like carbon nano-structured thin films. *Thin Solid Films* 2005, 492 (1-2), 124-130.
30. Meyyappan, M. A review of plasma enhanced chemical vapour deposition of carbon nanotubes. *Journal of Physics D-Applied Physics* 2009, 42 (21).
31. Koehne, J.; Chen, H.; Li, J.; Cassell, A. M.; Ye, Q.; Ng, H. T.; Han, J.; Meyyappan, M. Ultrasensitive label-free DNA analysis using an electronic chip based on carbon nanotube nanoelectrode arrays. *Nanotechnology* 2003, 14 (12), 1239-1245.
32. Yu, Z.; McKnight, T. E.; Ericson, M. N.; Melechko, A. V.; Simpson, M. L.; Morrison, B., III Vertically aligned carbon nanofiber arrays record electrophysiological signals from hippocampal slices. *Nano Lett.* 2007, 7 (8), 2188-2195.
33. Yu, Z.; McKnight, T. E.; Ericson, M. N.; Melechko, A. V.; Simpson, M. L.; Morrison, B., III Vertically aligned carbon nanofiber as nano-neuron interface for monitoring neural function. *Nanomedicine* 2012, 8 (4), 419-423.
34. Zhang, D. A.; Rand, E.; Marsh, M.; Andrews, R. J.; Lee, K. H.; Meyyappan, M.; Koehne, J. E. Carbon nanofiber electrode for neurochemical monitoring. *Mol. Neurobiol.* 2013, 48 (2), 380-385.
35. Shang, N. G.; Au, F. C. K.; Meng, X. M.; Lee, C. S.; Bello, I.; Lee, S. T. Uniform carbon nanoflake films and their field emissions. *Chemical Physics Letters* 2002, 358 (3-4), 187-191.

36. Heien, M. L. A. V.; Phillips, P. E. M.; Stuber, G. D.; Seipel, A. T.; Wightman, R. M. Overoxidation of carbon-fiber microelectrodes enhances dopamine adsorption and increases sensitivity. *Analyst* 2003, 128, 1413-1419.
37. Zestos, A. G.; Nguyen, M. D.; Poe, B. L.; Jacobs, C. B.; Venton, B. J. Epoxy insulated carbon fiber and carbon nanotube fiber microelectrodes. *Sensors and Actuators B-Chemical* 2013, 182, 652-658.
38. Takmakov, P.; Zachek, M. K.; Keithley, R. B.; Walsh, P. L.; Donley, C.; McCarty, G. S.; Wightman, R. M. Carbon microelectrodes with a renewable surface. *Anal. Chem.* 2010, 82 (5), 2020-2028.
39. Roberts, J. G.; Moody, B. P.; McCarty, G. S.; Sombers, L. A. Specific oxygen-containing functional groups on the carbon surface underlie an enhanced sensitivity to dopamine at electrochemically pretreated carbon fiber microelectrodes. *Langmuir* 2010, 26 (11), 9116-9122.
40. About.com . <http://metals.about.com/od/properties/a/Electrical-Conductivity-In-Metals.htm>. 2014.
41. Bath, B. D.; Michael, D. J.; Trafton, B. J.; Joseph, J. D.; Runnels, P. L.; Wightman, R. M. Subsecond adsorption and desorption of dopamine at carbon-fiber microelectrodes. *Anal. Chem.* 2000, 72 (24), 5994-6002.
42. Zachek, M. K.; Takmakov, P.; Park, J.; Wightman, R. M.; McCarty, G. S. Simultaneous monitoring of dopamine concentration at spatially different brain locations in vivo. *Biosensors & Bioelectronics* 2010, 25 (5), 1179-1185.
43. Phillips, P. E. M.; Wightman, R. M. Critical guidelines for validation of the selectivity of in-vivo chemical microsensors. *Trac-Trends in Analytical Chemistry* 2003, 22 (9), 509-514.
44. Williams, J. E.; Wiczorek, W.; Willner, P.; Kruk, Z. L. Parametric analysis of the effects of cocaine and cocaine pretreatment on dopamine release in the nucleus accumbens measured by fast cyclic voltammetry. *Brain Res.* 1995, 678 (1-2), 225-232.
45. Nguyen, M. D.; Lee, S. T.; Ross, A. E.; Ryals, M.; Choudhry, V. I.; Venton, B. J. Characterization of spontaneous, transient adenosine release in the caudate-putamen and prefrontal cortex. *Plos One* 2014, 9 (1), e87165.
46. Srivastava, S. K.; Vankar, V. D.; Kumar, V. Growth and microstructures of carbon nanotube films prepared by microwave plasma enhanced chemical vapor deposition process. *Thin Solid Films* 2006, 515 (4), 1552-1560.
47. Long, J. T.; Weber, S. G. Noise at microelectrodes and microelectrode arrays in amperometry and voltammetry. *Anal. Chem.* 1988, 60, 2309-2311.

48. Jacobs, C. B.; Vickrey, T. L.; Venton, B. J. Functional groups modulate the sensitivity and electron transfer kinetics of neurochemicals at carbon nanotube modified microelectrodes. *Analyst* 2011.
49. Peairs, M. J.; Ross, A. E.; Venton, B. J. Comparison of Nafion- and overoxidized polypyrrole-carbon nanotube electrodes for neurotransmitter detection. *Analytical Methods* 2011, 3 (10), 2379-2386.
50. Ross, A. E.; Venton, B. J. Nafion-CNT coated carbon-fiber microelectrodes for enhanced detection of adenosine. *Analyst* 2012, 137 (13), 3045-3051.
51. Xiao, N.; Venton, B. J. Rapid, Sensitive Detection of Neurotransmitters at Microelectrodes Modified with Self-assembled SWCNT Forests. *Analytical Chemistry* 2012, 84 (18), 7816-7822.

# Chapter 6: Conclusions and Future Directions

---

## 6.1. Overview

This thesis has explored alternative methods to make carbon-based electrodes for neurotransmitter sensing with fast scan cyclic voltammetry. Although glass capillary insulated carbon-fiber microelectrodes (CFMEs) have been used for over twenty-years, there are many reasons to explore alternative and novel electrode development. First, glass-insulated CFMEs cannot be utilized for some applications. Since glass can break and shatter, it cannot be used for novel chronic testing lasting several weeks or months<sup>1</sup>, in higher order primates<sup>2</sup>, or even in humans.<sup>3</sup> Second, carbon nanotube fiber microelectrodes cannot be insulated in pulled glass capillaries. The altered tensile strengths and thicknesses of the nanotube fibers do not pull well in the vertical capillary puller. Polyimide coated fused silica capillaries have been developed, however, this method is tedious, time-consuming, and not amenable to batch fabrication. Therefore, an alternative insulation for electrode development was necessary. Here, we have developed a novel epoxy insulation for carbon-fiber<sup>4</sup>, carbon nanotube fiber<sup>5</sup>, and carbon nanopetal coated metal wire microelectrodes for neurotransmitter detection. The epoxy insulation was primarily tested with carbon-fiber microelectrodes and then used to form alternative electrode materials such as carbon nanotube fiber microelectrodes and carbon nanopetal (CNP) coated metal electrodes. The epoxy insulation allowed us to develop several novel nanomaterial based electrodes that were tested and compared.

## 6.2 Comparison of Alternative Electrode Materials

Epoxy insulating carbon-fiber microelectrodes proved to be a significant method development to creating a novel electrode material. Since it does not require the vertically capillary puller, it could be used to create a wide variety of electrode materials such as PVA-CNT fiber microelectrodes (PVA-CNTFMEs), PEI-CNTFMEs, acid spun CNTFMEs, and carbon nanopetal (CNP) coated metal wire microelectrodes. The method was relatively easy and reproducible, allowing for a batch fabrication of many alternative nanomaterial based electrodes.

### 6.2.1. Synthesis and Characterization

The method of fabrication of each material is important in whether a batch fabrication of electrodes is possible. For this study, T-650 carbon fibers were readily available for purchase from Cytec Engineering. Wet-spun polymer (such as PVA and PEI) CNT fiber microelectrodes were manually produced by hand. They were separated via sonication and surfactants, and then were manually spun into ribbons in polymer solutions. The ribbons needed to be purified in methanol or water to wash away the polymer and form fibers, but evidence of polymer and surfactant impurities were still evident on the SEM images of the fibers. Acid spun CNT fibers were formed by dissolving CNTs in chlorosulfonic acid and then wetspinning into acetone, which produced CNT fibers. They did not have polymer and surfactant impurities unlike the PEI-CNT fibers with only aligned CNTs present on the SEM image. The CNP coated metal wires were the most amenable to batch fabrication because we could coat 15-20 fibers simultaneously using plasma enhanced chemical vapor deposition in 3.5 to 7

minutes. There was no purification necessary, which greatly expedited the process. Ridges of petal like carbon covered the entire surface of the metal wire, which created a novel and uniformly coated sensor.

Material	Sensitivity (LOD)	Electron Transfer (mV)	Ipc/Ipa	Temporal Resolution	Anti-Fouling
CFMEs	$24 \pm 2$ nM	$680 \pm 5$	Low	Low	No
Acid-CNTFMEs	$3 \pm 0.5$ nM	$570 \pm 7$	High	High	Not tested
PEI-CNTFMEs	$5 \pm 1$ nM	$670 \pm 6$	Medium	High	5-HT, 5-HIAA
PVA-CNTFMEs	$53 \pm 5$ nM	$970 \pm 3$	Medium	Not tested	Dopamine
Ta-CNPFMEs	$12 \pm 1$ nM	$520 \pm 1$	High	Not tested	Not tested

**Table 6.1:** Electrochemical Properties of alternative nanomaterial based electrodes.

### 6.2.2. Sensitivity

We compared the sensitivity of all five electrode materials. The limit of detection assumed that the signal was three-times the noise and was dependent on the surface area of the electrode. The acid-spun CNT fiber electrode had the lowest LOD of about 3 nM. We attribute this to the larger electroactive surface area of the acid spun CNT fiber (30-40 microns in diameter). We are currently examining novel techniques to make thinner fibers for FSCV testing. The nanopetal coated CNP wires also had significantly lower limits of detection (12 nM) than the CFMEs (24 nM) (see Table 1). This result is also attributed to surface area as metal wires 20-25 microns in diameter are coated in carbon nanopetals that increased the diameter to well over 30 micrometers as opposed to CFMEs that are 7 micrometers in diameter. The CNPs also add surface roughness, which provides more sites for adsorption for biomolecules to the surface. PEI-CNT fiber microelectrodes also have significantly lower LODs than CFMEs due to their larger diameters (~18 microns), but the same is not true for

PVA-CNTFMEs because they are coated in a non-conductive polymer (poly(vinyl alcohol), which decreases sensitivity by blocking adsorption sites on the CNT fiber.

### 6.2.3. Electron Transfer

CNT materials are used as electrodes for neurotransmitter detection because of their high conductivity, which is a function of their high  $sp^2$  hybridization caused by the delocalization of electrons. We also examined the electron transfer kinetics ( $\Delta E_p$ ) or peak separation of all of the electrode materials at 400 V/s. PVA CNT fibers had the slowest electron transfer ( $\sim 900$  mV) because of the aforementioned non-conductive PVA that coated the surface upon synthesis. The PEI-CNT fiber microelectrodes had  $\Delta E_p$  values that were about 300 mV less because the amine of the PEI physisorbs to the walls of the CNTs and undergoes an intermolecular charge transfer to increase conductivity 100 X (Table 1). However, the presence of the polymer impurities provides an explanation why the electron transfer kinetics of the PEI CNT fiber electrodes were not significantly faster than the graphitic CFMEs. We hypothesize this to be true because of polymer and surfactant impurities even though PEI does not diminish conductivity as much as PVA does. Furthermore, both acid spun CNTFMEs and CNP coated metal wires have significantly faster electron transfer kinetics than CFMEs. Again, acid spun CNTs are composed of purely CNT materials with no polymer or surfactant impurities. The synthesis also precludes the use of tissue sonication, which could diminish conductivity by shortening CNT lengths, which have more CNT-CNT junctions. The Ta-CNP metal electrode has

the fastest electron transfer, which is mainly attributed to the high conductivity of the metal substrate that has a conductivity, which is two orders of magnitude larger than that of carbon fiber. Acid-spun CNT fibers and Ta-CNP coated wires display promising electrocatalytic effects for neurotransmitter detection in comparison to CFMEs and polymer wet spun CNT fiber microelectrodes.

#### **6.2.4. Reversibility**

The oxidation of dopamine is quasi-reversible at CFMEs, which means that not all of the dopamine-o-quinone (DOQ) that is oxidized from dopamine is reduced back to dopamine. However, this property is not true with many of the carbon nanomaterial based electrodes. Again, the impurity free CNP coated metal wires and the acid spun CNT fibers had the highest peak cathodic peak: anodic ratios (.9) as opposed to .6 for CFMEs (Table 1). The reduction peaks appear to be almost as large as the oxidation peaks, which is not observed at CFMEs. The wet spun acid CNT fiber had cathodic : anodic peak ratios somewhere around .75. Again, the fact that they are not as reversible as acid spun CNT fibers may be due to the presence of polymer and surfactant impurities on the surface of the CNTs. The Sombers group also found that CVD grown carbon nanotube yarn microelectrodes had a greater reversibility than CFMEs illustrating the fact that many CNT-based electrodes have this unique property.<sup>6</sup> This may be attributed to the fact that DOQ is not desorbing as fast from the surface of the nanomaterial as it does from CFMEs as shown with the CNTYMEs. This would produce larger negative reduction peaks if less DOQ falls off the surface.

### 6.2.5. Temporal Resolution

We have also shown that CNT based nanomaterials have a sensitivity for dopamine that is independent of the wave application frequency. For CFMEs, upon increasing the frequency from 10 Hz to 100 Hz, there is an over 75% decrease in the peak oxidation current for dopamine (Table 1). This phenomenon occurs because, at higher frequencies, there is less time for the cationic dopamine to adsorb at the negative holding potential. Since dopamine is adsorption controlled to the surface of CFMEs, the peak oxidative current drops markedly at higher frequencies. However, for CNT fiber materials such as PEI and acid-spun fibers, sensitivity for dopamine does not decrease at higher frequencies. This property was also seen with CNTYMEs. The adsorption kinetics were modeled to show that DOQ and DA desorb at equal rates from CNTYMEs, while DOQ desorbs at a rate that is ten-times faster than dopamine at CFMEs. Therefore, the sensitivity is not dependent on the wave application frequency. Since both CNT fibers and yarns have this property, it is hypothesized that the frequency independent response is a property of the CNTs and not of the manner of construction of the electrode. The adsorption kinetics of dopamine on polymer and acid spun CNTs should be modeled to determine whether dopamine and DOQ desorb from the surface at equal rates as they do with CNTYMEs. Future work should include testing the metal coated CNP electrodes for the frequency independent response. Since they are not composed of solely CNTs, this would allow us to determine whether this property is CNT dependent or if it also extends to other nanomaterials.

### 6.2.6. Anti-fouling Properties

The Ewing group has illustrated the anti-fouling properties of PVA-CNT fiber microelectrodes to high concentrations of dopamine (100  $\mu$ M - 1 mM) over relatively long periods of time in comparison to CFMEs that fouled significantly<sup>7</sup>. Dopamine polymerizes at CFMEs, which blocks sites for adsorption and hence decreases sensitivity markedly at CFMEs. PEI-CNT fiber microelectrodes also displayed anti-fouling properties with respect serotonin and 5-HIAA. Both serotonin and 5-HIAA, a metabolite interferant of serotonin, undergo a free radical polymerization on the surface of the electrode, which also blocks sites for adsorption. PEI CNT fiber microelectrodes are fouling resistant to both molecules, while CFMEs are not. It is hypothesized that PVA and PEI CNT fiber microelectrodes are fouling resistant because the CNTs have a higher density of edge plane carbon as opposed to CFMEs, which is the catalytic site for dopamine and serotonin oxidation<sup>8</sup>. Ideally, this phenomenon should also occur at acid spun CNT fibers because they are also composed of CNTs, but these electrodes have not yet been examined for their anti-fouling properties. Likewise, Ta-CNP coated metal wires were also not examined for their anti-fouling properties yet. Testing this material for its anti-fouling properties would allow us to see if many non-CNT based materials are also fouling resistant and whether the CNPs could be useful for *in vivo* implantation.

### 6.2.7. Acid Spun CNT Fibers

Preliminary data in chapter 4 already has shown the promise of acid spun CNT fiber microelectrodes including low limits of detection, faster electron transfer kinetics, and more reversibility for dopamine oxidation in comparison to CFMEs and polymer wet-spun CNT fiber microelectrodes. However, the high conductivity and surface areas of acid-spun CNT fiber microelectrodes have also caused some problems such as overloading. Overloading is caused by highly conductive materials with larger surface areas that have background currents greater than current our potentiostat can handle (10  $\mu\text{A}$ ). Since we do not have access to the custom-built apparatus of the Smalley institute that stretches and compresses acid spun CNT fibers, it is harder for us to control the surface area<sup>9</sup>. If this is the case, then fibers with larger diameters (50 microns or more) may cause overloading, and hence, a non-functional electrode. Controlling the surface area and diameter of acid spun fibers would be a problem worth examining in the future.

## 6.3 Future Directions

### 6.3.1 *In vivo* testing

Further optimization of these electrode materials has been an ultimate goal of this project. As already mentioned in chapter 2, epoxy insulated CFMEs have been used to detect stimulated dopamine release *in vivo* in rats in the caudate. However, we have had some experimental issues with reproducibility with this method though. Unlike the glass insulated CFME, the epoxy insulated CFME is not tapered, has varied thicknesses, and a jagged and rough surface.

This is thought to possibly cause tissue damage, which could negatively affect *in vivo* testing.

The detection of neurotransmitters *in vivo* with novel electrode materials development has often been difficult to achieve. The Garris group had this issue when they developed their novel boron doped diamond electrode that had a larger surface area.<sup>10</sup> Although the electrode had interesting anti-fouling properties, it could not detect stimulated dopamine release without the use of a reuptake inhibitor, nomifensine, because of the larger electrode surface area. The Phillips group has developed a polyimide coated fused silica capillary electrode for chronic measurements that also has been used to insulate alternative nanomaterials when slid into glass capillaries.<sup>1</sup> However, the method of production is tedious and not amenable to batch fabrication. The 90 micron diameter capillary may also cause some tissue damage. We are currently trying to etch smaller and more uniform channels in Teflon molds to achieve the purpose of creating a small and uniformly shaped sensor. We have experimented with different epoxies such as Armstrong, SU-8, Epon 828, epoxylite, 5-minute epoxy, and silica gel for this end. An epoxy insulated PEI-CNT fiber was also slid into a pulled glass capillary, and the epoxy glass-interface was sealed with a two-hour epoxy. However, this created a leaky electrode with KCl running through holes of the epoxy.

The most promising method seems to be sliding a CNT fiber into a pulled glass capillary without the polyimide capillary. The challenging aspect of this procedure can be epoxying a larger glass-fiber interface, and the difficulty of

threading a fiber into a small opening. Up to this point, we have made a few *in vivo* measurements with this technique. Glass capillary insulated PEI-CNTFMEs were used to detect stimulated dopamine release in rats. Even though we saw the representative cyclic voltammogram for dopamine, the temporal resolution of the sensor was very poor with the signal not returning to baseline. We hypothesize that this occurred because the glass-fiber seal is very large relative to the tapered CFMEs, which causes poor insulation that leads to slower time responses *in vivo*. Ideally, acid spun CNT fiber microelectrodes could also be useful *in vivo* sensors if thinner fibers are able to be produced because of their high conductivity. Ta-CNP electrodes should also be tested *in vivo* due to the uniform surface coverage of carbon over the entire surface of the metal wire. This produced relatively large surface areas (25-30 microns in diameter) that usually do not overload, unlike acid spun CNT fiber microelectrodes. Ta-CNP microelectrodes have also been thoroughly sonicated in water as a control to see if the CNPs could come off the metal wire, and they have not appeared to do so after observing SEM images before and after the sonication. Therefore, it is also assumed that CNPs would not fall off the Ta wires after *in vivo* implantation, which should theoretically make these electrodes suitable as novel *in vivo* sensors.

### **6.3.2 Growth of Carbon Using Chemical Vapor Deposition**

An area where there is a lot of promise in novel electrode development is utilizing chemical vapor deposition to grow vertically aligned carbon. In this thesis, we have already shown that aligned carbon nanopetals can be grown

onto a variety of metal wires (palladium, tantalum, niobium, nickel, etc.) to create novel electrodes. We have also grown vertically aligned carbon nanopetals on carbon fibers, inconel, stainless steel, tungsten, molybdenum, and thinner nickel wires. This method does not require the deposition of a catalyst and has uniform surface coverage over the entire metal wire. However, growing vertically aligned carbon nanotubes to maximize surface area and sites for adsorption in a comb-like structure has been more challenging. Depositing an iron catalyst on a metal wire has been much more challenging than depositing it on other surfaces such as silica<sup>11</sup>. The uneven deposition of the catalyst creates sporadic, heterogeneous, and incomplete growth over the surface of the metal wire, which does not lead to the creation of sensitive electrode sensors<sup>11</sup>.

We are currently working with scientists at Oak Ridge National Lab to improve our growth of aligned CNTs on cylindrical metal wires. We are experimenting with alternative methods of depositing the Al buffer layer and metal catalyst. One catalyst deposition technique is achieved through physical vapor or electron-beam deposition<sup>12</sup>; however, this has led to uneven catalyst deposition. We have also tried to dip-coat and electrodeposit iron onto metal wires. The laser deposition of a TiO<sub>2</sub> buffer layer instead of the Al layer has also led to some interesting growth patterns. More effective methods of depositing buffer layers and catalysts onto the surface of metal wires have also included laser depositing (with pulse laser deposition) the catalyst. Future work could include the growth of vertically aligned carbon nanotubes on other materials such as carbon fibers and even carbon nanotube fibers. If we grew vertically aligned

carbon nanotubes onto carbon nanotube fibers, then ideally, there would be no real interface between the carbon. We would be growing carbon nanotubes onto carbon nanotubes. This theoretically could create a very sensitive electrode material without any convoluting of the signal or hindrance of electron transfer through different materials.

### 6.3.3. Conclusions and Future of the Field

In this work, we have shown that the use carbon nanomaterials in electrode technology is beneficial for sensitive neurotransmitter detection. Carbon nanotube materials lower limits of detection<sup>13-15</sup>, increase electron transfer kinetics<sup>16</sup>, and resist surface fouling<sup>17</sup> of electrode materials. The high aspect ratio of the cylindrical chemical structure is ideal for biomolecule adsorption to increase the sensitivity of the electrode material, while the high  $sp^2$  hybridization of the CNTs also increases conductivity and charge transfer. Also, the higher density of edge-plane carbon, the catalytic site for analyte oxidation, also helps resist surface fouling. We have shown that PEI CNT fiber microelectrodes resist surface fouling by serotonin and 5-HIAA relative to CFMEs, which could make them a novel *in vivo* sensor for serotonin that does not require the electrodeposition of nafion to the surface to repel interferants. The CNT fiber microelectrodes also displayed higher sensitivities, faster electron transfer, and more reversibility for dopamine oxidation relative to CFMEs.

A more thorough characterization of CNT fiber microelectrodes and other carbon nanomaterial electrodes is required to fully understand the chemistry behind the adsorption of biomolecules to the surface. For example, Raman

spectroscopy could allow us to map the ordered and disordered carbon regions on the surface of the CNT fiber. We also could use FT-IR, higher resolution scanning electron microscopy (SEM), transmission electron microscopy (TEM), x-ray photoelectron spectroscopy (XPS), energy-dispersive X-ray photoelectron spectroscopy (EDS), and other surface techniques to help us better characterize the surface morphology of CNT fibers and CNP-grown metal wires, which would allow us to further examine the electrochemistry of each type of microelectrode.

CNT based microelectrodes are useful not only for neurotransmitter detection with FSCV, but for other purposes as well, such as enzyme sensors to detect sugars such as glucose and galactose,<sup>18-21</sup> cholesterol,<sup>22</sup> and DNA.<sup>23,24</sup> The CNT fiber microelectrodes also could be used to detect vesicular release in single cells using amperometry as illustrated by the Ewing group.<sup>25,26</sup> The 2 ms temporal resolution of CNT fibers could provide the first FSCV measurements of single burst firing of dopamine on the millisecond timescale. The use of carbon nanomaterial based electrodes could open up many opportunities in the detection of a wide variety of biomolecules with high temporal resolution.

## Reference List

1. Clark, J. J.; Sandberg, S. G.; Wanat, M. J.; Gan, J. O.; Horne, E. A.; Hart, A. S.; Akers, C. A.; Parker, J. G.; Willuhn, I.; Martinez, V.; Evans, S. B.; Stella, N.; Phillips, P. E. Chronic microsensors for longitudinal, subsecond dopamine detection in behaving animals. *Nat. Methods* **2010**, *7* (2), 126-129.
2. Schultz, W. Behavior-related activity of primate dopamine neurons. *Revue Neurologique* **1994**, *150* (8-9), 634-639.
3. Kishida, K. T.; Sandberg, S. G.; Lohrenz, T.; Comair, Y. G.; Saez, I.; Phillips, P. E.; Montague, P. R. Sub-second dopamine detection in human striatum. *Plos One* **2011**, *6* (8), e23291.
4. Zestos, A. G.; Nguyen, M. D.; Poe, B. L.; Jacobs, C. B.; Venton, B. J. Epoxy insulated carbon fiber and carbon nanotube fiber microelectrodes. *Sensors and Actuators B-Chemical* **2013**, *182*, 652-658.
5. Zestos, A. G.; Jacobs, C. B.; Trikantopoulos, E.; Venton, B. J. Polyethyleneimine Carbon Nanotube Fiber Microelectrodes for Enhanced Detection of Neurotransmitters. Chapter 3. **2014**.
6. Schmidt, A. C.; Wang, X.; Zhu, Y.; Sombers, L. A. Carbon Nanotube Yarn Electrodes for Enhanced Detection of Neurotransmitter Dynamics in Live Brain Tissue. *ACS Nano* **2013**.
7. Harreither, W.; Trouillon, R.; Poulin, P.; Neri, W.; Ewing, A. G.; Safina, G. Carbon nanotube fiber microelectrodes show a higher resistance to dopamine fouling. *Anal. Chem.* **2013**, *85* (15), 7447-7453.
8. Guell, A. G.; Meadows, K. E.; Unwin, P. R.; Macpherson, J. V. Trace voltammetric detection of serotonin at carbon electrodes: comparison of glassy carbon, boron doped diamond and carbon nanotube network electrodes. *Physical Chemistry Chemical Physics* **2010**, *12* (34), 10108-10114.
9. Ericson, L. M.; Fan, H.; Peng, H.; Davis, V. A.; Zhou, W.; Sulpizio, J.; Wang, Y.; Booker, R.; Vavro, J.; Guthy, C.; Parra-Vasquez, A. N.; Kim, M. J.; Ramesh, S.; Saini, R. K.; Kittrell, C.; Lavin, G.; Schmidt, H.; Adams, W. W.; Billups, W. E.; Pasquali, M.; Hwang, W. F.; Hauge, R. H.; Fischer, J. E.; Smalley, R. E. Macroscopic, neat, single-walled carbon nanotube fibers. *Science* **2004**, *305* (5689), 1447-1450.
10. Arumugam, P. U.; Zeng, H.; Siddiqui, S.; Covey, D. P.; Carlisle, J. A.; Garris, P. A. Characterization of ultrananocrystalline diamond microsensors for dopamine detection. *Appl. Phys. Lett.* **2013**, *102* (25), 253107.

11. Nessim, G. D. Properties, synthesis, and growth mechanisms of carbon nanotubes with special focus on thermal chemical vapor deposition. *Nanoscale* **2010**, 2 (8), 1306-1323.
12. Meyyappan, M. A review of plasma enhanced chemical vapour deposition of carbon nanotubes. *Journal of Physics D-Applied Physics* **2009**, 42 (21).
13. Jacobs, C. B. Carbon Nanotube-based microelectrodes for enhanced detection of neurotransmitters. Dissertation . **2012**.
14. Jacobs, C. B.; Vickrey, T. L.; Venton, B. J. Functional groups modulate the sensitivity and electron transfer kinetics of neurochemicals at carbon nanotube modified microelectrodes. *Analyst* **2011**.
15. Jacobs, C. B.; Peairs, M. J.; Venton, B. J. Review: Carbon nanotube based electrochemical sensors for biomolecules. *Anal. Chim. Acta* **2010**, 662 (2), 105-127.
16. Britto, P. J.; Santhanam, K. S. V.; Rubio, A.; Alonso, J. A.; Ajayan, P. M. Improved charge transfer at carbon nanotube electrodes. *Advanced Materials* 1999, 11 (2), 154-157.
17. Swamy, B. E. K.; Venton, B. J. Carbon nanotube-modified microelectrodes for simultaneous detection of dopamine and serotonin in vivo. *Analyst* **2007**, 132, 876-884.
18. Sebez, B.; Su, L.; Ogorevc, B.; Tong, Y.; Zhang, X. J. Aligned carbon nanotube modified carbon fibre coated with gold nanoparticles embedded in a polymer film: Voltammetric microprobe for enzymeless glucose sensing. *Electrochemistry Communications* **2012**, 25, 94-97.
19. Zhu, Z. G.; Garcia-Gancedo, L.; Flewitt, A. J.; Xie, H. Q.; Moussy, F.; Milne, W. I. A Critical Review of Glucose Biosensors Based on Carbon Nanomaterials: Carbon Nanotubes and Graphene. *Sensors* **2012**, 12 (5), 5996-6022.
20. Zhu, Z. G.; Garcia-Gancedo, L.; Flewitt, A. J.; Moussy, F.; Li, Y. L.; Milne, W. I. Design of carbon nanotube fiber microelectrode for glucose biosensing. *Journal of Chemical Technology and Biotechnology* **2012**, 87 (2), 256-262.
21. Wen, H.; Nallathambi, V.; Chakraborty, D.; Barton, S. C. Carbon fiber microelectrodes modified with carbon nanotubes as a new support for immobilization of glucose oxidase. *Microchimica Acta* **2011**, 175 (3-4), 283-289.
22. Gopalan, A. I.; Lee, K. P.; Ragupathy, D. Development of a stable cholesterol biosensor based on multi-walled carbon nanotubes-gold nanoparticles composite covered with a layer of chitosan-room-temperature ionic liquid network. *Biosensors & Bioelectronics* **2009**, 24 (7), 2211-2217.

23. Kim, J. H.; Kataoka, M.; Jung, Y. C.; Ko, Y. I.; Fujisawa, K.; Hayashi, T.; Kim, Y. A.; Endo, M. Mechanically Tough, Electrically Conductive Polyethylene Oxide Nanofiber Web Incorporating DNA-Wrapped Double-Walled Carbon Nanotubes. *Acs Applied Materials & Interfaces* **2013**, 5 (10), 4150-4154.
24. Ko, J. W.; Woo, J. M.; Ahn, J.; Cheon, J. H.; Lim, J. H.; Kim, S. H.; Chun, H.; Kim, E.; Park, Y. J. Multi-Order Dynamic Range DNA Sensor Using a Gold Decorated SWCNT Random Network. *Acs Nano* **2011**, 5 (6), 4365-4372.
25. Sombers, L. A.; Maxson, M. M.; Ewing, A. G. Loaded dopamine is preferentially stored in the halo portion of PC12 cell dense core vesicles. *J. Neurochem.* **2005**, 93 (5), 1122-1131.
26. Sombers, L. A.; Hanchar, H. J.; Colliver, T. L.; Wittenberg, N.; Cans, A.; Arbault, S.; Amatore, C.; Ewing, A. G. The effects of vesicular volume on secretion through the fusion pore in exocytotic release from PC12 cells. *J. Neurosci.* **2004**, 24 (2), 303-309.